THE UNIVERSITY OF MANITOBA

THE SOLUTION OF THE NAVIER-STOKES AND ENERGY EQUATIONS FOR FREE CONVECTION FROM A VERTICAL FLAT PLATE BY NUMERICAL METHODS

by

ALI M. E. OMAR

A THESIS

SUBMITTED TO THE FACULTY OF GRADUATE STUDIES
IN PARTIAL FULFILLMENT OF THE REQUIREMENTS
FOR THE DEGREE OF MASTER OF SCIENCE

DEPARTMENT OF MECHANICAL ENGINEERING

WINNIPEG, MANITOBA
OCTOBER, 1974

THE SOLUTION OF THE NAVIER-STOKES AND ENERGY EQUATIONS FOR FREE CONVECTION FROM A VERTICAL FLAT PLATE BY NUMERICAL METHODS

by

ALI M. E. OMAR

A dissertation submitted to the Faculty of Graduate Studies of the University of Manitoba in partial fulfillment of the requirements of the degree of

MASTER OF SCIENCE

© 1974

Permission has been granted to the LIBRARY OF THE UNIVERSITY OF MANITOBA to lend or sell copies of this dissertation, to the NATIONAL LIBRARY OF CANADA to microfilm this dissertation and to lend or sell copies of the film, and UNIVERSITY MICROFILMS to publish an abstract of this dissertation.

The author reserves other publication rights, and neither the dissertation nor extensive extracts from it may be printed or otherwise reproduced without the author's written permission.

ABSTRACT

A numerical study has been carried out to analyze the laminar free convection heat transfer from an isothermal vertical flat plate into a fluid. The plate height varied between 0.1 and 23.64 cm. Depending on the temperatures of the plate and bulk fluid, the corresponding range of the Grashof number was from 1.0 to 0.4704×10^8. In addition, several values of the Prandtl number were attempted, ranging from 0.72, which is an average value for air, to 12.8, which is the average value of the Prandtl number for water in the temperature range from $0^{\circ}C$ to $4^{\circ}C$. The Boussinesq-approximated complete forms of the Navier-Stokes and energy equations were considered, since the boundary layer approach is not valid for cases involving low and moderate values of Grashof number.

Solutions of the steady-state and time-dependent governing equations were attempted by using several numerical techniques. For the steady-state case, results were obtained for Gr = 1.0 and Pr = 10.0 by applying the "Direct Substitution Simple Explicit" (DSSE) method. The "Simple Explicit" (SE) and the "Alternating Direction Implicit" (ADIP) techniques, on the other hand, were modified and used in attempts to solve for the time-dependent case, but no final results were obtained.

The results obtained for the steady-state situations illustrate the effects of the boundary conditions and of the initial values on the numerical solution. However, to circumvent the instability problem and to express the real physical situation in numerical terms, a new set of

boundary conditions, called the "Open-control-volume Boundary Conditions", were introduced. These new boundary conditions reduced the recirculation of the flow, and the appearance of strong eddies near the boundaries away from the heated plate.

When the bulk fluid was water near $4^{o}C$, uni-directional and bi-directional convective flow patterns were predicted. The boundaries between these flow-patterns were investigated and determined for a bulk temperature of $0^{o}C$. A map for the resulted convective flow regimes was obtained. This map showed that the regimes obtained for similar studies, but for the boundary-layer case, are not the same as those predicted in the present work.

Two new computational techniques were introduced. The first, referred to as the "Up-down" technique, was introduced mainly to solve for Laplacian and Poissonian fields. The other was referred to as the "Temporary-nodes" grid system and computational technique. Its function was to save computer storage and computational time.

The IBM 370/108 computer was used on computing and plotting the results.

ACKNOWLEDGEMENTS

I would like to express my gratitude to Dr. G. K. Yuill for his advice and kind encouragement, without which this work would not have been possible. I am also grateful to Professor G. E. Sims, Professor A. B. Thornton-Trump and all other staff members and fellow graduate students at the Mechanical Engineering Department of the University of Manitoba whose discussions have been very helpful.

I acknowledge gratefully the financial support of the Inland Waters Directorate of Environment Canada, who supported this research work.

Finally, I would like to present this work to my wife, Mona, as a result of her true love.

TABLE OF CONTENTS

LIST OF FIGURES

LIST OF TABLES

LIST OF SYMBOLS

English Symbols

C_1', C_2', C_3', C_4'	Constants
c	Specific heat
D_1, D_2, D_3	Density-temperature coeffecients, defined by equation (A-1)
f	Function of any dependent variable
g	Acceleration of gravity
h	Coefficient of convective heat transfer
h	Equally grid-spacing size, dimensionless
k	Thermal conductivity
k	Unequally grid-spacing ratio, h_y/h_x
L	Plate-height
T	Dimensional temperature
u', u	Dimensional and non-dimensional velocity-components in the x-direction
v', v	Dimensional and non-dimensional velocity-components in the y-direction
V'	Dimensional resultant velocity
x', x	Dimensional and non-dimensional distances in the direction perpendicular to the plate
X	x'-direction body force
y', y	Dimensional and non-dimensional distances in the direction parallel to the plate
Y	y'-direction body force

Greek Symbols

μ	Dynamic viscosity
ρ	Density
τ', τ	Dimensional and non-dimensional time
Φ	Dissipation function

ζ', ζ	Dimensional and non-dimensional vorticities, defined by equation (2.4)
ψ', ψ	Dimensional and non-dimensional stream-function, defined by equation (2.7)
θ	Dimensionless temperature
β	Coefficient of volumetric thermal expansion, defined by equation (A.2)
ν	Kinematic viscosity
α	Thermal diffusivity
ϕ	Any dependent variable
ω	Relaxation factor
γ	Angle defined in Figure (7-4)

Subscripts

r	Reference
p	At the plate
b	At the bulk of fluid
o	At $0^{o}C$
k	At the pivotal point considered for computation
i	At the column number i
j	At the row number j
x	In the x-direction
y	In the y-direction

Superscripts

k	At the computation step number k
n	At the present computational time-step

Dimensionless Groups

Gr_k	Node-Grashof number, defined by equation (2.17)
Pr	Prandtl number, $c\mu/k$
$\overline{Nu}$	Average Nusselt number, defined by equation (B.29)

CHAPTER 1

INTRODUCTION

1.1 Introduction to the Problem

Free convection flow results from the action of body forces on a fluid element. This kind of flow has usually been considered to be generated in a gravitational field, despite the fact that free convection can also be set up by the action of other forces [Refs. 12, (p.522), 38, 57].

Many practical applications of heat transfer by free convection, where the gravitational field creates the body forces, can be found. For instance, in the design of nuclear-reactor fuel elements, it is necessary to consider their behaviour during a coolant-pump failure. Under such circumstances, the heat may be transferred solely to the coolant by the free convection generated by the presence of the gravitational force.

Other practical problems can be found where the body forces are created by the presence of other fields. For instance, electric and magnetic fields can interact with a moving electrically conducting fluid, creating body forces. Consequently, free convection can be observed within the boundary layers on the walls of magnetohydrodynamic power generators [Ref. 57]. Also, in gas turbine rotor blade design, heat is transferred through the free convective flow produced by the action of the centrifugal force [Ref. 38].

The unusual variation of the density of water near $4^{o}C$ has motivated a number of workers [Refs. 51, 70, 77] to study free convection heat transfer from several geometric shapes to water in this

temperature range. The most interesting point here is the bi-directional convective flow which has been observed experimentally and has been predicted by the numerical solution of the boundary-layer equations [Ref. 77].

Generally speaking, free convection can be distinguished, as far as the analytical treatment is concerned, by the interrelation of the momentum and energy equations. The convective fluid-flow is generated by the change in density due to the transfer of heat. Once the fluid starts to move, convective transfer of heat will take place and this, in turn, will affect the momentum transfer. Steady state can be achieved when both the momentum and energy fields reach an equilibrium state.

The study of the problem of free convection heat transfer from a vertical flat plate to fluids began in 1879 with an experimental investigation by Oberback* with some analytical work. In recent years, since 1950, numerous theoretical analyses have appeared in the literature. However, the analysis of the general case of free convection heat transfer has rarely been carried out. Most workers have dealt with the boundary-layer approximate formulae because of their greater simplicity.

1.2 Scope and Format of the Thesis

The aim of the present work is to solve the general and simplified forms of the Navier-Stokes and energy equations which govern the case of heat transfer by free convection from a vertical flat plate to liquids, with emphasis on water near $4^{o}C$. Numerical solutions for the steady-state and time-dependent cases have been obtained using a digital computer. Several numerical methods have been attempted to find the best

*See reference 14

technique to achieve steady and stable temperature and velocity fields.

The formulation of the governing general equations and Boussinesq-approximated expressions are presented, with the controlling boundary conditions, in Chapter 2. Ten numerical methods and their stability analyses are discussed in detail in Chapter 3 after an introductory presentation of finite-difference and iterative techniques. In Chapter 4, two new computation techniques to improve and broaden the range of convergence of some numerical methods are presented. The factors which affect the stability and accuracy of the present solutions are discussed in Chapter 5. Following some preliminary results presented in Chapter 6, Chapter 7 includes detailed interpretation and analysis of the results obtained. Finally, conclusions are presented in Chapter 8.

The appendices at the end of the thesis contain step-by-step derivations of some finite-difference formulae, tables of numerical values, and computer-programme listings for some useful numerical subroutines.

1.3 Previous Work on Related Problems

1.3.1 Steady State Problems

Many workers have dealt with steady state free convection heat transfer from a vertical flat plate to fluids. Most of these have attempted to solve the approximate boundary-layer equations.

The first researcher who attacked this problem was Oberback in 1879*. He tried to solve the general form of the governing equations

---

*See reference 14

by expressing them in series in terms of the volumetric thermal expansion coefficient β. Three years later, Lorenz* obtained practicable straight forward solutions by simplifying the problem of Oberback with the introduction of some sweeping assumptions. This led to results in good agreement with some associated experiments on one hand, but on the other hand, these results did not predict the variation of the heat transfer coefficient h as a function of the distance from the plate leading-edge.

A significant advance in the problem of vertical flat plate is due to Schmidt and Beckmann [Ref. 55]. In 1930, their measurements indicated that the boundary region may be thin compared with the plate height and hence, as a result, the boundary layer assumption could be introduced. In an attempt to solve Schmidt and Beckmann's resulting equations, Pohlhausen** introduced a new definition of a stream function to satisfy the continuity equation; as well as similarity parameters to convert the relevant equations to ordinary differential equations. Pohlhousen's theoretical solution for Pr = 0.733 was adjusted to agree with the experimental results of Schmidt and Beckmann.

In 1939, for the same problem of vertical flate plate, Saunders [Ref. 50] obtained further solutions for air, mercury and water by an approximate method which did not have to fall back on experimental data.

Touloukian, Hawkins and Jakob [Ref. 69] carried out some measurements of the heat transfer coefficient h for the case of free convection from a 2.75 inch diameter cylinder to water and glycol. They found that the influence of curvature was so small that the results

---

*See references 14 and 55
** See reference 55

did not differ appreciably from that for vertical flat plate.

Almost all work done before 1948 has been summarized by Jakob [Ref. 29, p. 522].

In 1953, Ostrach [Ref. 38], in collaboration with Albers, obtained an exact numerical solution for the case of an isothermal vertical semi-infinite flat plate. Eight values of Pr from 0.01 to 1000 were used to get solutions by means of computer. These results confirmed those of Schmidt and Beckmann. The type of flow was found to be dependent solely on the Grashof number. For high values of Gr, the flow was of the boundary layer type and the problem was reduced to one analogous to Prandtl's forced-flow model. The Prandtl number Pr, on the other hand, was found to affect the thickness of the boundary layers. Increasing the value of Pr appeared to reduce the thickness of the thermal boundary layer while decreasing the value of Pr was found to thicken both layers.

The method developed by Ostrach appeared to work well for the case of constant heat flux if the heat transfer coefficient and Grashof number be expressed in terms of the value of the constant heat flux, q. This was the approach used by Sparrow and Gregg [Ref. 61] to obtain similarity solutions for such circumstances.

Additional cases of similarity solutions were carried out by Sparrow and Gregg [Ref. 63] and Yang [Ref. 75] for plate-temperature variation of the form $T_p - T_b = Cy^n$, where C is constant and n can be lower or higher than zero, or zero for the isothermal case.

In many problems, the variation of the density with temperature is not the only factor to be considered. The viscosity μ

and the thermal conductivity k are also sensitive to any temperature change. This was the problem attacked by Sparrow and Gregg [Ref. 62] for the case of variable fluid properties in free convection from a vertical flat plate. They showed that properties other than β should be evaluated at the following reference temperature

$$T_r = T_p - 0.38\ (T_p - T_b) \qquad (1.1)$$

This has been stated as a better choice than that of the film temperature.

Schechter [Ref. 51] and Schechter and Isbin [Ref. 52] studied the case of free convection heat transfer from an isothermal vertical flat plate to water near 4^oC. They considered the thermal expansion coefficient β as the only temperature-dependent variable. They observed three regions for the convective fluid flow depending on the values of the plate and water-bulk temperatures. By varying the plate-temperature and keeping the water-bulk temperature below 4^oC, they observed upwards and downwards unidirectional flow regions in addition to a bi-directional flow region.

In 1972, Yuill [Ref. 77] considered the thermal expansion coefficient β and the viscosity μ as temperature-dependent variables for the same problem of Schechter and Isbin. He obtained a similarity solution by using the Runge-Kutta technique to solve the boundary layer problem. In that effort, the results of some experiments carried out are in good agreement with the numerical solutions obtained.

Previous researchers have performed solutions of not only the boundary layer approximate equations but also the governing equations in the Boussinesq-approximated general

form. For instance, Yang and Jerger [Ref. 76] performed perturbation solutions for the two cases of Pr = 0.72 and 10.0. They used the boundary layer approach as a zero-order approximation to get the first-order approximate solution. Suriano, Yang and Donlon [Ref. 66] solved the same case for extremely low Grashof numbers by applying the perturbation technique. Their solution was limited by the nature of the perturbation series itself as being valid only for $Gr < 1.0$.

In 1966, Suriano and Yang [Ref. 65] solved the problem of free convective heat transfer to liquids from vertical and horizontal plates for a Grashof number range $0 < Gr < 69.5$. They used the initialised disturbances technique which has been adopted by Lester [Ref. 33] in his attempt to solve the Navier-Stokes equations of fluid flow.

Free convection from a vertical flat plate and through a fluid contained in a long horizontal cylinder of non-uniform wall temperature has been studied by Hellums and Churchill [Ref. 27]. After some simplification of their governing equations, their numerical solutions agreed with some experimental data of Martini and Churchill [Ref. 35].

Up-wind difference techniques were applied by Runchal, Spalding and Wolfshtein [Ref. 48] to solve the elliptic equations for vorticity, heat and mass transfer in two dimensions. The generalized case of recirculating flows was analysed by Gosman et al. [Ref. 25].

Heat transfer by free convection in a rectangular enclosure, between two parallel plates or cylindrical annuli, is of importance here since the vertical flat plate case can be considered as an asymptotic situation when one of the surfaces goes to infinity. One of the

early studies of this subject was done by Poots [Ref. 42]. He used orthogonal polynomials, suggested by Batchelor [Ref. 3], to solve two simultaneous equations governing the cases of horizontal, oblique and vertical air layers. He performed the computations by hand for five value of the Rayleigh number. Eckert and Carlson [Ref. 11] used the Zehnder-Mach interferometer to study the temperature fields in such fluid layers for a wide range of Pr. Other solutions for the same circumstances were obtained by different numerical methods. Elder [Ref. 15] used an iterative technique to solve five decomposed second-order equations for vorticity, velocities in the two co-ordinate directions, stream-function and temperature. Numerical stability was achieved by imposing the condition that the normal gradient of the vorticity vanishes on the horizontal boundaries of the vertical cavity. This arbitrary condition, which has no physical meaning, was claimed to affect the end regions. For a set of fourth-order equations, De Vahl Davis [Ref. 8] used a similar iterative procedure, but the vorticity was not retained as a variable. Consequently, the vorticity boundary-conditions problem did not arise. The same set of the fourth-order equations were solved by Rubel and Landis [Ref. 46]. They considered an intermediate iterative step for the computation of the final temperature, and applied an inner iterative method to solve for the value of the stream function. The variable fluid property problem was also attacked for such cases by Rubel and Landis [Ref. 47]. For gases, they showed that the density variations are of the same importance as viscosity and thermal conductivity variations.

An analytic solution of the boundary layer equations for external free convection flow from a sphere, with various prescribed

thermal conditions on the surface, was obtained by Chiang, Ossin and Tien [Ref. 6] by the series expansion method. Schenk and Schenkels [Ref. 53] studied free convection in water around melting ice spheres. They photographed and observed the flow phenomena. Similar experimental investigations were performed by Vanier and Tien [Ref. 71].

1.3.2 Time-dependent Problems

The time-dependent solution of the relevant equations, for both the boundary layer and general forms, have been analysed by several different numerical techniques.

An early analysis of one-dimensional free convection about a semi-infinite flat plate, undergoing a step function change in temperature, was carried out by Illingworth [Ref. 28]. The solution was obtained in exponentials and error-functions, giving the velocity as a function of position and time. Sugawara and Michiyochi [Ref. 64] treated a step-function change in plate temperature by using a method of successive approximation. In this method, the heat was considered to be transferred only by conduction for the first approximation. Dimensionless temperature and velocity distributions were given for two times for a fluid having a Prandtl number of 1.0.

In 1958, a comprehensive study of the transient case of free convection from a semi-infinite vertical flat plate was presented by Siegel [Ref. 57] who used the integral method. The plate was subjected to step changes in temperature and heat flux in two different trials. Three stages of behaviour were observed: laminar pure conduction, a transient region, and full convection. The time required to reach the first and final stages were stated as follows:

The conduction regime ends at time

$$\tau = 1.80 \{(1.50 + Pr)/Gr\}^{\frac{1}{2}} \quad (1.2)$$

and the steady convective regime is attained at a time

$$\tau = 5.24 \{(0.952 + Pr)/Gr\}^{\frac{1}{2}} \quad (1.3)$$

A similar study was done by Gebhart [Ref. 22] to develop an approximate solution for the transient behaviour associated with a constant heat flux density at the plate. No comparable results have been presented for the corresponding case of an isothermal plate.

A perturbation solution for vertical cellular heat transfer was obtained by Kuo [Ref. 32]. He expanded the dependent variables in a series of orthogonal functions, and expanded the coefficients of these functions as power series in chosen perturbation parameters. The values of these parameters have to be kept less than one for all finite values of the Rayleigh number Ra.

Fromm [Ref. 19] introduced the time-central difference technique to solve for the velocity and stream-function equations governing two-dimension fluid flow. He studied the stability of the finite-difference form for the vorticity equation, and, as a result, he modified this equation by multiplying all the terms by a factor depending on the grid size, kinematic viscosity and time-iterative increment. One year later, Fromm [Ref. 20] used this technique again to solve the Boussinesq-approximated Navier-Stokes equations of a fluid layer heated from below. Very recently, in 1972, this technique was tried by Kettleborough [Ref. 30] to solve the problem of free convection in a rectangular cavity, but he stated that it did not give satisfactory results.

The use of the Alternating-Direction Implicit (ADIP) method, introduced primarily by Peaceman and Rachford [Ref. 41], was adopted by Wilkes and Churchill [Ref. 74] in an attempt to obtain the temperature and velocity distribution for a rectangular cavity. They solved the initial value problem of a fluid initially at rest and suddenly subjected to a prescribed thermal boundary condition. The ADIP method has the advantage of yielding information on the transient conditions which exist prior to the establishment of the steady state. On the other hand, it has the disadvantage that the Rayleigh number must be below 75000.

A good survey on the stability limits and the applicability of several numerical methods to the solution of diffusion equations has been carried out by Barakat and Clark [Ref. 2]. In addition, they introduced the Alternating-Direction Explicit (ADEP) technique to solve such problems. Trials were done by Kettleborough to apply the ADEP to problems like that of the present study, but it was found that the technique did not work for this kind of equation. No matter how small the time step was made, irregularities soon built up in the calculated field.

An experimental and analytical study of transient free convection in moderate and high Prandtl number fluids was presented by MacGregor and Emery [Ref. 34]. The effects of the Grashof and Rayleigh numbers, the aspect ratio and variable properties were discussed. An explicit finite-difference technique was used in conjunction with a Gauss-Seidel iterative method for the solution of their relevant equation. Comparisons were presented of their computed and experimental results.

In 1972, Kettleborough [Ref. 30] studied the entrance effect on the transient laminar two-dimension heat and fluid flows between two

isothermal vertical parallel plates. Comparisons were done between results using the Simple Explicit (SE) technique alone and using the combination of the SE and ADIP procedures. Good agreement between the two approaches was obtained.

For other geometries and dimensions, De Vahl Davis and Thomas [Ref. 9] obtained a numerical solution for the cases of free convective fluid motion in a closed annular cavity formed by two concentric isothermal cylinders and two horizontal planes. The former case was further studied by Thomas and De Vahl Davis [Ref. 68]. Here, a secondary flow was induced at a critical Rayleigh number, causing multicellular motion. Aziz and Churchill [Ref. 1] presented a finite difference technique for the numerical solution of three-dimensional free convection in an enclosure. An alternating direction method was applied to the solutions of the transient parabolic equations, the energy and vorticity transport, while a successive overrelaxation (S.O.R.) technique was used for the determination of the vorticity. Although some results were given, their report consisted mostly of a discussion of the various methods available for both two and three dimensions.

The turbulent free convection boundary layer was analysed by Eckert and Jackson [Ref. 13] for a flat plate. The main result of their work lies in the estimation of the critical Rayleigh number. They found that the transient regime between laminar and turbulent free convection occurred at values of Ra between 10^8 and 10^{10}, usually taken as 10^9 [Ref. 29, p. 529]. A similar analysis was carried out by Deardorf [Ref. 7] for two-dimensional convection between horizontal parallel plates. He studied the effect of the width-height ratio on the formation of convective plumes. The effect of replacing the rigid-surface boundary conditions

by free-surface conditions was found to increase the heat transfer by 190%.

From the above survey of previous related studies, it can be seen that most progress has been made in the solution of the Boussinesq-approximated boundary-layer equations, for both steady-state and time-dependent free-convection heat transfer problems. This is due to the fact that all earlier experimental investigations have been carried out on free-convection heat transfer at high values of Grashof number, Gr, where the boundary layer exists.

It is noticeable also that some work has been done using several different analytical and numerical approaches to solve the free-convection Boussinesq-approximated general equations. The major difficuly in attacking such problems lies in finding the proper way to initialize the solution and to state adequate boundary conditions.

As a general remark, it can be said that the Direct Substitution Simple Explicit (DSSE) method appeared to work smoothly for solving steady-state problems. Also, the Simple Explicit (SE) and the alternating direction implicit (ADIP) methods seemed to be the most promising techniques for solving the time-dependent equations.

CHAPTER 2

GOVERNING EQUATIONS

The postulates which will be applied in developing the governing equations are those pertaining to free convection heat transfer from a smooth isothermal flat plate to water. The convective flow is generated solely by the temperature-dependent density variation of water, in conjunction with a gravitational field of strength g. This density variation is a result of the heat transfer by all modes from the plate into water.

Many textbooks* have discussed and analysed the set of formulae governing the case considered in this report. These formulae are usually designated as the Navier-Stokes, energy and continuity equations. These equations can be derived for an isotropic, compressible, Newtonian and Stokesian fluid by considering momentum, energy and mass conservation respectively. For two-dimensions, this yields [Ref. 54, pp. 51 and 254]

$$\rho\frac{Du'}{D\tau'} = X - \frac{\partial p}{\partial x'} + \mu\,(\nabla'^2 u') + \frac{1}{3}\mu\,\frac{\partial}{\partial x'}(\text{div}\,\bar{V}') \qquad (2.1\text{-a})$$

$$\rho\frac{Dv'}{D\tau'} = Y - \frac{\partial p}{\partial y'} + \mu\,(\nabla'^2 v') + \frac{1}{3}\mu\,\frac{\partial}{\partial y'}(\text{div}\,\bar{V}') \qquad (2.1\text{-b})$$

$$\rho c\frac{DT}{D\tau'} = \frac{Dp}{D\tau'} + k\,\nabla'^2 T + \mu\Phi \qquad (2.2)$$

and

$$\frac{\partial \rho}{\partial \tau'} + 2\left(u'\frac{\partial \rho}{\partial x'} + v'\frac{\partial \rho}{\partial y'}\right) + \rho\left(\frac{\partial u'}{\partial x'} + \frac{\partial v'}{\partial y'}\right) = 0 \qquad (2.3)$$

---

*See references 12, 21, 29, 36, 40, 45, 54 and 56

with the assumption that all properties except density are constant.

The left-side term in equations (2.1) and (2.2) is frequently called the "inertia" or "convective" term. It presents the contribution of the convection flow to momentum and energy transfer. For low velocity fields, e.g. at the very first time-iterative steps, this term can be neglected to retain the case of pure conduction heat transfer [Ref. 28].

Equation (2.2) implies neither sources nor sinks within the control volume, and neglects the heat transfered by radiation. This last assumption is reasonable since the temperature differences involved in the considered case are very small.

Now, we can eliminate the pressure-gradient term in equations (2.1-a) and (2.1-b) by differentiating the first with respect to y', and the second with respect to x' and subtracting. Also, we can introduce a dimensional vorticity function ζ' defined as

$$\zeta' = \frac{\partial v'}{\partial x'} - \frac{\partial u'}{\partial y'} \tag{2.4}$$

Consequently, with some lengthy algebraic manipulation, equation (2.1-a) and (2.1-b) can be combined into one equation of the form

$$\rho \frac{D\zeta'}{D\tau'} - \mu \nabla'^2 \zeta' - \frac{\partial}{\partial x'}(Y) + \frac{\partial}{\partial y'}(X)$$

$$= \rho \zeta' \operatorname{div} \bar{V}' + \frac{Du'}{D\tau'} \frac{\partial \rho}{\partial y'} - \frac{Dv'}{D\tau'} \frac{\partial \rho}{\partial x'} \tag{2.5}$$

2.1 Simplified Dimensional and Non-dimensional Time-dependent Forms

For the case under consideration, the Boussinesq approximation can be introduced. This is based on the assumption that $(T_p - T_b)$ is sufficiently small to (a) neglect the density variation in all terms of equations (2.2), (2.3) and (2.5) except for the y'-direction buoyancy term; (b) assume all transport and thermodynamic properties (apart from the density) to be independent of temperature; (c) neglect the compressibility effect. This last assumption means that the time and spatial variation of density, and as a result the pressure, can be omitted [Ref.38] and (d) neglect the heat dissipation by viscous effects since the dissipation number [Refs, 23,24] is very small for water $(10^{-4} - 10^{-7})$ under the present circumstances.

On this base of assumptions, the continuity equation (2.3) can be reduced to be

$$\frac{\partial u'}{\partial x'} + \frac{\partial v'}{\partial y'} = 0 \qquad (2.6)$$

We are now in a position to introduce a new function which satisfies equation (2.6) and includes u' and v' in one function, that is the stream-function ψ', defined by

$$u' = \partial\psi'/\partial y' \quad \text{and} \quad v' = -\partial\psi'/\partial x' \qquad (2.7)$$

The stream-function ψ' physically represents the volumetric rate of flow per unit length. It has the dimensions of $ft^3/(sec.\ ft)$.

On the other hand, by applying the aforementioned assumptions, and substituting the value $-\rho g$ for the y'-direction body force Y,

equation (2.5) will be

$$\rho\frac{D\zeta'}{D\tau'} - \mu\nabla'^2\zeta' + g\frac{\partial\rho}{\partial T}\frac{\partial T}{\partial x'} = 0 \qquad (2.8)$$

By making use of equation (A - 2) in Appendix A, we can say that

$$(\partial\rho/\partial T)_k = -\beta_k\rho_k \qquad (2.9)$$

and equation (2.8) can be written in an expanded form as

$$\frac{\partial\zeta'}{\partial\tau'} + u'\frac{\partial\zeta'}{\partial x'} + v'\frac{\partial\zeta'}{\partial y'} = g\beta_k\frac{\partial T}{\partial x'} + \nu_k\nabla'^2\zeta' \qquad (2.10)$$

Similarly, the energy equation (2.2) can also be simplified to take the form

$$\frac{\partial T}{\partial\tau'} + u'\frac{\partial T}{\partial x'} + v'\frac{\partial T}{\partial y'} = \alpha_k\nabla'^2 T \qquad (2.11)$$

Other forms of equations (2.10), (2.11) and (2.6) can be rephrased by introducing the definitions of the stream-function (2.7) and the vorticity (2.4). This yields

$$\frac{\partial\zeta'}{\partial\tau'} + \frac{\partial\zeta'}{\partial x'}\frac{\partial\psi'}{\partial y'} - \frac{\partial\zeta'}{\partial y'}\frac{\partial\psi'}{\partial x'} = g\beta_k\frac{\partial T}{\partial x'} + \nu_k\nabla'^2\zeta' \qquad (2.12)$$

$$\frac{\partial T}{\partial\tau'} + \frac{\partial T}{\partial x'}\frac{\partial\psi'}{\partial y'} - \frac{\partial T}{\partial y'}\frac{\partial\psi'}{\partial x'} = \alpha_k\nabla'^2 T \qquad (2.13)$$

and

$$0 = \zeta' + \nabla'^2\psi' \qquad (2.14)$$

This set of equations presents the dimensional forms of the time-dependent vorticity, temperature and stream-function formulae respectively. For the case under consideration, these equations are associated with the

following initial and boundary conditions:

For $\tau' < 0$;

$$T = T_b \text{ and } u' = v' = \psi' = \zeta' = 0 \qquad (2.15\text{-a})$$

For $\tau' \geq 0$ and

at $y' = \pm \infty$ and $0 \leq x' \leq + \infty$;

$$u' = 0, \qquad \text{i.e. } \partial \psi' / \partial y' = 0$$

$$\partial v' / \partial y' = 0$$

$$\partial^2 T / \partial y'^2 = 0 \qquad (2.15\text{-b})$$

at $x' = + \infty$ and $- \infty \leq y' \leq + \infty$;

$$u' = 0, \qquad \text{i.e.} \qquad \psi' = C_2'$$

$$\partial v' / \partial x' = 0 \quad \text{and hence} \qquad \zeta' = 0$$

$$\partial T / \partial x' = 0 \qquad (2.15\text{-c})$$

at $x' = 0$ and $-L/2 \leq y' \leq L/2$;

$$u' = 0 \quad \text{therefore} \qquad \psi' = C_1'$$

$$v' = 0 \qquad \text{and} \quad \partial \psi' / \partial x' = 0$$

$$T = T_p \qquad (2.15\text{-d})$$

and at $x' = 0$, $- \infty \leq y' < -L/2$ and $L/2 < y' \leq + \infty$;

$$u' = 0 \quad \text{therefore} \qquad \psi' = C_1'$$

$$\partial v' / \partial x' = 0 \qquad \text{and} \qquad \zeta' = 0$$

$$\partial T / \partial x' = 0 \qquad (2.15\text{-e})$$

The physical meaning of these boundary conditions will be discussed in Chapter 5.

It is convenient, for the sake of simplifying the numerical solution, to non-dimensionalize the equations involved in the analysis. To do so, we will set the plate height to be unity, and will identify the following dimensionless parameters

co-ordinates: $x = x'/L,\ y = y'/L$ (2.16-a)

velocities : $u = u'/\nu_k,\ v = v'/\nu_k$ (2.16-b)

dependent variables: $\psi = \psi'/\nu_k,\ \zeta = \zeta' L^2/\nu_k$

$$\theta = (T - T_b)/(T_p - T_b) \quad (2.16\text{-c})$$

and

time: $\tau = \tau'\ \nu_k/L^2$ (2.16-d)

In addition, the variable node-Grashof number Gr_k will be defined as

$$Gr_k = g\ \beta_k\ (T_p - T_b)\ L^3/\nu_k^2 \quad (2.17)$$

By using the dimensionless parameters of equation (2.16) and the variable Grashof number Gr_k, equations (2.12) to (2.14) can respectively be rephrased to take the forms

$$\frac{\partial \zeta}{\partial \tau} + \frac{\partial \zeta}{\partial x}\frac{\partial \psi}{\partial y} - \frac{\partial \zeta}{\partial y}\frac{\partial \psi}{\partial x} = \nabla^2 \zeta + Gr_k \frac{\partial \theta}{\partial x} \quad (2.18)$$

$$\frac{\partial \theta}{\partial \tau} + \frac{\partial \theta}{\partial x}\frac{\partial \psi}{\partial y} - \frac{\partial \theta}{\partial y}\frac{\partial \psi}{\partial x} = \frac{1}{Pr}\nabla^2 \theta \quad (2.19)$$

and

$$\underbrace{\quad}_{\text{Transient term}} \quad \underbrace{\qquad\qquad 0}_{\text{Convection term}} = \underbrace{\nabla^2 \psi}_{\text{Diffusion term}} + \underbrace{\zeta}_{\text{Source term}} \quad (2.20)$$

associated with the following initial and boundary conditions

For $\tau < 0$;

$$\theta = 0 \text{ and } u = v = \psi = \zeta = 0 \quad (2.21\text{-a})$$

For $\tau \geq 0$, and

at $y = \pm \infty$ and $0 \leq x \leq +\infty$;

$$u = 0 \qquad \text{i.e. } \partial \psi / \partial y = 0$$

$$\partial v/\partial y = 0$$

$$\partial^2 \theta/\partial y^2 = 0 \quad (2.21\text{-b})$$

$$\underline{\text{at } x = +\infty \text{ and}} \; -\infty \leq y \leq +\infty \; ;$$

$$u = 0 \qquad \text{i.e.} \qquad \psi = C_2$$

$$\partial v/\partial x = 0 \qquad \text{therefore} \qquad \zeta = 0$$

$$\partial \theta/\partial x = 0 \qquad (2.21\text{-c})$$

$$\underline{\text{at } x = 0 \text{ and}} \; -0.5 \leq y \leq +0.5 \; ;$$

$$u = 0 \qquad \text{therefore} \qquad \psi = C_1$$

$$v = 0 \qquad \text{and} \qquad \zeta = 0$$

$$\theta = 1.0 \qquad (2.21\text{-d})$$

and $$\underline{\text{at } x = 0 \text{ and}} \; -\infty \leq y < -0.5 \text{ and } +0.5 < y \leq +\infty \; ;$$

$$u = 0 \qquad \text{therefore} \qquad \psi = C_1$$

$$\partial v/\partial x = 0 \qquad \text{and} \qquad \zeta = 0$$

$$\partial \theta/\partial x = 0 \qquad (2.21\text{-e})$$

The similarity of the terms in equations (2.18) to (2.20) is obvious. Consequently, one or both of equations (2.18) and (2.19) will be considered for any numerical discussion to follow.

2.2 Simplified Dimensional and Non-dimensional Steady State Forms

By steady state is meant a state of equilibrium in which the dependent variables change solely with the spatial co-ordinates. This state can be reached as the final situation at the end of a transient process, and it might be either stable or unstable from the numerical point of view.

By a similar manner to that used to derive the time-dependent set of equations, and by considering all the aforementioned assumptions to be valid, the steady state forms of the governing equations can be easily formulated. Here, the transient term of equations (2.12) to (2.14) can be omitted to yield

$$\frac{\partial \zeta'}{\partial x'} \cdot \frac{\partial \psi'}{\partial y'} - \frac{\partial \zeta'}{\partial y'} \cdot \frac{\partial \psi'}{\partial x'} = g\, \nu_k \frac{\partial T}{\partial x'} + \nu_k \nabla'^2 \zeta' \qquad (2.22)$$

$$\frac{\partial T}{\partial x'} \cdot \frac{\partial \psi'}{\partial y'} - \frac{\partial T}{\partial y'} \cdot \frac{\partial \psi'}{\partial x'} = \alpha_k \nabla'^2 T \qquad (2.23)$$

and

$$0 = \zeta' + \nabla'^2 \psi \qquad (2.24)$$

associated with the boundary conditions (2.15-b) to (2.15-e).

To formulate the non-dimensional forms of the steady state case, the dimensionless parameters (2.16-a) to (2.16-c) and the variable node-Grashof number, Gr_k, can be substituted into equations (2.22) to (2.24) . This will yield

$$\frac{\partial \zeta}{\partial x} \cdot \frac{\partial \psi}{\partial y} - \frac{\partial \zeta}{\partial y} \cdot \frac{\partial \psi}{\partial x} = Gr_k \frac{\partial \theta}{\partial x} + \nabla^2 \zeta \qquad (2.25)$$

$$\frac{\partial \theta}{\partial x} \cdot \frac{\partial \psi}{\partial y} - \frac{\partial \theta}{\partial y} \cdot \frac{\partial \psi}{\partial x} = \frac{1}{Pr} \nabla^2 \theta \qquad (2.26)$$

and

$$0 = \zeta + \nabla^2 \psi \qquad (2.27)$$

associated with the set of boundary conditions (2.21-b) to (2.21-e).

CHAPTER 3

NUMERICAL CONSIDERATIONS AND STABILITY ANALYSIS

The general formulation of many physical problems involving rates of change with respect to two or more independent variables, such as time, length or angle, leads to a partial differential second-order equation of the form [Ref. 58]

$$a\frac{\partial^2\phi}{\partial x^2} + b\frac{\partial^2\phi}{\partial x\partial y} + c\frac{\partial^2\phi}{\partial y^2} + d\frac{\partial\phi}{\partial x} + e\frac{\partial\phi}{\partial y} + f\phi + g = 0 \qquad (3.1)$$

where a, b, c, d, e, f and g may be functions of the dependent variable ϕ. This possibility occurs frequently because such equations usually represent the mathematical form of one of the conservation laws in physics. Equation (3.1) is said to be elliptic when $b^2 - 4ac < 0$, parabolic when $b^2 - 4ac = 0$ and hyperbolic when $b^2 - 4ac > 0$.

The mathematical solution of partial differential equations usually involves some difficulties and challenges. In order to circumvent these difficulties, several numerical methods have been developed. Of these, the finite-difference methods are the most effective and commonly used ones.

3.1 Finite-Difference Approaches

Finite-difference approaches are basic in numerous branches of numerical analysis. Their importance lies in the ease with which many complicated operations and functions can be discretized. Operations, such as integration and differentiation, can then be performed not upon continuous functions but rather, approximately, in terms of numerical

values over a discrete point set. The resulting finite-difference forms are arithmetically simple and can conveniently be programmed for digital computers.

Now, by using the symbols shown in Figure (3 - 1), the first derivative $f'_x = df/dx$ at any particular point x, can be approximated

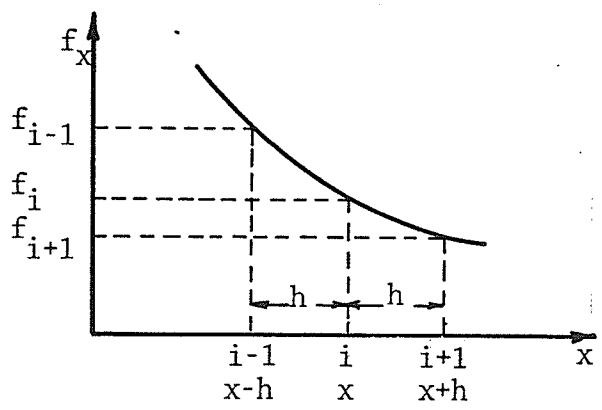

Figure (3 - 1) : Forward-, Backward- and Central-Differences

by the forward-difference formula as

$$f'_i = (f_{i+1} - f_i)/h \tag{3.2}$$

by the backward-difference formula as

$$f'_i = (f_i - f_{i-1})/h \tag{3.3}$$

or by the central-difference formula as

$$f'_i = (f_{i+1} - f_{i-1}) / 2h \tag{3.4}$$

All forms (3.2) to (3.4) are explicit ones. The truncation error (see Chapter 5) for forward- and backward-difference derivative approximations are of the order (h), while that for the central-difference formula is of the order (h^2)

Alternatively, numerical approximate forms for the first derivative can be expressed explicitly in terms of the values at 3, 5 or more points on one side of the considered pivotal point i [Ref. 31, p. 660].

The more the points considered in the formula, the higher the accuracy and the lower the truncation error will be. The "three-point one-sided derivative" formula is a good example to be considered. Here, the forward and backward forms can be written as

$$f_i' = (-3f_i + 4f_{i+1} - f_{i+2})/2h \tag{3.5}$$

and

$$f_i' = (3f_i - 4f_{i-1} + f_{i-2}) / 2h \tag{3.6}$$

respectively. In this case, the truncation error is of the order (h^2) (see Appendix B).

In general, forward- and backward-difference formulae are required to compute derivatives at the boundaries of any specified control volume. The central-difference formula is preferred and should be used if function-values are available on both sides of the considered pivotal point [Ref. 73].

The second derivative, at point i of Figure (3 - 1), can be expressed explicitly in terms of the numerical values of the function f, at the three points i - 1, i and i + 1, as

$$f_i'' = (f_{i-1} - 2f_i + f_{i+1})/h^2 \tag{3.7}$$

with a truncation error of the order (h^2). This approximation is consistent with the idea of fitting a second-order polynomial to three pivotal points. Usually, we can gain some increase in accuracy by using higher-order polynomials. For instance, as an alternative to expression (3.7), the second derivative can be obtained for five pivotal points as

$$f_i'' = (-f_{i-2} + 16f_{i-1} - 30f_i + 16f_{i+1} - f_{i+2})/ 12\, h^2 \tag{3.8}$$

with a truncation error of the order (h^4) (see Appendix B).

Unfortunately, the round-off error controls the accuracy of the expression as well. For expressions of higher order of approximation, the gain achieved by reducing the truncation error is quickly compensated by the loss occasioned by the increase of the round-off error. Other formulae for numerical differentiation have been obtained by Bickley [Ref. 4].

The most important derivative-operator in the present work is Laplacian operator ∇^2. In two-dimensional Cartesian co-ordinates, it can be expressed as

$$\nabla^2 = \frac{\partial^2}{\partial x^2} + \frac{\partial^2}{\partial y^2} \tag{3.9}$$

Applying equation (3.7) independently in both x and y directions,

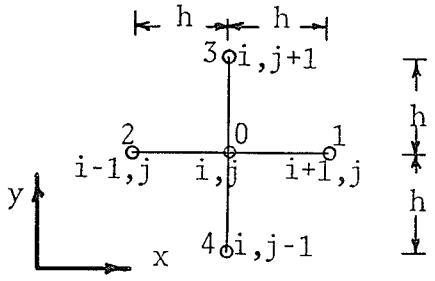

Figure (3 - 2) : The Five pivotal points for two-dimensional operators.

and adding, the resulting expression will be

$$(\nabla^2 f)_0 = f_{i+1,j} + f_{i-1,j} + f_{i,j+1} + f_{i,j-1} - 4f_{i,j})/h^2 \tag{3.10}$$

in the notation of Figure (3 - 2).

Finite-difference Laplacian operators are available in many co-ordinate systems other than the Cartesian. For example, Salvadori and Baron [Ref. 49, pp. 237-252] present cylindrical and spherical co-ordinate forms.

Pivotal points are not always equally spaced. For such cases, finite-difference derivative operators can be derived as well. This is obvious since approximate polynomials can be fitted to unequally spaced pivotal-point values. Expressions for the Laplacian operator ∇^2 for such cases have been presented by Salvadori and Baron [Ref. 49, pp. 231 - 234].

3.2 Iterative Techniques

The use of finite-difference formulae to solve for parabolic and elliptic partial differential equations produces a set of linear, or non-linear, algebraic equations. Iterative methods are usually the most successful way to solve such set of equations.

The first step in developing the iterative techniques was the introduction of the "relaxation methods" by Southwell [Refs.59, 60]. We are required to solve the simultaneous algebraic equations

$$A\underline{f} = \underline{b} \tag{3.11}$$

where A is a symmetric, positive and finite matrix. The aim of the relaxation process is to examine the components of the residual, or displacement, vector

$$r^k = b - Af^k \tag{3.12}$$

for the current approximate solution f^k, and make successive changes in the components of f^k so that the components of the residual vector are steadily reduced to negligible amounts.

Generally speaking, iterative procedures are to be classified into two main categories: In one, use is made of matrix inversion techniques as part of the iterative cycle [Ref. 72]. These are frequently referred as "block" methods; other methods use only the procedure of successive substitutions, and they are known as "point" methods.

Within the last category, there is a choice of several alternatives [Refs. 16, 17, 58]. Of these, the Point-Jacobi, Gauss-Seidel and Successive Overrelaxation (S.O.R.) methods are of interest here.

In the Point-Jacobi method*, during each cycle of iteration, only the values of the variables produced by the previous cycle of iteration are used. In the Gauss-Seidel method, the updated values are used as soon as they become available.

The most speedy method is, in fact, the successive overrelaxation (S.O.R.) method**. Here, at each step of iteration, the variables are overcorrected by a factor ω called the relaxation factor. The value of this factor is often altered between successive scans of the considered equation-set in an attempt to speed up the rate of convergence. The value of ω at which the maximum rate of convergence occurs is called the optimum value. The S.O.R. procedure has a definite advantage, for some type of computer applications, over other methods in that it requires carrying as computer memory not more than one complete set of dependent-variable values.

Frankel [Ref. 18] carried out some computer experiments on different numerical methods to differentiate between their speed of convergence. He concluded that the S.O.R. procedure would prove more rapidly convergent and more convenient for digital computers than other methods including the second-order Richardson method.

---

*This iterative method has many different other names. Of these, the "Method of Simultaneous Displacements" and the "Richardson Iterative Method" [Ref. 72].

**This method is called the "Accelerated Liebmann Method" by Frankel (1955) [Ref. 18] and many subsequent authors.

3.3 Applicable Numerical Methods and Their Stability Analysis

Numerous methods have been devised for solving the governing vorticity, temperature and stream-function equations. These methods can be divided into two main classes. The first deals with the solution for the steady state case and the other concerns the time-dependent or transient situation.

3.3.1 Methods for the solution of the steady state equations

Several numerical methods have been applied to solving the equations of the steady state case. The finite-difference approximations have usually been used in these methods for numerical computations. Three of these methods will be discussed here along with their stability analysis and their applicability for our case.

3.3.1.1 Direct Substitution Simple Explicit (DSSE) Method

The DSSE method is based on the explicit finite-difference direct representation of each term in the equation to be solved. For instance, by considering equations (2.25) and (2.26) in conjunction with Figure (3 - 2), the values of the vorticity and dimensionless temperature at the pivotal point 0 can be expressed explicitly in terms of other dependent variables at the surrounding nodes 1, 2, 3 and 4 respectively as

$$\zeta_0 = \frac{1}{4}(\zeta_1 + \zeta_2 + \zeta_3 + \zeta_4) - \frac{1}{16}\{(\zeta_1 - \zeta_2)(\psi_3 - \psi_4) - (\zeta_3 - \zeta_4)(\psi_1 - \psi_2)\} + Gr_k \frac{h}{2}(\theta_1 - \theta_2) \qquad (3.13)$$

and

$$\theta_0 = \frac{1}{4}(\theta_1 + \theta_2 + \theta_3 + \theta_4) - \frac{Pr}{16}\{(\theta_1 - \theta_2)(\psi_3 - \psi_4) - (\theta_3 - \theta_4)(\psi_1 - \psi_2)\} \qquad (3.14)$$

By initializing the entire field with suitable values as a first guess, the two sets of equations (3.13) and (3.14) can be easily programmed for computer solutions. The S.O.R. technique recommended by Frankel is usually used to achieve such solutions. The main difficulty lies in the estimation of the simultaneous optimum ω - values necessary for maximizing the convergence rate. However, it seems likely in many such complex problems that an appreciable improvement in convergence rate can be achieved by a suitable guess of ω - values. Moreover, approximate optimum ω - values can be found by computer experiments without great effort.

The stability of equations (3.13) and (3.14) mainly depends on the linearity of these equations and is greatly influenced by the order of magnitude of each term with respect to others. The convergence of the above equations is found to be restricted by three stability conditions: (a) The sum of the moduli of the dependent variable on the right-hand side must be less than or equal to unity at each node of the mesh; (b) This sum must be less than unity for at least one pivotal point; and (c) These moduli, and the source term, must not vary too much from one cycle of iteration to another.

The first condition is obviously satisfied for the two equations since the sum of moduli is equal to one regardless of the node considered. The second condition can be satisfied by considering any boundary-node subjected to a Dirichlet boundary-condition. In this case, the sum of

moduli is equal to zero. The third condition is already satisfied for equation (3.14) since the source term equals zero. For equation (3.13), it is found that to satisfy the third stability-condition, the value of the variable node-Grashof number Gr_k should not exceed 100. The DSSE method applicability for our case is therefore limited by this value of Gr_k. For values of $Gr_k > 100$, the DSSE method can be applied but previous results must be supplied as initial values to any succeeding run with an increment value of 5 to 10 in Gr_k. This is what Gosman at al. [Ref. 25, p. 128] asked about in their effort to define the "sufficiently small" variations.

In addition, a major factor is found to affect the convergence of equations (3.13) and (3.14), namely, the value of the acceleration factor ω. Forsythe and Wasow [Ref. 16, p. 237] stated that there is a certain optimum value of ω, at which the convergence rate of an iterative scheme can be maximized, for each scan of computation. This value is usually not known prior to the solution and it may vary from one iterative step to the next. Improper choice of this value may decrease the rate of convergence. Omar [Ref. 37] performed computer experiments to test these statements for simple Laplacian and Poissonian fields. Some accelerating values for ω have been observed. At these values, the rate of convergence was found to be fast but still slower than that corresponding to the optimum values. However, some useful schemes exist for successivly estimating the optimum relaxation factors for the solution of equations in one dependent variable [Refs. 5, 26, 43, 44].

It is very important to emphasize at this stage that when the source term varies significantly from one iteration to the next, causing instability, the use of under-relaxation is highly recommended. "Under-relaxation" implies that an acceleration factor, ω, between 0 and 1.0 is to be

used to achieve smoothly oscillating convergence or even stability. This subject was studied in 1953 by Ostrowski [Ref. 39]. As a general rule, the vorticity equation presents the main source of instability. Consequently, the underrelaxation process must be used here.

3.3.1.2. Up-wind Differences Method

This is a method in which the first-order differential coefficients in the convective terms of equations (2.12) and (2.13) can be replaced by finite-difference forms dependent on the direction of flow. Gosman et al. [Ref. 25] introduced this approach to circumvent the instability exhibited when non-linear equations governing recirculating fields of mass and heat flows are solved.

In the present study, several trials have been carried out applying this method to solve the governing equations of free convection. The procedure exhibited instability even for very low values of Gr_k.

3.3.1.3 Initialised-Disturbances Method

In 1960, Lester [Ref. 33] developed a method for computing the vorticity and stream-function by applying the DSSE technique on an extended node-set including 13 neighbouring nodes. The idea of the solution was to assume a specific disturbance initially imposed on the dependent variable at the considered pivotal point. This would yield the so-called new value. By applying the DSSE form on the closest four surrounding nodes, other values would be obtained to be used through the DSSE process to recalculate the value of the dependent variable at the pivotal point. The difference between the recalculated

and the new values is presumably fixed to be some figure. At this stage, a correlation could be formed between these fixed figures and the originally guessed diturbances. Through this correlation, a new guess for the imposed disturbance could be calculated to be added to the value of the dependent variable for further repetitions. The same process was applied by Suriano and Yang [Ref. 65] in an attempt to solve for the case of free convection heat transfer from vertical and horizontal plates to liquids.

The first workers who analyzed the stability of this method were Thom and Apelt [Ref. 67]. Their approach was dependent on initial disturbances imposed one at a time on the dependent variables of a fluid flow problem. Later on, Lester [Ref. 33] applied Thom and Apelt's approach but with simultaneous initial disturbances imposed on the dependent variables. Suriano and Yang [Ref. 65] also used the same technique to determine a convergence criterion for vorticity and temperature transport. Despite the independent imposing of the initial diturbances on the dependent variables, the convergence criterion derived was mathematically complicated and had no physical meaning. However, their approach seemed to work well for low and moderate values of Gr_k, up to 70.

For the present woek, it can be seen that the restrictions stated for the use of the DSSE method for higher Gr_k are still valid. In fact, the computation time is expected to be longer. No trials were carried out to solve the equations of free convection using this technique. The reason can be illustrated through the following analysis: The values of Gr_k considered by Suriano and Yang were 0.139, 1.0 and 69.5. No predictions were stated for the applicability of their procedure to other situations involving higher values of Gr_k. However,

to get an idea about the range of usefulness of their process, let us consider the dominant factor in their convergence criterion. For the very first computation step, this factor, for the temperature equation, can be reduced to be

$$-192 < h^3 \, Gr_k \, . \, Pr \, (\Delta\theta)_k < 320 \qquad (3.15)$$

Now, for $h = 0.1$, $\Delta\theta = 0(10^{-1})$ and $Pr = 10$, the maximum allowable Gr_k value will be 3.2×10^5. Therefore, for laminar free convection limit, $Ra = 10^8$, h must be 3.2×10^{-2} for $\Delta\theta = 0(10^{-1})$, or $\Delta\theta$ should be $0(3.2 \times 10^{-3})$ for $h = 0.1$. In both cases we need a large mesh with a small grid size. This will worsen the accuracy and the stability of the computation process (see Chapter 5).

3.3.2 Methods for Solving the Time-dependent Equations

According to Kuo [Ref. 32], a steady state can be defined as the final equilibrium state between the temperature field and the fluid flow field. If this equilibrium state is stable, it must be reached asymptotically through the use of a time-dependent approach. On the other hand, if it is unstable, it will be replaced by another state which may be numerically stable but not steady.

In the subsequent sub-sections, we will study some numerical methods which are usually used for seeking the steady state by solving the time-dependent forms of the relevant equations.

3.3.2.1 Perturbation Technique

The perturbation technique is usually used to obtain solutions at different orders of approximations. The zero-order solution is often that corresponding to a very idealized and simplified case. For instance, pure conductive heat transfer can be considered as a zero-order approximation for the free convection case at the beginning of the fluid motion. The first-order approximation usually gives a better representation of the problem. Second- and higher-order solutions usually present more accurate or more sophisticated cases.

The essence of the perturbation technique lies in the choice of a proper perturbation parameter. For similarity solutions, the similarity parameter is usually taken as the perturbation parameter. In other cases, the Grashof number itself can be considered as the perturbation parameter.

The perturbation method cannot be used to solve our governing set of equations. The nature of the perturbation series itself limits the value of Gr_k to be less than unity [Ref. 66].

3.3.2.2 Finite-Difference Methods

The finite-difference methods used to solve the time-dependent relevant equations can be classified into two main categories; namely, "Explicit" and "Implicit" techniques.

For the following discussion, we shall consider equation (2.19) in conjunction with Figure (3 - 3).

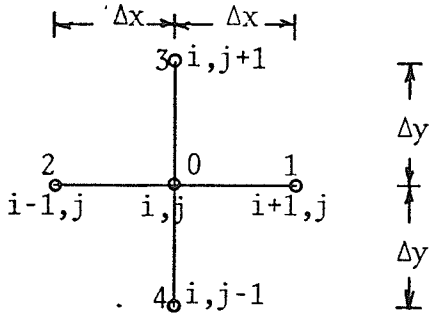

Figure (3-3) : Grid system for finite-difference formulation.

The node of interest here is (i, j). It is surrounded by four nodes distant Δx and Δy as shown. Let n designate the n^{th} time-step, therefore, n - 1 and n + 1 will stand for the preceding and the succeeding time-steps respectively.

I Explicit Methods

I.1 Simple Explicit (SE) Method

The SE method is one of the easiest and most commonly used techniques to solve time-dependent formulae. Here, the dependent variable at (i, j) and time (n + 1) can be expressed explicitly in terms of its values at the five points (i + 1, j), (i - 1, j), (i, j), (i, j + 1) and (i, j - 1) and present time n. Accordingly, equation (2.19) can be rephrased to be

$$(\theta_0^{n+1} - \theta_0^n)/\Delta\tau = \{(\theta_1^n - 2\theta_0^n + \theta_2^n)/\Delta x^2 + (\theta_3^n - 2\theta_0^n + \theta_4^n)/\Delta y^2\}/Pr$$
$$-\{(\theta_1^n - \theta_2^n)(\psi_3^n - \psi_4^n) - (\theta_3^n - \theta_4^n)(\psi_1^n - \psi_2^n)\}/4\Delta x\Delta y \qquad (3.16)$$

and for this case, stability can be achieved if

$$\Delta\tau \leq \left\{\frac{|(\partial\psi/\partial x)_{max}|}{\Delta y} + \frac{|(\partial\psi/\partial y)_{max}|}{\Delta x} + \frac{2Pr}{(\Delta x)^2} + \frac{2Pr}{(\Delta y)^2}\right\}^{-1} \qquad (3.17)$$

The SE method was used successfully by MacGregor and Emery [Ref. 34] to solve for the transient situation of free convection in a square enclosure. The results obtained were in good agreement with their experiments. In 1972, Kettleborough [Ref. 30] used the SE method in conjunction with the ADIP technique (see Article II.8 in Section 3.3.2.2) to observe analytically the entrance effect on free convection in a rectangular cavity.

The SE method has the advantage of being simple and easy for programming. The restriction of small $\Delta\tau$ usually requires a huge number of time steps and represents the essential disadvantage of this method. Another disadvantage was shown during an attempt by the author to solve the problem of this study by the SE method; that is, the great sensitivity of the method to the values initialising the computation process. Improper values caused instability and divergence no matter how small $\Delta\tau$ was made.

I.2 Alternating-Direction Explicit (ADEP) Method

This method was introduced by Barakat and Clark [Ref. 2] to solve diffusion equations (equations like (2.19) without the convective term). The basic principle of this method is to assume that the value of the dependent variable θ at the pivotal point 0 and at the time level n+1, θ_0^{n+1}, can be represented by two functions α_0^{n+1} and β_0^{n+1} so that

$$\theta_0^{n+1} = (\alpha_0^{n+1} + \beta_0^{n+1})/2 \qquad (3.18)$$

associated with the condition that α and β satisfy the original considered diffusion equation.

By applying the finite-differences in an alternating-direction technique [Ref. 2], α_0^{n+1} and β_0^{n+1} can be presented for numerical computation by the following forms (see Figure (3 - 3) for notations)

$$\alpha_0^{n+1} = f(\alpha_0^n, \alpha_1^n, \alpha_3^n, \alpha_2^{n+1}, \alpha_4^{n+1}) \tag{3.19}$$

and

$$\beta_0^{n+1} = f(\beta_0^n, \beta_1^{n+1}, \beta_3^{n+1}, \beta_2^n, \beta_4^n) \tag{3.20}$$

Now, α_0^{n+1} can be computed explicitly, through equation (3.19), by marching from the point 0(1, 1) to the point at the opposite end $F(i_{max}, j_{max})$ by increasing the indices i and j by unity. Also, β_0^{n+1} can be computed explicitly, by the use of equation (3.20), by marching in the reverse direction. As a result, θ_0^{n+1} can be calculated at this time-step (n+1) using equation (3.18).

Barakat and Clark declared that the ADEP method did not have severe restriction on the time step and it had the simplicity of the SE method. However, Kettleborough [Ref. 30] tried to solve equations like that involved in the present work but the method appeared to be unsuccessful regardless of the value of $\Delta\tau$.

I.3 Central-Difference Explicit (CDEP) Method

This method was introduced by Fromm [Ref. 19] in an attempt to achieve stability in the solution of the finite-difference form of the vorticity equation. The essence of this method is the use of time- and space-centered finite-differences; i.e., the dependent variable at a time $(\tau + \Delta\tau)$ can be calculated in terms of the values at both τ and

$(\tau - \Delta\tau)$ time-steps. By applying this technique on the vorticity equation, and using velocity values at mid-points between the mesh-nodes (e.g. $(i, j+\frac{1}{2})$, $(i+\frac{1}{2}, j)$, etc.), Fromm developed a modified vorticity equation to satisfy two requirements for stability, namely,

$$(|u'|+|v'|)\ \Delta\tau'/(hL) \leqslant 1 \tag{3.21}$$

and

$$\nu\,\Delta\tau'/(hL)^2 \leqslant 1/4 \tag{3.22}$$

Conditions (3.21) and (3.22) are quite similar to the inequality (3.17) for stability of the temperature equation (2.19).

The CDEP method was used successfully by Fromm [Ref. 20] to solve the equations governing free convection from a heated fluid layer. Kettleborough [Ref. 30] attempted to apply the CDEP technique to solve for the case of free convection in a rectangular enclosure, but the method did not appear to give satisfactory results.

II Implicit Methods

To circumvent the time-step restrictions stated for the stability of the explicit methods, numerous implicit techniques have been devised.

By using these methods, the dependent variable at any time level n+1 can be expressed explicitly in terms of the variable-values at the neighbouring nodes at time level n, and/or implicitly at the same time level n+1. Consequently, the use of this technique requires the solution of a large number of simultaneous algebraic equations at each time step. Iterative methods, such as Gauss-Seidel or Liebmann S.O.R. methods, usually appear to be the most suitable way to solve such simultaneous equations. On the other hand, according to

Fromm [Ref. 19], the smaller the value of the time-step, the more rapid the computation is. This is obvious since the speed of the computation process depends on the speed of the iterative cycles. The closer the first guesses, the faster the iterative cycle can be. Consequently, by halving the time-step, one can make the first guesses much closer and the number of steps required for convergence can be decreased by more than 50%.

Three implicit methods will be discussed below: the simple implicit, the Crank-Nicolson, and the alternating-direction implicit methods.

II.1 Simple Implicit (SI) Method

This is the most direct method in which the dependent variable at the time level n+1 can be expressed implicitly in terms of the values at the surrounding nodes at the same time level.

By applying this technique, in conjunction with Figure (3.-3), and by assuming $\Delta x = \Delta y = h$, equation (2.19) can take the form

$$(\theta_0^{n+1} - \theta_0^n)/\Delta\tau = \{\theta_1^{n+1} + \theta_2^{n+1} + \theta_3^{n+1} + \theta_4^{n+1} - 4\theta_0^{n+1}\}/Pr\ h^2$$
$$- \{(\theta_1^{n+1} - \theta_2^{n+1})(\psi_3^n - \psi_4^n)$$
$$- (\theta_3^{n+1} - \theta_4^{n+1})(\psi_1^n - \psi_2^n)\}/4h^2 \qquad (3.23)$$

This equation is unconditionally stable.

The main disadvantage of the SI method is the large number of iterations required for each time interval.

II.2 Crank-Nicolson Implicit Method

According to this method, equation (2.19) can be represented by the form

$$(\theta_0^{n+1} - \theta_0^n)/\Delta\tau = \{\theta_1^{n+1} + \theta_2^{n+1} + \theta_3^{n+1} + \theta_4^{n+1} - 4\theta_0^{n+1}\}/2Prh^2$$
$$+ \{\theta_1^n + \theta_2^n + \theta_3^n + \theta_4^n - 4\theta_0^n\}/2Prh^2$$
$$- \{(\theta_1^{n+1} - \theta_2^{n+1})(\psi_3^n - \psi_4^n) - (\theta_3^{n+1} - \theta_4^{n+1})(\psi_1^n - \psi_2^n)\}/8h^2$$
$$- \{(\theta_1^n - \theta_2^n)(\psi_3^n - \psi_4^n) - (\theta_3^n - \theta_4^n)(\psi_1^n - \psi_2^n)\}/8h^2 \qquad (3.24)$$

Expressions like (3.24) are unconditionally stable but require a large number of iterations for each time-step.

It should be emphasized here that the application of forms like (3.23) and (3.24) will be unconditionally stable regardless of the choice of the time-interval as a function of the grid size. So, condition (3.22) is not necessary to be applied. However, the restriction on the value of the time-interval in connection with the absolute values of the velocity components is still valid. This means that for the stability of the iterative process within any time-step, a condition like (3.21) should be satisfied.

II.3 Alternating-Direction Implicit (ADIP) Method

This method was introduced by Peaceman and Rachford [Ref. 41] in an attempt to solve elliptic and parabolic equations. Forsythe and Wasow [Ref. 16] discussed and analysed this technique in more detail.

The process is composed of two steps to pass from the time τ to the time $\tau + \Delta\tau$. During the first step, implicit differences are

used for the derivatives in direction x and explicit differences are used for the y-direction derivatives. For the second step, the reverse procedure is applied to each of the two directions.

For equation (2.19), the numerical ADIP form will be

$$(\theta_0^{n+\frac{1}{2}} - \theta_0^n)/(\Delta\tau/2) = (\theta_1^{n+\frac{1}{2}} - 2\theta_0^{n+\frac{1}{2}} + \theta_2^{n+\frac{1}{2}})/Pr(\Delta x)^2 + (\theta_3^n - 2\theta_0^n + \theta_4^n)/Pr(\Delta y)^2 - \{(\theta_1^{n+\frac{1}{2}} - \theta_2^{n+\frac{1}{2}})(\psi_3^n - \psi_4^n) - (\theta_3^n - \theta_4^n)(\psi_1^n - \psi_2^n)\}/4\Delta x\Delta y \qquad (3.25)$$

for the first step, followed by

$$(\theta_0^{n+1} - \theta_0^{n+\frac{1}{2}})/(\Delta\tau/2) = (\theta_1^{n+\frac{1}{2}} - 2\theta_0^{n+\frac{1}{2}} + \theta_2^{n+\frac{1}{2}})/Pr(\Delta x)^2 + (\theta_3^{n+1} - 2\theta_0^{n+1} + \theta_4^{n+1})/Pr(\Delta y)^2 - \{(\theta_1^{n+\frac{1}{2}} - \theta_2^{n+\frac{1}{2}})(\psi_3^n - \psi_4^n) - (\theta_3^{n+1} - \theta_4^{n+1})(\psi_1^n - \psi_2^n)\}/4\Delta x\Delta y \qquad (3.26)$$

for the second step.

The number of iterations required for each time interval is much less than that required for any other implicit method, but still somewhat larger than that required for any explicit technique [Ref. 18].

The ADIP method was applied by Wilkes and Churchill [Ref. 74] to solve the governing equations of free convection in a rectangular enclosure. The main disadvantage of this method was found to lie in the evaluation of the vorticity at the boundaries. The vorticity values at the boundary nodes were those calculated from the previous velocity fields. Hence, these values were always one time interval behind the rest of the values.

The ADIP method was applied by the author, with some modifications, to solve the present problem. The computation sequence was carried out in a manner such that the velocity field was updated at each iterative step within each time-interval. More details of this technique are given in Chapter 6.

CHAPTER 4

IMPROVED COMPUTATIONAL TECHNIQUES

By computational technique we mean the path to be followed while the numerical calculations are being carried out from one node to the next. A good technique of computation is that which produces the closest solution to the exact one in as few computational steps as possible.

Generally speaking, the computation process is carried out in two main steps. The first step usually deals with the computation of the dependent variables at interior nodes. This can be done by expressing the governing equations in numerical forms according to a specific numerical method. The second step concerns the evaluation of the dependent variables at the boundary nodes. For Dirichlet boundary conditions, the boundary values can be directly substituted. For Neumann or mixed boundary conditions, specific formulae should be derived and then used. Improper formulae may initiate irregularities and cause instability or even provoke divergence of the solution.

The most commonly used technique of computation is the "Ordinary Technique". Here, the procedure starts by point (1, 1) at $x = 0$ and $y = 0$ and the computations advance forward, in one node increment in both directions, to end at point (IN, JN) at $x = x_{max}$ and $y = y_{max}$ (see Figure 4 - 1). This procedure of computation is found to be very useful if the property being transported has a tendency towards a specific direction. Also, it allows flexibility in choosing

the origin for the numerical calculations. This choice is sometimes as important as the method itself. In fact, improper choice of the origin may distort the physical meaning of the results. The main disadvantage of the ordinary technique lies in its not being fast enough to compute symmetrical or homogeneously distributed fields.

The "Alternating-Direction"Technique" is another process for the computation procedure. In this technique, the procedure is carried out for one cycle from point (1, 1) to point (IN, JN) and the following cycle from point (IN, JN) to point (1, 1). This can be done by increasing and decreasing the indices i and j by unity for each cycle respectively. The alternating-direction technique is useful in expressing some numerical explicit forms to circumvent the instability problem in solving diffusion equations [Ref. 2].

4.1 Up-down Technique

This technique is improved and tried in the present work to be used for Laplacian and Poissonian fields. In such fields, Dirichlet boundary conditions, on one or more sides, present the main source of diffusion into the field of the property being considered; for instance, heat or mass transfer from a source of any shape to the surrounding fluid.

To clarify this idea, the problem of a flat plate located at $i = 1$ and $JL < j < JH$ (see Figure 4 - 1) will be considered. If the plate is isothermal and there is no fluid flow, equation (2.26) will be

$$\nabla^2\theta = 0 \tag{4.1}$$

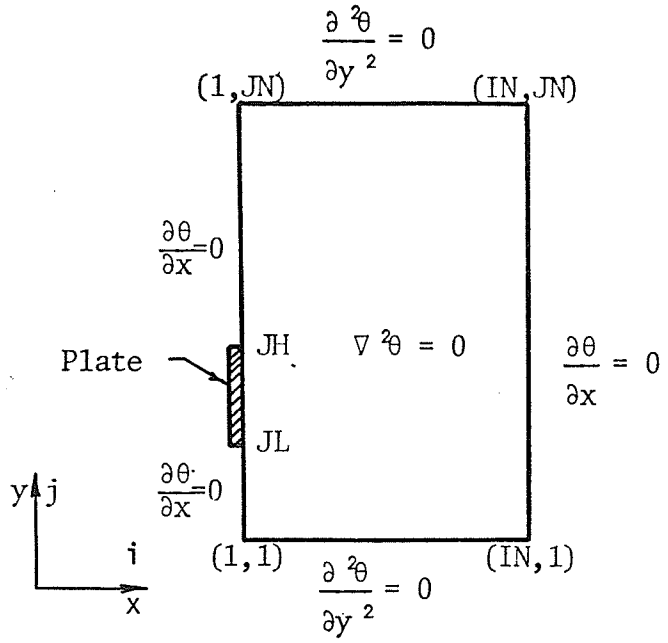

Figure (4 - 1) Co-ordinate system at boundary condition for Laplacian conduction field

Expression (4.1) presents the steady state Laplacian heat-conduction temperature field.

Applying the up-down technique, the finite-difference computation of such field is carried out by following two steps: The first step is embodied in the equation

$$\theta_{i,j} = (\theta_{i,j-1} + \theta_{i-1,j} + \theta_{i+1,j} + \theta_{i,j+1})/4.0 \qquad (4.2)$$

The computation process will start from point (1, 1) and end at point (IN, JN). The second step can then be carried out by using the equation

$$\theta_{i,j} = (\theta_{i,j+1} + \theta_{i-1,j} + \theta_{i,j-1} + \theta_{i+1,j})/4.0 \qquad (4.3)$$

and by marching from point (1,JN) to point (IN,1).

Algebraically, there is no difference between equations (4.2) and (4.3), but a remarkable difference exists if the sequence of computation is taken into account. As the field is being swept from point (1,1) to point (IN,JN) through equation (4.2), the plate acts as a

heat source and will diffuse, numerically, the heat into the region above the plate. If the procedure is to be continued in an ordinary computation technique, the region below the plate will be swept downwards row by row and, as a result, the convergence of the entire process will be very poor. Alternatively, by the use of the up-down technique, the field can be swept in the second cycle of computation from point (1,JN) to point (IN, 1) following equation (4.3) and the heat can be diffused faster into the region below the plate. By repeating this sequence of computation, the diffusion of heat over the entire field can be achieved quickly, to a reasonable approximation, in a few steps. For instance, if JL = 15, at least 14 steps are required to cover the region below the plate by acceptable values. On the other hand, using the up-down technique this can be achieved in two steps. Moreover, a reasonable solution can be obtained in these 14 steps.

Listing (C - 1) in Appendix C presents a programme for the up-down technique in conjunction with the S.O.R. method to solve for the Laplacian temperature field.

4.2 Temporary-Nodes (TN) Technique

Frequently, the user of the numerical techniques is urged to halve the grid size h or to double the mesh size to achieve certain accuracy. At the same time, he might be limited by the availability of large computer-storage or long computation time. For such circumstances, the TN technique of computation is highly recommended.

The essence of this approach lies in the way the pivotal points are distributed over the entire mesh. By this method, computer-storage saving can be gained by using dummy nodes for temporary computations.

The mesh nodes are divided into two sets of pivotal points; coded by Round and Cross nodes. Figure (4 - 2) shows a sample of these nodes in the proposed grid system.

Consider a mesh of size 21 x 31 for discussion. Here then, the round nodes will occupy 11 x 16 sites, the cross nodes will occupy 10 x 15 sites, and temporary nodes a, b, c, d, e and f will occupy

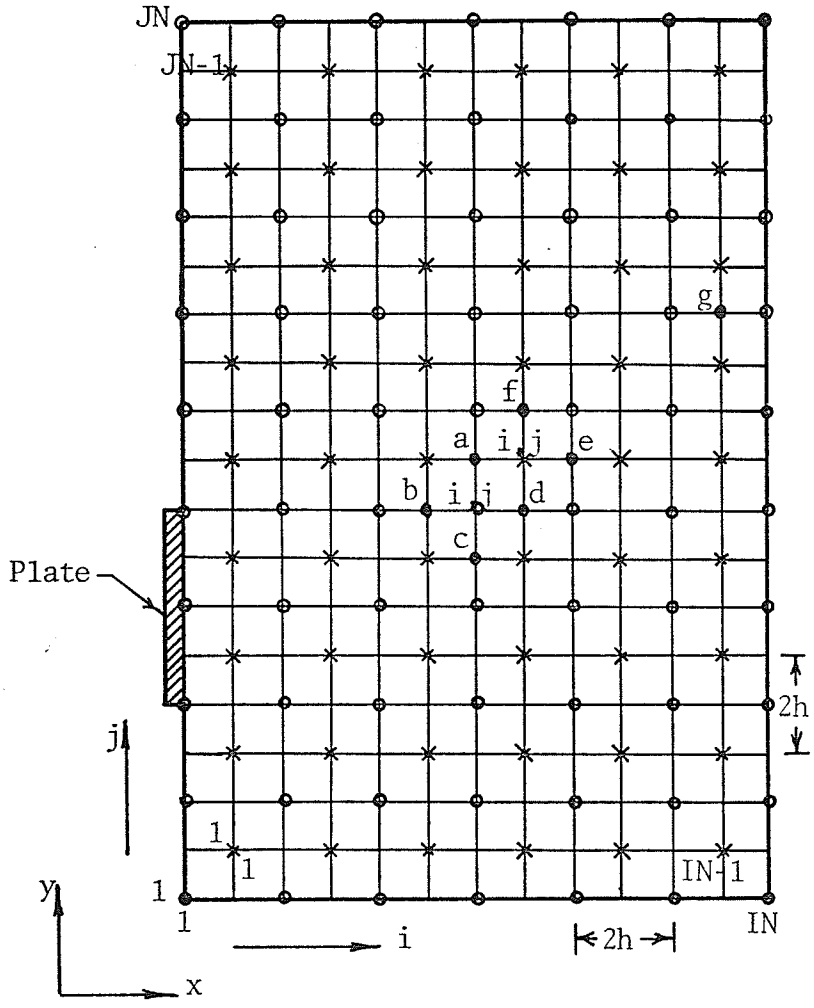

Figure (4 - 2) Round and Cross nodes in the Grid System of the TN Computation technique

the vacant sites in between. By this technique, 319 nodes out of 651 can be saved from the computer storage (49%).

Two procedures may be applied to carry out the computations. In the first, the computations may progress by keeping j constant and changing the column-index i. This technique is called horizontal sweeping. Vertical sweeping, on the other hand, can be carried out by keeping i constant and changing the index of rows j.

In these two techniques, the goal of the computational procedure is to evaluate simultaneously the dependent variables at each of the (i,j)'s cross and round nodes in the same computational step.

Generally speaking, the value of any dependent variable at a particular pivotal point can be computed by the use of the updated values of all dependent variables at the four surrounding nodes. This is true in all finite-difference formulae which have been derived in the present work. On this base, if the round and cross nodes, over the whole mesh, are initialized by suitable values, the temporary values of the dependent variables at the nodes a,b,c,d,e and f can easily be computed by applying the corresponding finite-difference formulae. These temporary values will not be stored until the computational cycle is terminated, but instead, they will be cancelled by the new temporary values which will be computed in the next computational step. That is why this technique does not need storage as large as that required for an ordinary grid system.

At this stage, the (i,j)'s round and cross nodes are surrounded by four updated computed values at the temporary nodes. Hence, by substituting these temporary values into the proper finite-difference formulae, the values of the dependent variables at the (i,j)'s round and cross pivotal points can be computed simultaneously in the same computational step. These updated values at the round and cross nodes have to be

stored for the subsequent computational cycle.

To proceed further, the computational process of the dependent variables can be advanced horizontally to the (i+1,j)'s round and cross nodes, or vertically to the (i,j+1)'s nodes. In either approach, as it was mentioned earlier, new associating temporary values have to be computed at new sites of the nodes a,b,c,d,e and f using the already computed updated values of the dependent variables at the (i,j)'s round and cross nodes.

At the end of any computational cycle, all values of the dependent variables at the interior round and cross nodes would be computed and stored, while the temporary values would be cancelled except the last six values for the last computational step.

For the nodes in the vicinity of the boundaries, the temporary values at the boundary-nodes can be substituted directly for Dirichlet boundary conditions, or they can be taken as an arithmetic average for Neumann boundary conditions. For other situations, formulae have to be derived.

For the boundary nodes (round nodes only), a temporary value has to be computed at a mid-way pivotal point, such as point g. This temporary value, in turn, is to be substituted into the corresponding finite-difference formula.

It should be mentioned here that the truncation error of a numerical approach depends mainly on the numerical formulation, and the round-off error depends on the total number of the computational steps. On the other hand, it can be said , from present computer experiments, that the stability of any computational

procedure mainly depends on the mesh and grid parameters as well as the type of equations to be solved. The grid system and computation technique influence both the convergence rate and the accuracy of the results.

For a TN technique, in conjunction with an iterative method, the truncation error depends on the order of approximation considered in the Taylor's expansion used and also on the grid size. The stability and convergence criteria are those corresponding to an ordinary grid system, i.e., for the steady state equations (2.25), (2.26) and (2.27), the following inequality should be satisfied [Ref. 33]

$$0 < hL\sqrt{u'^2 + v'^2}/\nu < 40 \tag{4.4}$$

By applying the TN technique, the accuracy can be improved by halving the grid size. This will require the same computer storage needed for an ordinary technique with doubled grid size.

This technique has two main advantages. Namely a reduction in computer memory by nearly one half can be achieved and, an appreciable shortening of the time required for computation is obtainable.

The main disadvantage of the TN technique is the complexity in the programming process.

Program-listing (C - 2), in Appendix C, presents the TN computation technique in conjunction with the DSSE method. This subroutine can be used to solve the steady state equations (2.25) to (2.27) with a value of Gr_k as high as 500.

CHAPTER 5

OTHER FACTORS INFLUENCING THE COMPUTATIONAL PROCEDURE

5.1 Boundary Conditions

It is vey important to define the physical and numerical meanings of the infinity-distance for boundary conditions. Physically, it means that the boundaries are far enough from the considered region that they do not interfere with the process. Numerically, it means that the boundary conditions which are applied should not significantly affect the solution or even force it to represent another physical situation.

For the case of the vertical flat plate considered in this work, improper representation of the infinity-distances may have an appreciable effect which might convert the problem to the case of free convection in a rectangular cavity. This situation was observed in some trials (see Chapter 6) using an infinity-distance of three to six times the plate-height. A distance of six to ten times the plate-height was found to adequately approximate the infinity-distance and to give satisfactory results.

On the other hand, the boundary conditions which are to be imposed on a numerical solution should be selected carefully. Inadequate assumption of one of the boundary conditions may cause divergence or produce solutions which are stable but do not conform to the physical problem.

In the present work, it was found that it is very difficult to apply the boundary conditions, which were used previously in experimental studies, to get the corresponding numerical solution. The reason for that will be discussed later in this chapter, in section 5.5.1.

Generally speaking, the boundary conditions have to satisfy two requirements; (a) They must have a real physical meaning; and (b) They must produce consistent results with previous theoretical or experimental work for the same case. Despite these two requirements, Elder [Ref. 15] introduced vorticity-boundary conditions which had no physical meaning, and Suriano and Yang [Ref. 65] proposed contradictory zero values for the vorticity and velocities on the boundaries at infinity.

In the present work, several boundary conditions were attempted. The result of these trials with some physical and numerical discussion will be given in Chapter 6.

The final results, presented in Chapter 7, were obtained by applying the following boundary conditions (see Figure (5 - 1)):

a) Isothermal Rigid Wall

This condition was applied on the plate-surface facing the control volume under consideration. The plate is assumed to be isothermal at a temperature , T_p , $(\theta_p = 1.0)$ for the steady state case. For the time-dependent solutions, the plate was assumed to be at the bulk temperature ,T_b ,$(\theta_b = 0)$ for $\tau < 0$. At $\tau = 0$, the plate-surface temperature was subjected to a step change from T_b to T_p and kept constant at T_p thereafter. Neither functional variation in the plate-surface temperature nor constant heat flux cases were tried.

Assuming no slip on the plate-surface and no flow into or out of that surface, it is obvious that $u = 0$ and $v = 0$. This implies that the plate-surface is a stream line of constant value $\psi = C$ and the normal gradient $\frac{\partial \psi}{\partial x} = 0$. The value of C was arbitrarily chosen as 0. These assumptions

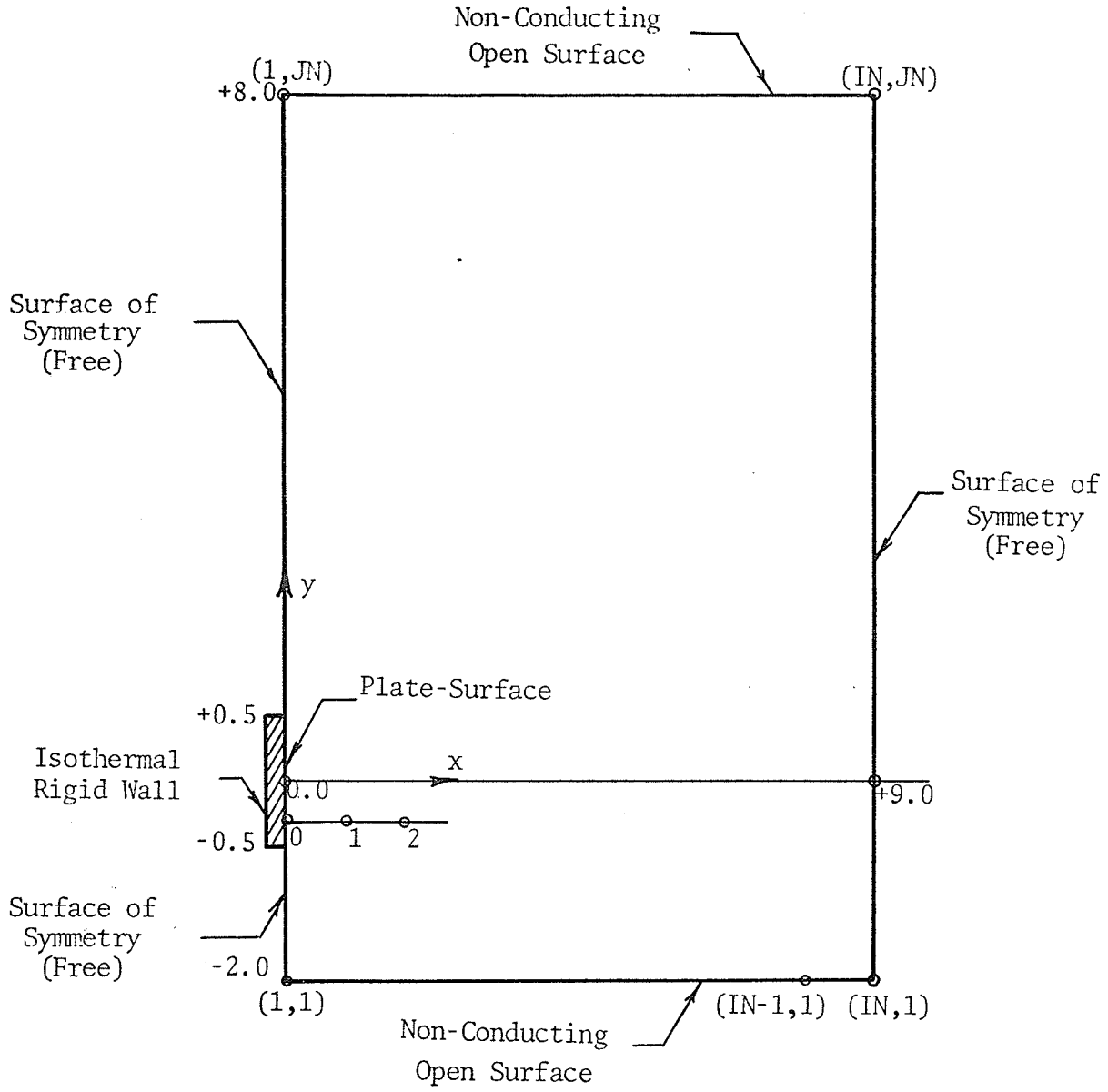

Fig. (5-1) : Co-ordinate System, Numerical Dimensions and Boundary Conditions

also verify the existence of eddies in the vicinity of the plate surface. The vorticity at a boundary node 0 can be computed by using the values of the stream-function and vorticity at the closest two pivotal points in the x-direction. The formula used is presented in detailed derivation in Appendix B. The use of the three-point one-sided derivative formula, to substitute for the first derivatives, produces equation (B.13) with a truncation error of the order (h^2). Since $\psi_0 = 0$, equation (B.13) can be simplified to be

$$\zeta_0 = (-4\psi_1 + \psi_2)/h^2 + (4\zeta_1 - \zeta_2)/3 \qquad (5.1)$$

b) Surface of Symmetry or Free Surface

This condition was applied to the boundaries at $x = 0$, $+0.5 < y \leq +8.0$ and $-2.0 \leq y < -0.5$; and at $x = +9$, $-2.0 \leq y \leq +8.0$. In this case, the velocity in the normal direction to the boundary, u, is assumed to be zero. Physically, this means that there is no fluid flow across the boundary which now presents a constant value streamline $\psi = C$. The value of C was arbitrarily chosen to be zero on the left side boundaries, and to take the computed value of ψ at the node (IN-1,1) for the right side boundary.

It was assumed also that there is no shear stress at such boundaries on the control-volume surface, i.e., $\partial v/\partial x = 0$. This, with the assumption that $u = 0$, implies that the vorticity will be zero according to equation (2.4).

The surfaces of symmetry were assumed to be adiabatic. The boundary condition which satisfies this requirement is $\partial\theta/\partial x = 0$. For the numerical solution, a three-point one-sided derivative formula is used to compute θ at the boundary nodes.

c) Non-Conducting Open-Surface

Two conditions for temperature and velocities were applied here

For temperature, there is no heat transfer by conduction in the y-direction, i.e., $\partial\theta/\partial y = 0$. Thus the heat is transferred only by the free convective flow. The finite-difference formula used to evaluate the temperature at the boundary nodes for such surfaces is presented in detail in Appendix B, Section B.5. Equations (B.17) and (B.18) present the forward and backward formulae to be applied for the lower and upper boundaries respectively.

For velocities, it was assumed that the horizontal velocity u vanishes, while the gradient of vertical velocity v, in the y-direction, is equal to zero. That means that the fluid is crossing the boundaries in a vertical direction with that velocity which has been achieved at the boundary due to the action of the buoyancy force.

As a result, the normal gradient of the stream-function vanishes, and the value of ψ at these boundaries can be computed by applying the three-point one-sided derivative formula. The vorticity, on the other hand, can be evaluated by using equation (2.4) for the non-dimensional case.

5.2 Initial Values

The choice of the initial values is a major factor which controls the speed, stability and accuracy of the numerical solution.

As a general approach, the initial values can be one of the following possibilities:

a) Zero or Constant Values

These can be supplied for all nodes except those of Dirichlet boundary conditions. For the present work, the zero-value assumption is

found to be very poor for convergence especially when the expected results are of high order of magnitude (10^4 - 10^6). The finite-difference approximate solution revealed instability for the steady state case regardless of the values of the relaxation factors. For the time-dependent solution, very low values for the time increment should be used for the first computational steps. Consequently, zero initial values were an improper choice to start with. However, great improvement is achieved by assuming very low uniform initial values for temperature, 3×10^{-4}, and keeping the initial values for the vorticity and stream-function as zeros. This is the technique by which the final results presented in Chapter 7 were obtained.

b) Arithmetically-Averaged Values

This means that the arithmetic average of the minimum and maximum values, stated by Dirichlet boundary conditions, can be used to initiate the entire nodes over the control volume.

This assumption may help in solving simple problems such as Laplacian or Poissonian fields. However, in the present complicated, non-linear case with three dependent variables, the arithmetic average assumption was found to distort the results at the regions far from the plate. Moreover, it provoked divergence and severe instability.

c) Linearly-Distributed Values

In this case, the initial values are linearly distributed over the control volume by using the Dirichlet boundary conditions, which might be specified in the problem, as minimum and maximum values.

For the two-dimension case considered in this thesis, the initial values were distributed linearly by columns and by rows in two

different attempts to achieve stability, but this technique did not help much. Better stable procedure could be achieved by using rectangular linear distribution but the results were not consistent with any previous experimental work.

d) Precomputed Results of a Simplified Similar Case

This is the most efficient and highly recommended technique to initialise a complicated problem. The computation procedure is started by obtaining a solution for a simplified form of the governing equations with the same boundary conditions as the main problem. This can be carried out using one of the previous initialising techniques. The resulting approximate solution is used thereafter as a first guess for the required case.

Another technique is to start with the same governing equation but for dependent variables of low order of magnitude. For instance, results of a process for Gr = 0(1.0) can be used to initialise a programme for Gr = 0(20.0). This, in turn, can be used to initialise a Gr = 0(100.0) programme, and so on.

These two techniques were applied in some trials described in Chapter 6. Some results were obtained, but they were not reasonable. The reason for this lies in the nature of the equations governing any free convection case. Since the momentum and heat transfer equations are interrelated, the principle of superposition could not be applied.

5.3 Exit Criterion

The choice of the exit criterion is very critical and important for any numerical procedure. By this criterion we mean the parameter by which the user of the numerical techniques can judge

the convergence and accuracy of the results. At the same time, the criterion can be used to stop the program when it reaches a specific value.

The frequently used criteria are the displacement vector, displacement norm and relative displacement norm.

The displacement vector $\underline{D}$ at the m^{th} step of computation is defined as the difference between two succesive values of $f_{i,j}$ produced by the m^{th} and the $(m - 1)^{th}$ steps. It can be expressed as

$$\underline{D}^{(m)} = \underline{f}^{(m)} - \underline{f}^{(m-1)} \tag{5.2}$$

The displacement norm $||D||$ can be defined as

$$||D|| = \sqrt{\sum_i D_i^2} \tag{5.3}$$

$$||D|| = \sum_i |D_i| \tag{5.4}$$

or

$$||D|| = |D_{i_{max}}| \tag{5.5}$$

Any of the forms (5.3), (5.4) and (5.5) can be used successfully for a preliminary check on the convergence rate. It is hoped that as the solution proceeds, $||D||$ value decreases to reach the terminating value. Form (5.5) is very useful to find the location of maximum error.

The relative displacement norm can be defined as

$$||\underline{D}||/||\underline{f}|| \tag{5.6}$$

$$||\underline{D}||/\text{number of mesh nodes} \tag{5.7}$$

or

$$(||\underline{D}||/||\underline{f}||)_m - (||\underline{D}||/||\underline{f}||)_{m-1} \tag{5.8}$$

where $||\underline{f}||$ is the dependent variable norm defined as $\sum_i |f_i|$, and f_i's are the updated values.

Form (5.6) is the most commonly used one. It gives a fairly good idea about the rate of convergence. The criterion will have a high value where the computation procedure is started by any kind of initializing process. As the procedure progresses, ||D|| will decrease. As a result the criterion will decrease until it reaches the terminating value. The smaller the value of the criterion at the terminating step, the closer the final numerical solution will be to the exact one.

Form (5.7) gives a very good measure of the convergence rate, but it cannot be used as an exit criterion especially if high accuracy is required.

Form (5.8) is very useful in checking the convergence of a time-dependent procedure. It is a very sensitive tool with high accuracy.

5.4 Relaxation Factor "ω"

The relaxation factor is sometimes called the "kicking factor" This name is based on the function of that factor. It kicks the numerical solution forwards or backwards to a better and more stable one by using over- or under-relaxation techniques respectively.

The over-relaxation process is usually applied in an attempt to improve the rate of convergence. Under such circumstances, the relaxation factor is found to be at its optimum value. Numerous formulae can be found for the estimation of that optimum value, but all of these deal with one equation in one dependent variable. As a general rule, estimated values give a good guess for ω_{opt} to start the solution with. Computer experiments carried out by Omar [Ref. 37] showed that the exact values of ω_{opt} always differed from the estimated ones by 5 to 15 percent. The reason for this lies in the apparent

difference between the idealized calculated estimates and the real values computed.

For more than one dependent variable, the analytical estimation of ω_{opt} is very difficult. It is much easier in such cases to carry out some computer experiments to find the value of ω_{opt}.

Under-relaxation is frequently used when the convergence features severe oscillation. For such cases, a value $0 < \omega_{opt} < 1$ will help as a damping factor.

For the case studied in this work, the analytical estimation of ω_{opt}, for the three dependent-variable equations, was out of the question. Alternatively, some computer experiments were carried out using values for ω's between 0.2 and 1.9. Two sets of three optimum relaxation factors for vorticity, stream function and temperature respectively have been achieved. They are (0.82, 1.83, and 1.67) and (0.82, 1.655 and 1.47).

5.5 Errors

5.5.1 Theoretical and Idealized Assumptions Error

In comparing experimental and theoretical works, the difficulties of duplicating in an experiment the idealized situation encountered in the numerical treatment should be considered. These difficulties can be summarized as follows [Ref. 14]:

a) The theoretical postulates state that the only motion in the fluid is that which results from the existence of the heated surface. In practice, convection currents (caused by outside effects or other parts of the apparatus) and other flow disturbances are extremely difficult to suppress entirely.

b) Despite the precision with which the heat input can be measured and controlled, some usually leaks by processes other than free convection. Conduction along support and leads and radiation may not be estimated accurately.

c) The "infinite volume of fluid at a uniform temperature" may in fact be a comparatively small bulk of fluid in a finite enclosure.

d) A finite flat plate must have edges, and their shape and size is not accounted for in the numerical treatments.

e) It is difficult to insure that the flow of fluid and heat are substantially two-dimensional.

5.5.2 Truncation Error

The truncation error is the major error in all numerical solutions and it is very important to be considered. This error is a result of ignoring higher order terms in the Taylor's expansion used to derive all finite-difference formulae. The value of this error depends mainly on the grid size h. It might be of the order of h, h^2 or h^3 according to the order of approximation.

The truncation error cannot be made vanishingly small by any computation technique, since the method itself is an approximate one. To get better approximations, higher order polynomials, or smaller grid sizes can be considered in deriving the numerical formulae. In these two cases, the required accuracy may be achieved but with more computation steps. On the other hand, these processes are limited in their applications because another error becomes important as the number of operations in the computation increases. This is the round-off error.

5.5.3 Round-off Error

Round-off error is mainly a computational error. It depends on the way in which the computer reads, stores and expresses numbers. Any number is rounded-off, leaving an approximate figure to be used in computation. The larger the number of computational steps, the larger the accumulation of the round-off error will be.

Generally speaking, the value of the round-off error is fairly small compared with the value of the truncation error. However, for huge numbers of computations, the loss in accuracy due to the accumulated round-off error may reach an appreciable value which balances the gain achieved by reducing the truncation error.

5.5.4 Computation-technique Error

This error can be controlled by the choice of the exit criterion, that is, how precise the final result should be. An exact solution can never be achieved numerically even for an infinite number of computations. This is obvious since the numerical formulae used have been already approximated and a truncation error always exists.

The computation-technique error is mainly influenced by the choice of the initial values. The closer the choice to the exact solution, the lower the value of the error. Also, this error depends on the number of computations and the programming technique in addition to the numerical technique used for computation.

5.6 Grid System

Different grid systems can be used for the computation procedure. The choice of any particular grid system mainly depends on the required accuracy, the geometry of the problem and the type of the numerical approach used.

The ordinary, equally-spaced grid system is the most commonly used one. In such systems, the grid size h can be as high as 0.2 and as low as the round-off error accumulation permits. Unequal grid-spacing in two directions can be applied. The ratio "k" between the two grid sizes can be as high as 4. Values over 4 may cause severe instability. This is due to the nature of the Taylor's expansion and the approximations involved in it. Functional spacing may be used to study a required region near the boundaries or study the entrance regions in heat transfer problems. Two or more regions with different grid sizes can be used when it is required to study a particular region with some emphasis. This approach is recommended to achieve high accuracy within this particular region and at the same time, prevent the accumulation of the round-off error over the entire control volume.

CHAPTER 6

RESULTS OF PRELIMINARY TRIALS OF COMPUTATIONAL TECHNIQUES

6.1 Steady-State Solutions

The Direct Substitution Simple Explicit (DSSE) method which was discussed in Chapter 3, Section 3.3.1, was used to solve for the steady-state case of the present work. The results which will be presented in this Chapter, Section 6.1.2, and in Chapter 7, had the same features of the convergence, accuracy and reliability discussed in detail in Appendix E. All the preliminary and final results for the steady-state and other cases, with their numerical conditions, are summarized in Table (6-1). Detailed discussion about each case will be done when it is necessary.

6.1.1 DSSE Method with Ordinary and TN Grid Systems (Closed-control - volume Boundary Conditions)

6.1.1.1 General Remarks and Observations

Equations (2.25), (2.26) and (2.27) were solved by the use of the Direct Substitution Simple Explicit (DSSE) method. The finite-difference forms were similar to expressions (3.13) and (3.14). The resulting set of simultaneous equations were solved by applying the Successive Over-Relaxation (S.O.R.) technique. The boundary conditions were those corresponding to an enclosed recirculating control volume. This means that the whole region was enclosed by a stream line of a constant value ($\psi = 0$). The lower and upper boundaries were treated as isothermal rigid walls in some trials, or as

TABLE (6-1): Summary of Preliminary and Final Results

Numerical technique	Numerical Parameters						Boundary conditions	Consistency with the present physical situation
	Grid system	Gr range	Pr range	Initial values	Mesh size	Grid size		
DSSE	Ordinary (Ord.)	1.0 to 100	0.72 to 12.8	Zero	21x31	0.2	E.C.V.*	No
				Previous results	30x53	0.2	E.C.V.	No
				Linearly distributed by columns or rectangles	30x50	0.1	E.C.V.	No
					31x81	0.1	E.C.V.	No
	Temporary-nodes (TN)	1.0 to 500	9.0 to 12.8	Zero	16x41 + 15x40	0.1	E.C.V.	No
				Previous (TN) results for Gr = 20	16x41 + 15x40	0.1	E.C.V.	No
				Previous (Ord.) results for Gr = 100	16x41 + 15x40	0.1	E.C.V.	No
	Ordinary (Ord.)	Constant value of 1.0	Constant value of 10.0	Very low values for temperature and zero values for ψ and ζ	91x101	0.1	O.C.V.**	Yes
				Pure conduction	91x101	0.1	O.C.V.	No
	Ordinary (Ord.)	Function of θ, -0.237 to 40.9	Constant value of 10.0	Very low value for temperature and zero value for ψ and ζ	91x101	0.1	O.C.V.	Yes
SE	Ordinary (Ord.)	1.0 to 0.4704×10^8	9.0 to 10.0	Zero	31x81	0.1, 0.051, and 0.025	E.C.V.	No
							O.C.V.	No
				Pure conduction	31x81	0.1	E.C.V.	No
ADIP	Ordinary (Ord.)	Constant value of 1.0	Constant value of 9.0	Zero	41x81	0.1	E.C.V.	No
				Zero	91x101	0.1	O.C.V.	No

* Enclosed Control Volume
** Open Control Volume

adiabatic free surfaces in others. At the right boundary, an isothermal rigid wall boundary condition was applied.*

Eighty-eight running trials were carried out by applying different initializing processes and by using different values of the relaxation factor, ω, with several mesh and grid sizes. Also, the effects of the sequence of computing the three dependent variables, and the procedure used for the computational process were studied. In addition, the effects of changing the Prandtl and Grashof numbers were investigated by computer. The following results were obtained:

a) By using an ordinary grid system, solutions were obtained for values of Gr up to 100. Values of Prandtl number of 0.72, 9.0, 10.0 and 12.8 were successfully attempted. The last value, 12.8, represents the average value of Prandtl number for water in the temperature range of interest (between $0^{o}C$ and $4^{o}C$). For Gr > 100, instability occurred in the vorticity computational cycle. Stable solutions were found to be achievable for such cases if previous results were used as initial values for any subsequent trial, with Grashof number increments of 5 or less.

b) Solutions for Grashof number up to 500 were obtained by using the DSSE method with a Temporary-Nodes (TN) grid system. The initial values used were either the results of a trial for Gr = 100, in which an ordinary grid system was used, or previous results for a low Grashof number trial in which the TN computational technique itself was used. A Grashof number increment of 25 to 50 for two successive runs could be used in the latter case.

---

* See Chapter 5, Section 5.1 for the physical meaning of the boundary conditions.

c) When zero initial values for all dependent variables were used, the convergence rate was found to be very slow. On the other hand, it was observed that the rate of convergence was appreciably improved by initializing the temperature field with values linearly distributed by columns from 1.0 to 0.0, or by using rectangular linear distribution for the stream-function in addition to column linear distribution for the temperature field. The vorticity was always initialized by zero values in all cases.

d) Different combinations of the relaxation factors were used with their values lying between 0.2 and 1.0. The following results were observed:

d-1) Under-relaxation was found to be more successful for the iterative solution of the vorticity equation. The higher order of magnitude of the source term in such equations with respect to other terms, necessitated the use of under-relaxation as a damping process. It was found that values between 0.6 and 0.9 could be used successfully as under-relaxation factors.

d-2) The stability of the ψ-equation was found to be dependent mainly on the stability of the ζ-equation. Over-relaxation was applied with values for the over-relaxation factor, ω, between 1.1 and 1.9. The choice of the ω-value for the ψ-equation depended on the choice of the value of ω used for the θ-equation. In fact, the value of ω used for the ψ-equation was found to be always higher than that used for θ-equation.

d-3) The convergence of the temperature equation was found to be absolutely stable unless the convergence of the ζ-equation was severely unstable. Over-relaxation was used successfully with ω-values ranging between 1.2 and 1.8. Under-relaxation of the θ-equation appeared to create instability in the convergence of the other dependent-variables equations.

e) Different mesh and grid sizes were used

21 x 31 with h = 0.2

30 x 53 with h = 0.2

30 x 50 with h = 0.1

31 x 81 with h = 0.1, and

16 x 41 + 15 x 40 with h = 0.1 for a TN computational technique.

As a general remark, it was found that the larger the mesh size, the better the boundary conditions at infinity were represented.

f) The best sequence of computation of the three dependent variables was found to be $\theta \rightarrow \zeta \rightarrow \psi$. This was depended on the nature of the dependent-variables equations. They were interrelated in such a way that the resulting updated numerical values of any variable had to be used as soon as they became available (See equations (2.25) and (2.27)). Alternative sequences were used, such as $\psi \rightarrow \theta \rightarrow \zeta$ and $\zeta \rightarrow \psi \rightarrow \theta$, but the rates of convergence in both cases were found to be slower.

6.1.1.2 Results and Plots

Of all the preliminary trials which have been carried out in the present work, two particular ones are discussed here. In spite of the fact that they were not representing the physical situation considered in the present work, yet they gave a good idea about the difficulties in imposing improper boundary conditions and using inadequate distances for the boundary conditions at infinity.

In the first trial, the steady state equations (2.25) to (2.27) were solved by using the DSSE method with an ordinary grid system. The mesh size used was 30 x 50 with h = 0.1. The plate was located at a

distance of 1.7 times the plate height away from the lower boundary. The enclosed-control-volume boundary conditions were applied and over-relaxation was used with ω-values of 0.9, 0.9 and 1.6 for ζ-, ψ-, and θ-equations respectively. The sequence of computing the dependent variables was $\theta \rightarrow \zeta \rightarrow \psi$. A constant value of 100 was assigned for the Grashof number and the Prandtl number was chosen to have a constant value of 9.0. Using previous results of a Gr = 20 run, as initial values, the computational process converged after 64 iterative steps with relative displacement norms less than 1% for all dependent variables.

In the second trial, the DSSE technique was used with a TN grid system. The mesh size was 31 x 81 (16 x 41 + 15 x 40) with h = 0.1. The same values for the relaxation factors and the same sequence of computation were used. The plate was located a distance of 3.2 times the plate-height from the lower boundary.

Typical stream lines produced by the DSSE method with a TN grid technique are shown in Figure (6-1). The value of the Grashof number was kept constant at 100, and β was assumed to be constant and positive. As a result, the convective flow near the plate was fully upward.

From Figure (6-1), the effect of the enclosing boundary conditions is noticeable. No flow is allowed to cross the constant $\psi = 0$ boundaries, and the recirculating stream-line pattern results.

The flow approaching the plate at low velocities is accelerated by the convective heat transferred in the plate-region. In this region, the horizontal component of velocity almost vanishes while the vertical component of velocity reaches its maximum value. At the upper boundary,

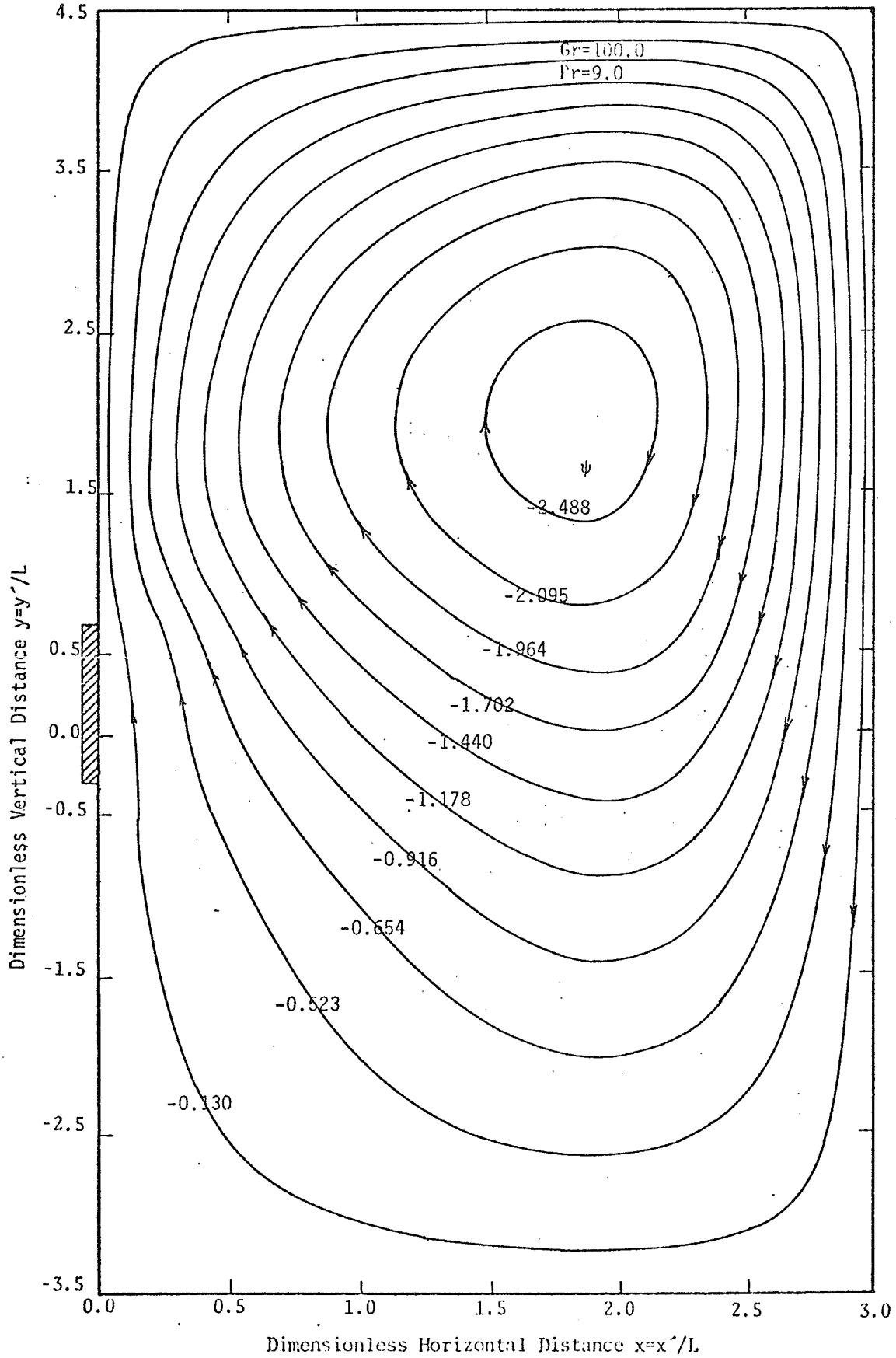

Fig (6-1) : Typical Stream Lines Produced by DSSE Method with a TN Grid System for Gr=100 and Pr=9.0 .

the fluid is forced to flow horizontally and the vertical component of velocity vanishes. The stream-line loops are closed by downward vertical flow at high speed near the right boundary at x = 3.0, and almost horizontal flow at the y = -2 boundary. The stream-line loops have been observed by Suriano and Yang [Ref. 65] for the vertical flat plate and all other work done for free convection in a rectangular enclosure [e.g., see Refs. 8, 20, 30, 34].

Typical vertical velocity profiles, produced by applying the DSSE method with ordinary and TN grid systems are shown in Figure (6-2). The velocity at the plate is zero (no-slip assumption). As the distance x increases, the velocity increases until it reaches its maximum value, then decreases passing the zero value to reach its maximum negative value and then increases again to a prescribed zero value at the x = 3.0 boundary. The positive and negative values of velocity correspond to the upward and downward directions respectively.

Figure (6-2), like Figure (6-1), shows the effects of the improper choice of the boundary conditions and the inaccurate presentation of the infinity-distances on the numerical solutions. By comparing each of these two stream-line loops with those for a rectangular cavity obtained by De Vahl Davis [Ref. 8, Figs. 2 and 7], it can be seen that the application of these improper conditions distorted the solution to that which corresponds to the case of free convection in a rectangular enclosure.

The constant-vorticity lines, shown in Figure (6-3) illustrate the reason for the instability which characterizes the numerical approach used to solve the vorticity equation, when improper boundary conditions

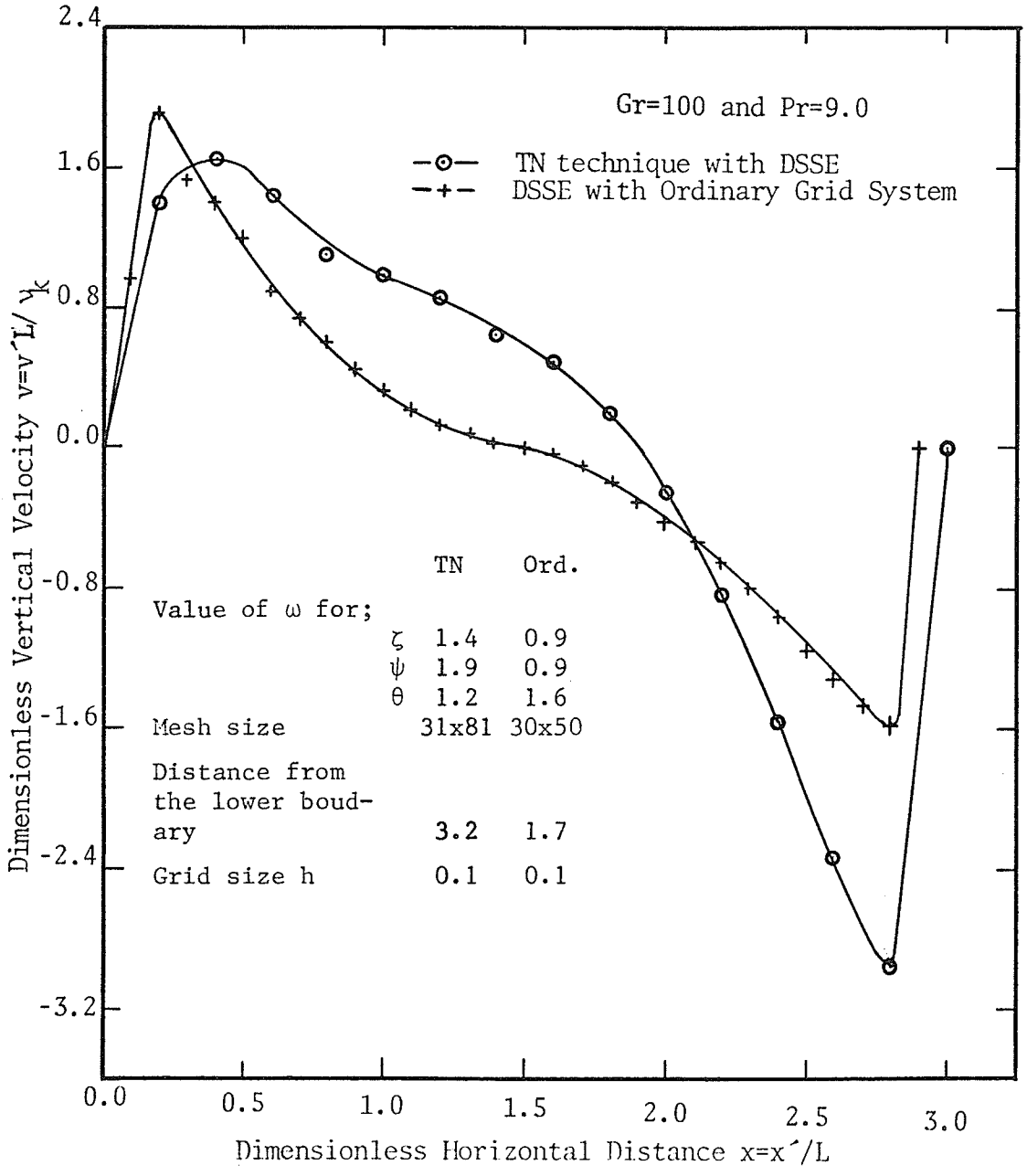

Fig. (6-2) : Vertical Velocity Profiles for Gr=100 and Pr=9.0 at y=0.0 .

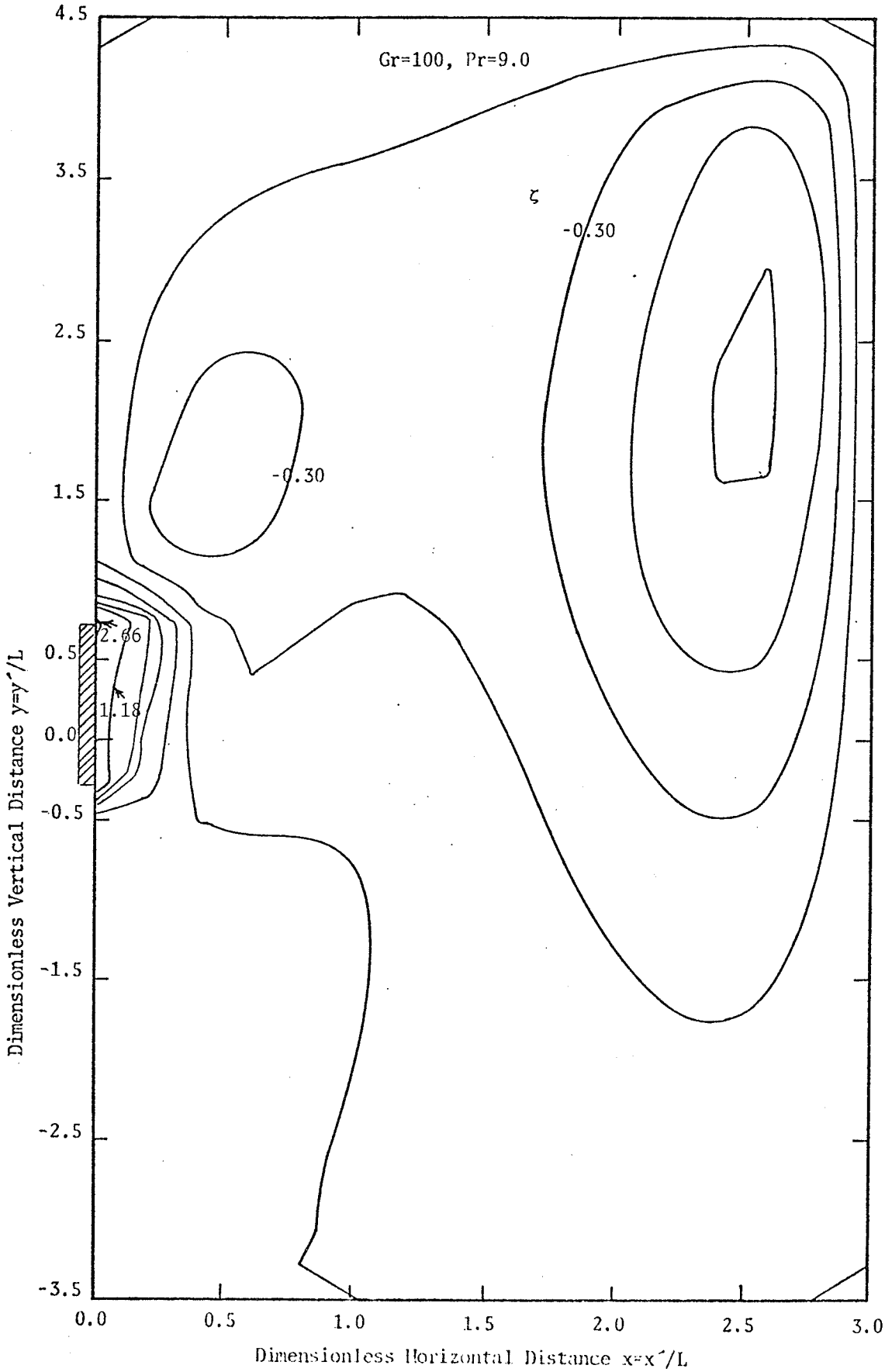

Fig (6-3) : Typical Constant-Vorticity Lines Produced by DSSE Method with a TN Griding System for Gr=100 and Pr=9.0 .

are applied. Very strong, positive, small eddies are generated adjacent to the plate while the bulk region is covered by large, weak, negative eddies. Very strong but small positive eddies are observed at the plate edges. In this particular case, they have appreciable influence on the entire field, since the mesh size is not large enough. In the trial which will be discussed in Section 6.2, open boundary conditions were used to eliminate the flow-recirculation and the eddies generated at the infinity boundaries.

The isotherms shown in Figure (6-4) have the same shape as those obtained by Suriano and Yang [Ref. 65] for Ra = 50. At the upper boundary, the boundary conditions compel the high-temperature fluid to flow downward near the right boundary. This behaviour can be clearly noticed in the y = 0 temperature-profile shown in Figure (6-5). Close to the plate, the temperature gradients are in fairly good agreement with those of the boundary layer solution obtained by Ostrach [Ref. 38] for Gr = 100 and Pr = 10. Far from the plate, the recirculated fluid at high temperature appeared to distort the profile causing a positive temperature gradient starting at x = 0.8. Close to the right boundary, the temperature starts to decrease again to reach the prescribed value of zero at the boundary itself.

The computed average Nusselt numbers* are 3.0317 and 4.2057 for ordinary and TN grid systems respectively, with the associated numerical parameters for each. Based on a formula stated for the boundary-layer similarity solution of Ostrach, and derived by Gebhart [Ref. 21, p. 336],

---

* Derivation and formulation of the $\overline{Nu}$ expression may be found in Appendix B.

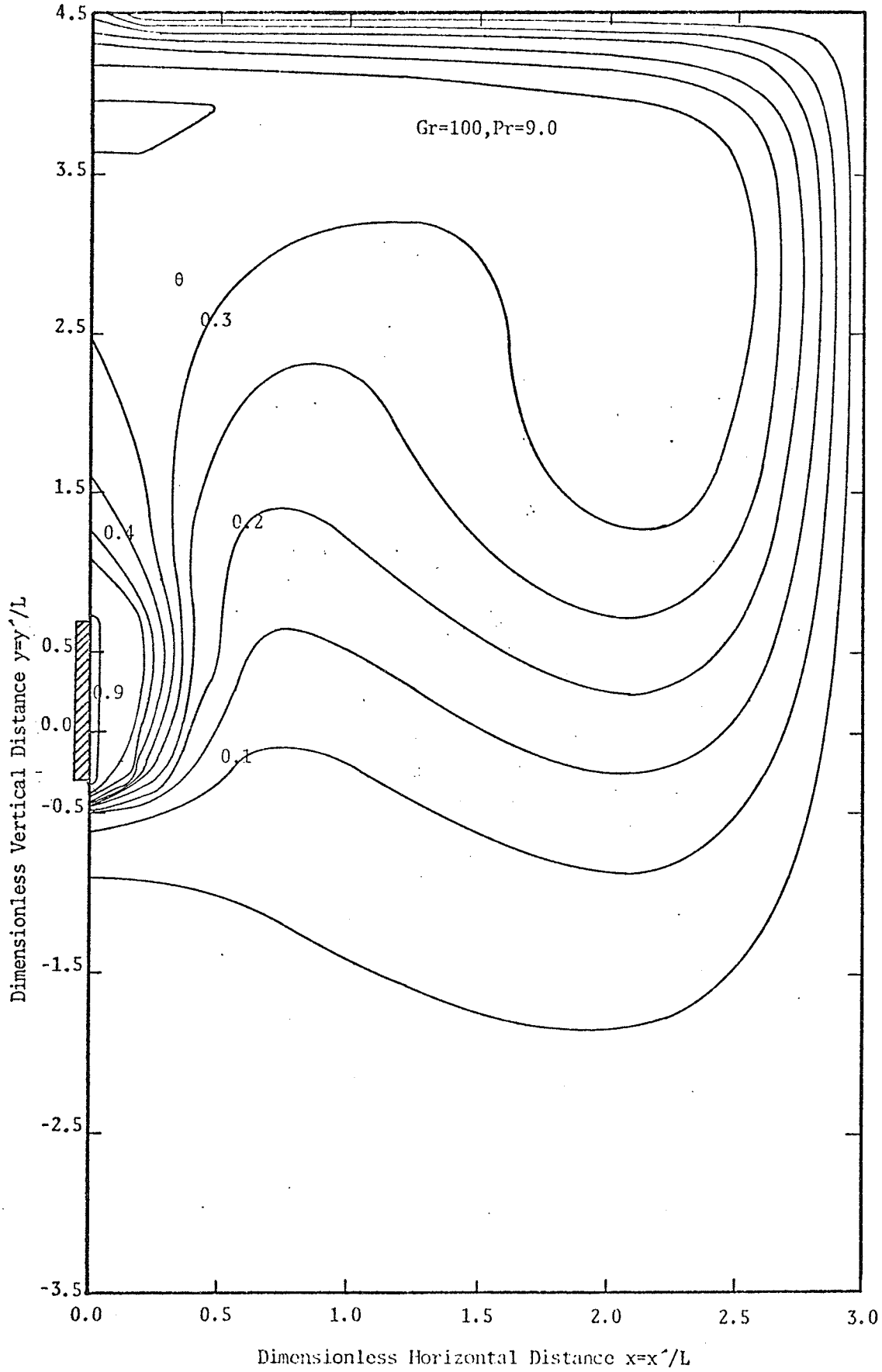

Fig (6-4) : Typical Isotherms Produced by DSSE Method with a TN Griding System for Gr=100 and Pr=9.0 .

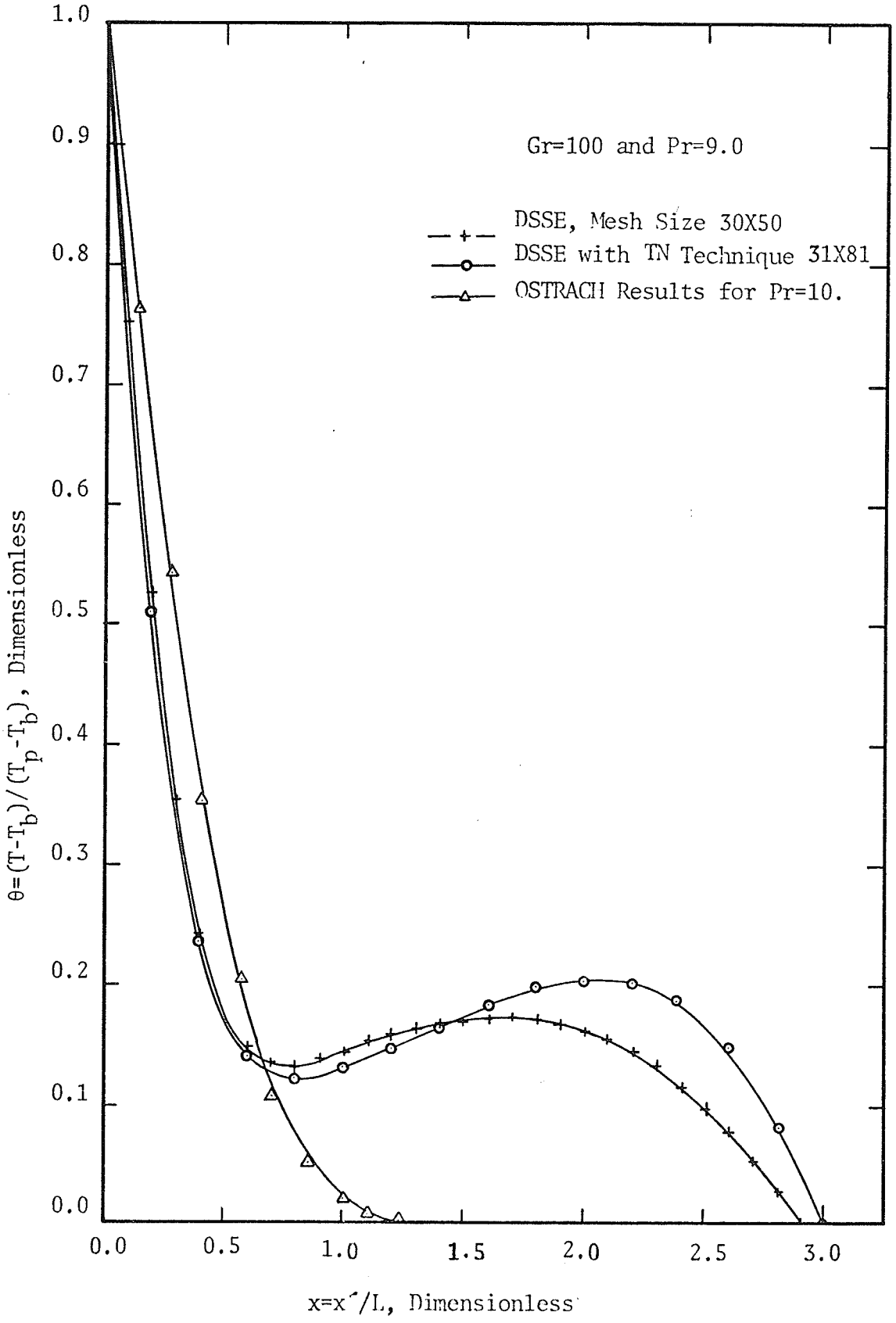

Fig (6-5) : Dimensionless Temperature Profiles for Gr=100 and Pr=9.0 .

the calculated value of $\overline{Nu}$ is 3.4827. By comparing the present results with this boundary-layer calculated value, it can be seen that the present values have maximum deviation of 20.7%.

6.1.2 DSSE Method with Ordinary Grid System (Open-Control-Volume Boundary Conditions)

The open boundary conditions have been stated by equations (2.21-b) and (2.21-c), and have been presented in Section 5.1. Under such conditions, the fluid was supposed to flow vertically at the lower and the upper boundaries. As a result, the stream lines would be normal to these boundaries. The right boundary was treated as a free surface. The other boundaries have been treated as described in the previous trial which has been studied in Section 6.1.1. These boundary conditions were applied for a mesh size of 91 x 101 with h = 0.1 to solve the steady-state equations (2.25) to (2.27). An over-relaxation technique was used with ω-values of 0.82, 1.83 and 1.67 for ζ-, ψ-, and θ-equations respectively. The Grashof number was maintained constant at a value of 1.0 and β was assumed negative. The Prandtl number was fixed at 10.0.

For an isothermal vertical flat plate located at a dimensionless distance of 2.0 from the lower boundary, typical stream lines are presented in Figure (6-6) for Gr = 1.0. It is very noticeable from this figure that the recirculation is reduced and the fluid is flowing vertically into and out from the control volume at the lower and the upper boundaries. Also, it can be noticed from the constant-vorticity lines shown in Figure (6-7) that the vorticity at the outer boundaries is completely eliminated. The only

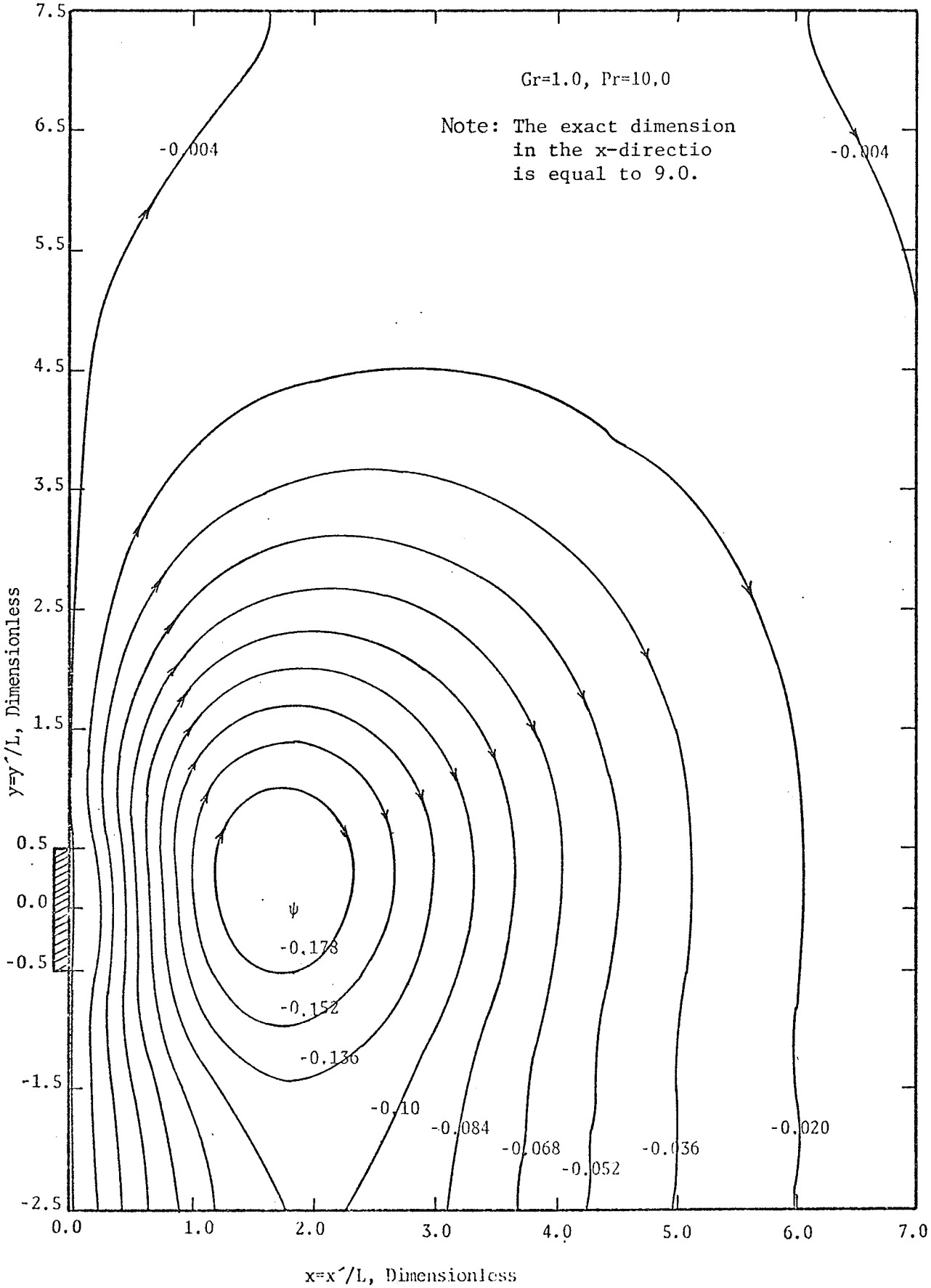

Fig (6-6) : Typical Stream Lines for Open Boundary Conditions Gr=1.0 and Pr=10.0 .

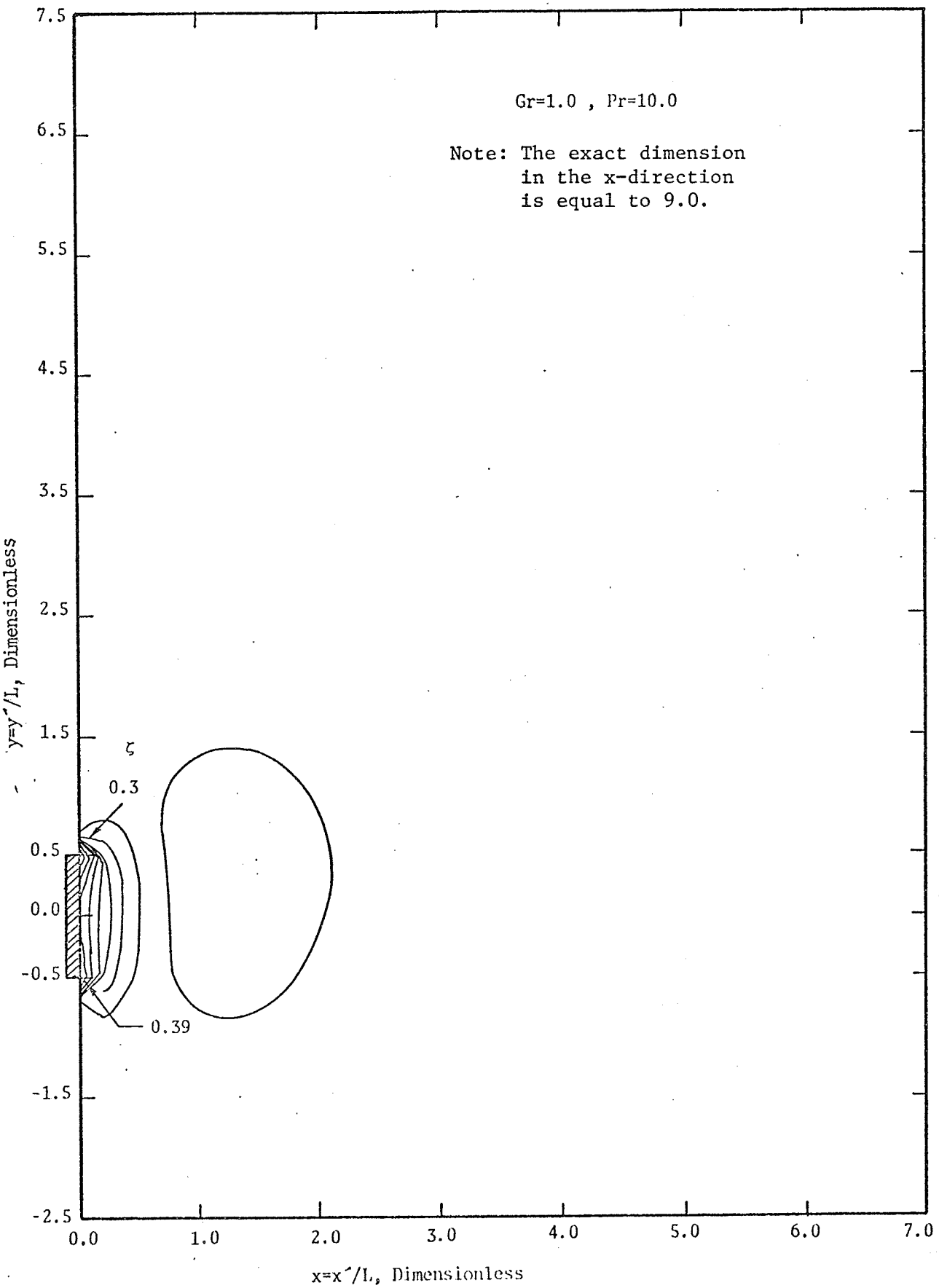

Fig (6-7) : Typical Constant-Vorticity Lines for Open Boundary Conditions . Gr=1.0 and Pr=10.0 .

remaining ones are; two at the plate-edges, a large one adjacent to the plate and a compensating core-eddy in the bulk of the fluid.

The velocity profile at y = 0.0 is shown in Figure (6-8). A very smooth curve results with a maximum value of 0.1704 at x = 0.5 and a minimum value of -0.05111 at x = 2.8. The results of Suriano and Yang [Ref. 65] for Gr = 1.0 and Pr = 10.0 are also presented. A complete and comprehensive comparison is not available since exact numerical values are not presented in Suriano and Yang's report. However, the difference between the influence of the open boundary conditions, suggested in the present work, and the closed zero-vorticity boundary conditions, imposed by Suriano and Yang on the behaviour of the solution is very obvious.

By an examination of the isotherms shown in Figure (6-9), it can be seen that the effect of the convective flow is not strong, since the value of Grashof number is low (Gr = 1.0). The resulting temperature profile at y = 0.0 shown in Figure (6-10) is in good agreement with that obtained by Suriano and Yang [Ref. 65] for the same value of Grashof and Prandtl numbers.

The computed average Nusselt numbers are plotted against the number of iterations in Figure (6-11). In the very first iterative steps, high values of $\overline{Nu}$ are obtained. As the number is increased, the value of $\overline{Nu}$ decreased rapidly until it reached an asymptotic value of 1.189 at the 104^{th} iterative step. This value conformed to the corresponding value of 1.107 computed by Suriano and Yang, with a relative error of 2.355%.

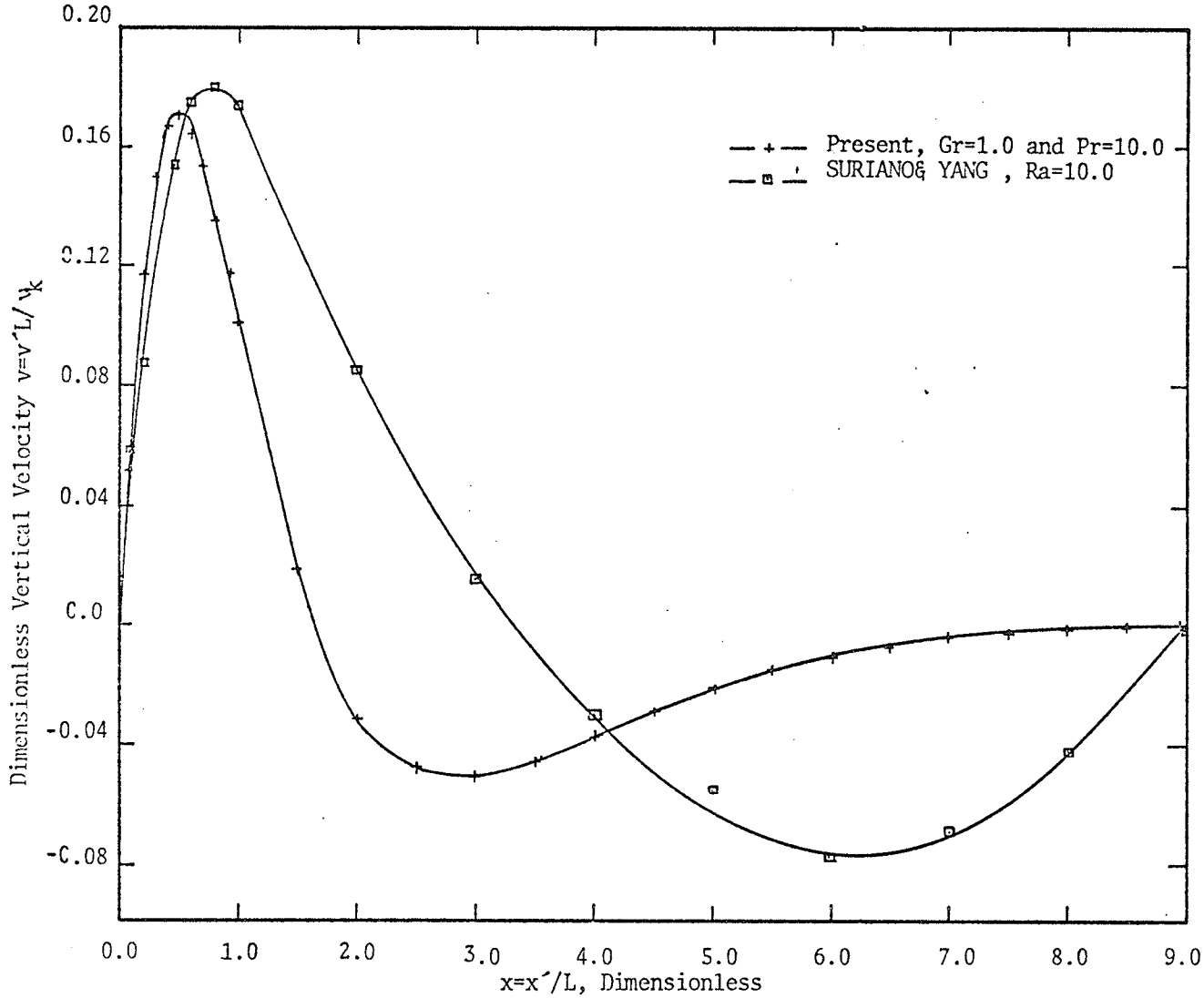

Fig (6-8) : Vertical Velocity Profile for Open Boundary Conditions

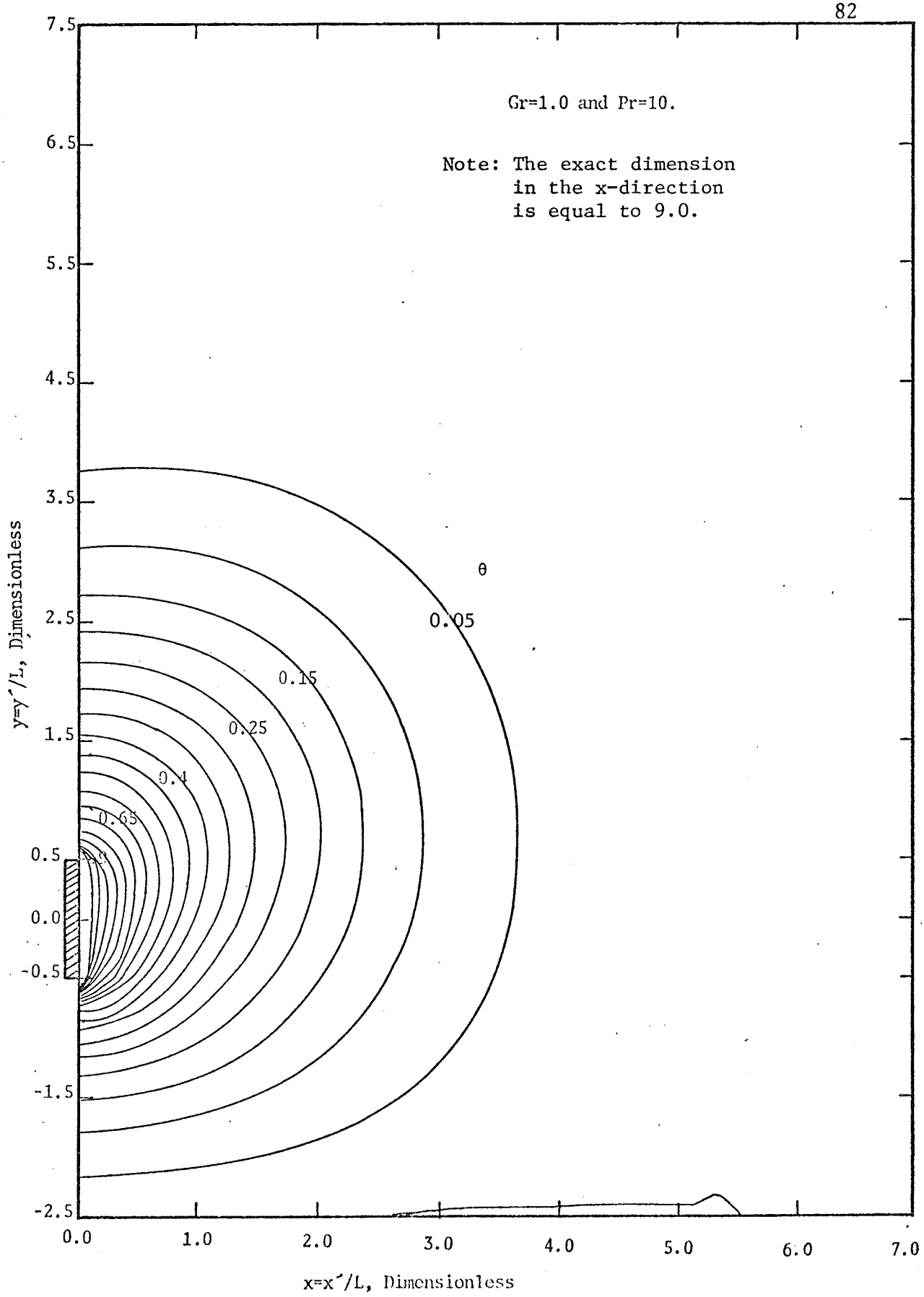

Fig (6-9) : Typical Isotherms for Open Boundary Conditions
Gr=1.0 and Pr=10.0 .

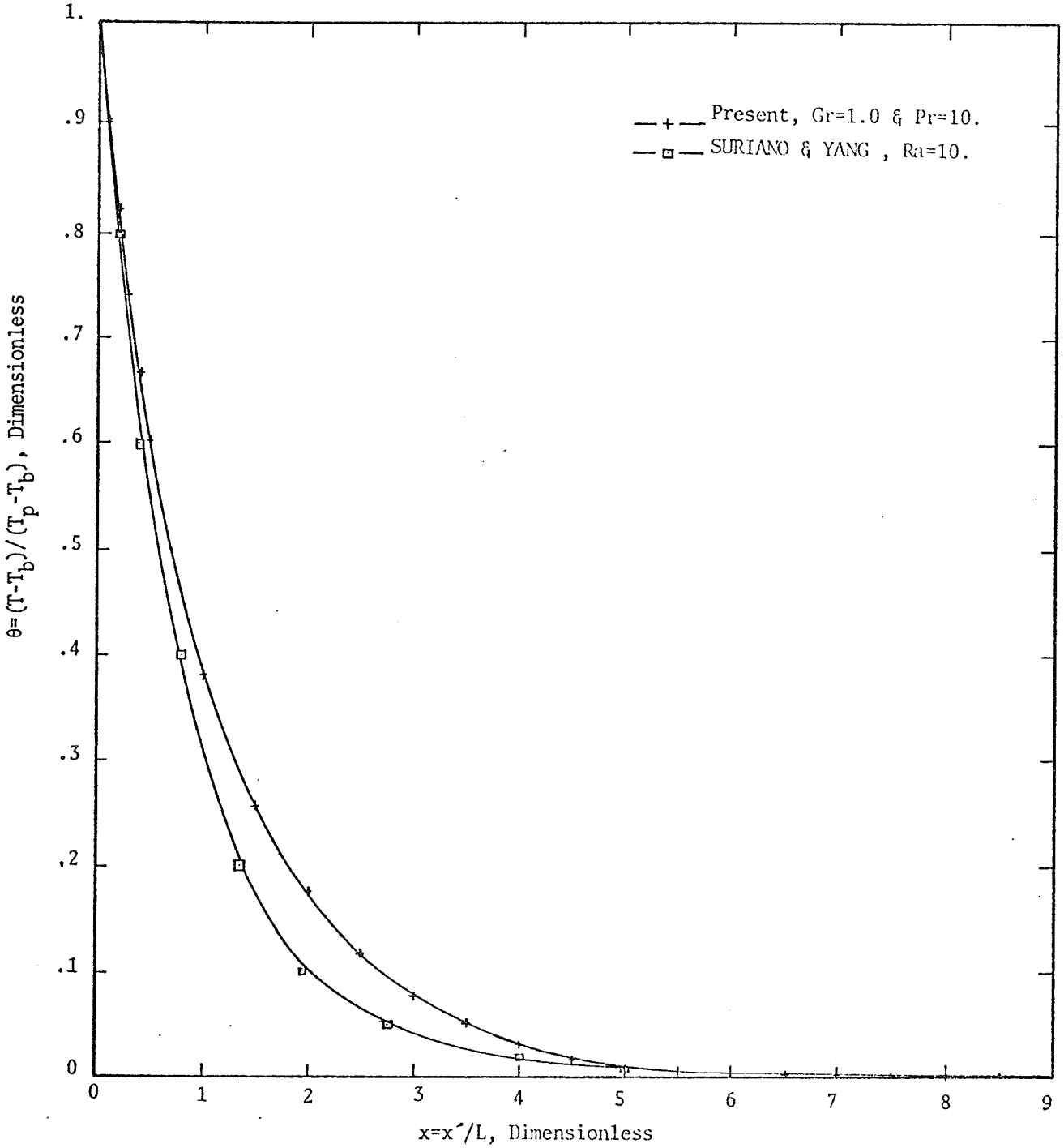

Fig (6-10) : Temperature Profile for Open Boundary Conditions at y=0 .

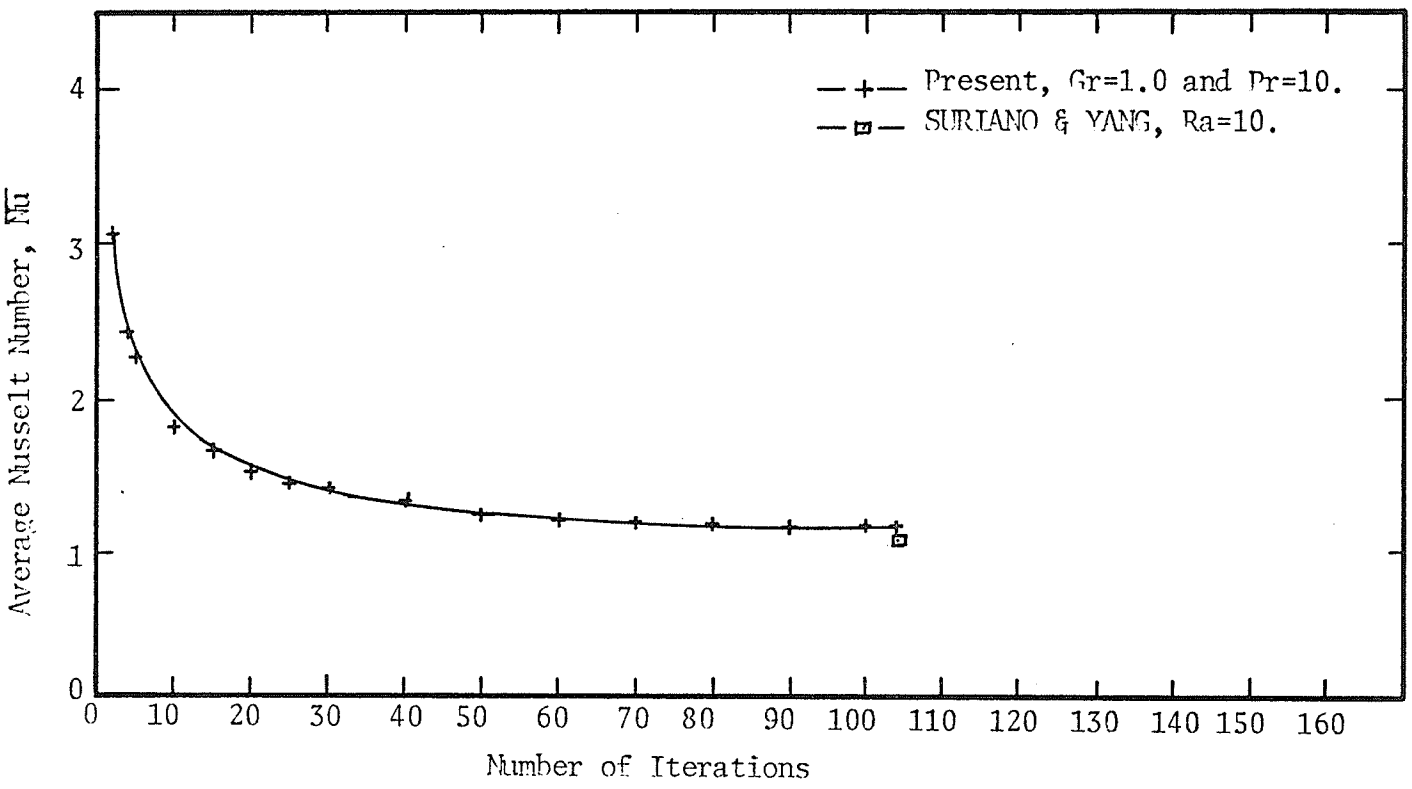

Fig. (6-11) : Variation of Nusselt Number with the number of iterations.

6.2 Time-Dependent Solutions

6.2.1 SE Method with an Ordinary Grid System

Equations (2.18) to (2.20) were solved numerically by the use of the Simple Explicit (SE) finite-difference method. Fifty-three running trials were carried out with the following variety of parameters:

a) Meshes with one or several regions were attempted, including

Equi-spaced 31 x 81 mesh with h = 0.1,

Double-spaced (k=2) two-region 31 x 81 mesh with h_x = 0.05 and 0.1,

Double-spaced (k=2) three-region 31 x 81 mesh with h_x = 0.025, 0.05 and 0.1, and

Quadruple-spaced (k=4) two-region and double-spaced single-region 31 x 81 mesh with h_x = 0.025, 0.05 and 0.1 respectively.

From these trials, it was found that the higher the number of fine regions, the more stable the solution would be.

b) Time-increment values between 10^{-7} and 0.2377×10^{-3} were tried. These were estimated to satisfy condition (3.17) which is necessary for the convergence and the stability of the procedure. The plate height was varied between 0.1 and 23.64 cm.. The corresponding values of Grashof number for $T_p = 15^oC$ and $T_b = 9^oC$ were between 1.0 and 0.4×10^8.

c) Many different boundary conditions were attempted. The enclosed control volume boundary conditions gave successful results up to $Gr = 1.632 \times 10^7$. The main disadvantage of this approach was the distortion of the results in such a way that they no longer represented the physical situation considered in the present work. The assumption of open-control-volume boundary

conditions, with zero initial values, was found to work well for the present case. The main drawback was the appearance of negative values in the temperature field when the computations were carried out for high values of Gr (10^3 - 10^7), no matter how low the values of time-increment were. This was found to be due to the high speed of the rate of convergence of the ψ-equation. In all the trials that were carried out here, the S.O.R. technique was used to compute the ψ-value at any pivotal point by direct and simple substitution in the corresponding finite-difference formula. This approach was found to be inadequate. The reason for that lies in the high velocity "concentration" which has been observed in the vicinity of the plate. This concentration, in turn, created negative values for temperatures at the nodes right in front of the plate-nodes.

No final results were obtained because of the very long computer-time required to carry out the computations. As a conclusion of these trials, it was found that the finite-difference formulation of the ψ-equation has to be modified to include the effect of the time-increment $\Delta\tau$, since the direct substitution of the value of ζ, which involves this effect, did not help to eliminate the velocity concentration near the plate.

6.2.2 ADIP Method with an Ordinary Grid System

The Alternating-Direction Implicit (ADIP) method used by Wilkes and Churchill [Ref. 74] to solve the momentum and heat transfer equations governing free convection from a vertical flat plate has been modified here by updating the ζ boundary-values instantaneously at each iterative step.

The sequence of computation of the modified method was started by solving the temperature equation for the complete computational cycle carried out for a time period between n and $n+\frac{1}{2}$. By using these updated temperature values, the vorticity could be directly calculated for the first iterative step, of the same computational cycle for the same time period by applying its finite-difference formula. The computations were performed thereafter in the same iterative step for the stream-function and velocities fields followed by the evaluation of the dependent variables at the boundary nodes. In any subsequent iterative step, this computational sequence was repeated until the first time-period cycle was completed. Through this technique, the updating procedure of the values of ζ, ψ and the velocities was carried out step by step to achieve the final updated values at the end of the first time-period cycle. For the second time-period cycle, from $n+\frac{1}{2}$ to $n+1$, the same procedure is repeated to yield updated values for one complete time-increment cycle.

Twelve trials were carried out in an attempt to circumvent the instability problem by using the modified sequence. Some stable steps of computation were achieved. No final results were obtained since the procedure needed a large number of computational steps. However, the modified sequence appeared to be a promising technique.

A computer subroutine-listing for the modified sequence is presented in Appendix C.

CHAPTER 7

FREE CONVECTION TO WATER NEAR 4°C

7.1 Introduction

In all trials which were presented in Chapter 6, the volumetric thermal expansion coefficient, β^*, was assumed to be constant over the temperature range of interest. This is why an average value for β was used. This approach appeared to be reasonable for most fluids which possess monotonic temperature-density relationship.

For a fluid with a non-monotonic density variation, β is not constant and, furthermore, it might change its sign in the temperature range of interest. This is the situation which occurs in bismuth, water, antimony and gallium. In such cases, the density-temperature relationship exhibits unusual behaviour. Starting from the freezing point, the density increases as the temperature increases and, accordingly, β will have a negative sign. This behaviour is continued on up to a particular temperature at which the density reaches a maximum value and β will be zero. Passing this maximum and critical point, the density starts to decrease with the increase of temperature and, consequently, β will have a positive sign.

The effect of this unusual behaviour of the density in its relation with temperature has been studied by Schechter [Ref. 51] and Schechter and Isbin [Ref. 52] for the case of free convection heat transfer from a vertical flat plate to water. Their numerical solution

---

* Defined by equation (A.2)

was obtained by introducing the similarity assumptions into the boundary layer equations governing the case. Their experimental measurements and observations of the uni-directional and bi-directional convective flow were in good agreement with their theoretical results.

Vanier and Tien [Ref.70] studied the effect of the maximum density on free convection heat transfer from a vertical flat plate to water near $4^{o}C$. They solved the boundary layer equations numerically by forward integration. They predicted numerous convective-flow regions covering a wide range of the plate and bulk temperatures.

In 1972, Yuill [Refs.77,78] studied the effects of the variation of the viscosity and the density, as functions of the temperature, on the free-convection heat transfer from a vertical isothermal flat plate to water near $4^{o}C$. The boundary layer equations were solved numerically by introducing the similarity assumptions. A correlation was developed and presented for the local Nusselt number as a function of the local Grashof and Prandtl numbers. This correlation includes a factor whose value is dependent on the temperatures of the plate and the bulk fluid.

7.2 Physical Description of the Phenomenon

The physical phenomenon can be described by considering free convection heat transfer from an isothermal vertical flat plate into water at $0^{o}C$. When the plate temperature is between $0^{o}C$ and $8^{o}C$ the layer of water adjacent to the plate becomes denser than the bulk of the fluid. As a result it sinks down. For a plate temperature slightly over $8^{o}C$, the inner layer adjacent to the plate becomes lighter than the bulk fluid, but it continues to flow downward. This is because the

buoyancy force generated in this inner layer is not strong enough to overcome the viscous force exerted on it by the outer layer, which is denser than the bulk fluid and thus moves downward. When the buoyancy force of this inner layer becomes high enough to compensate for the downward viscous force, a zero vertical velocity gradient at the plate surface occurs. In this particular situation, heat is transferred from the plate into the water by conduction through the stagnant surface-film. At a particular temperature, depending on the fluid under consideration, the inner layer becomes light enough to move upward and as the plate temperature increases, the upward convective flow in this layer becomes stronger and its thickness will increase. This behaviour continues on until the plate temperature reaches another particular value after which the flow becomes a fully upward uni-directional one.

7.3 Present Results and Plots

The effect of the unusual variation of the density of water with the temperature was studied for the case of free convection heat transfer from an isothermal vertical flat plate to a bulk of water near $4^{o}C$.

The steady state governing equations, (2.25) to (2.27), were solved by using the Direct Substitution Simple Explicit (DSSE) technique with an ordinary grid system. Thirty-one running trials have been carried out using a mesh size of 91 x 101 with h = 0.1. The plate-height was 0.1 cm., and the plate itself was located at a dimensionless distance of 2.0 away from the lower boundary. Open boundary conditions similar to those used in Section 6.1.2 were applied. Fully upward and downward uni-directional flows were observed in the vicinity of the plate. Also, for a particular region of both the plate and bulk temperatures, bi-directional flow was predicted.

Typical vertical velocity profiles for a bulk temperature of $0^{o}C$ and numerous plate temperatures are presented in Figures (7-1) and (7-2). Curve A of Figure (7-1) shows a typical fully downward profile at a plate temperature of $2.0^{o}C$. Here, the velocity reached a maximum downward value, then increased, passing its zero value and thereafter increased to pass a maximum upward value to decrease again to reach a very small value ($0(10^{-4})$) at the other boundary. For plate-temperatures of $8.0^{o}C$ and $9.0^{o}C$, curves B and C of Figure (7-1) show the distortion which occurred in the fully downward flow adjacent to the plate due to the insufficiently buoyant inner layer which was being dragged down by the outer layer. This is why these velocity profiles are slightly shifted upward very close to the plate. Curve D of Figure (7-1) presents the boundary between the downward unidirectional flow and the bi-directional flow. The resulting numerical value of the velocity at the pivotal point next to the plate-node was -0.5699×10^{-4}. The plate-temperature at this boundary was $9.9597^{o}C$. However, it is important to mention here that the similarity solution [Ref. 70,78] predicted this boundary to be at a plate-temperature of $12.4^{o}C$.

For plate temperatures above $9.597^{o}C$, bi-directional convective flow was observed. Curve E of Figure (7-1) and curves F and G of Figure (7-2) present such cases. Here, the vertical velocities close to the plate reached comparatively high maximum values depending on the value of the plate temperatures. It is noticed that, the positions of these

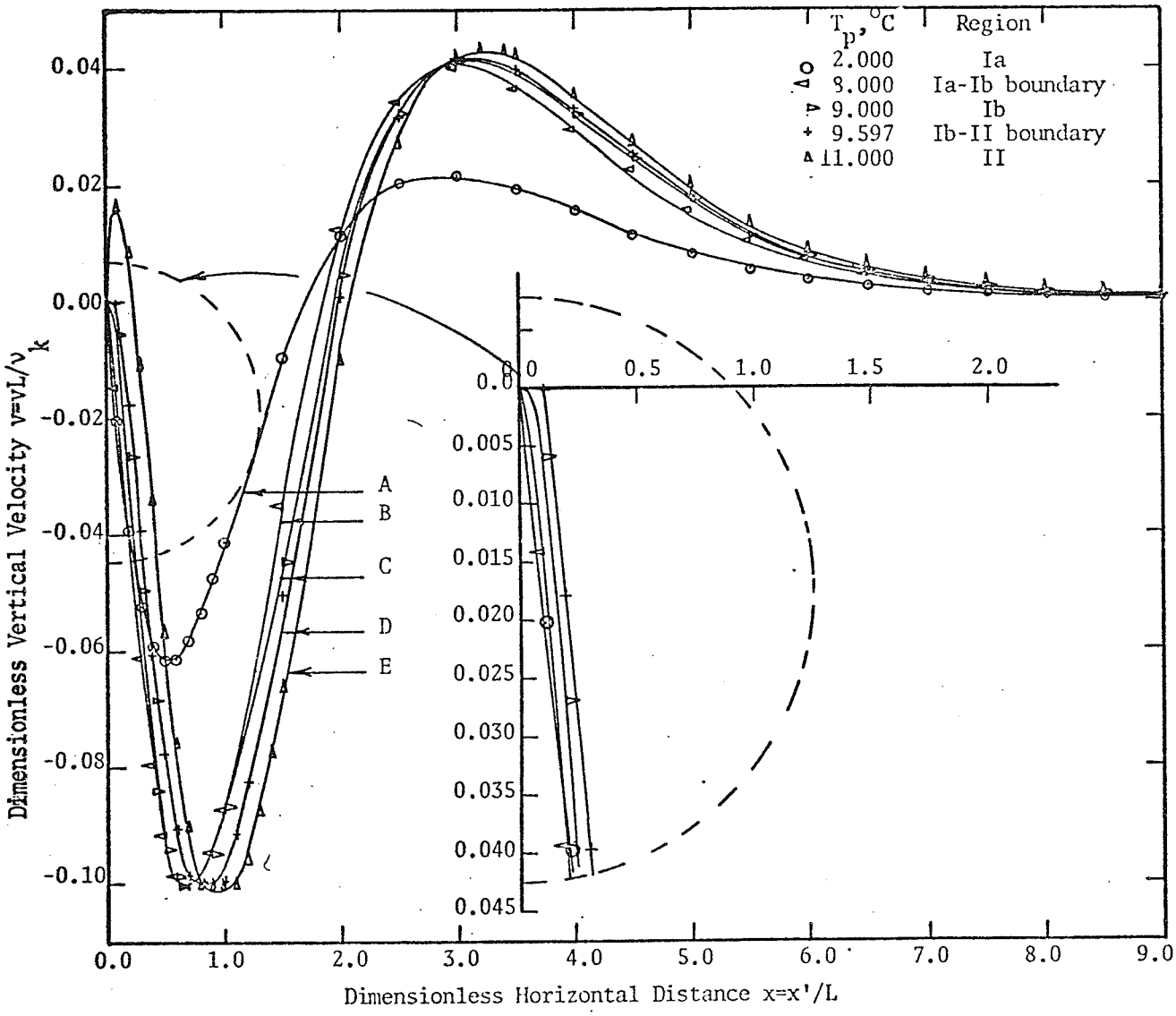

Fig (7-1) : Vertical Velocity Profiles for Downward Uni-Directional and Bi-Directional Flows for Bulk Temperature of 0°C .

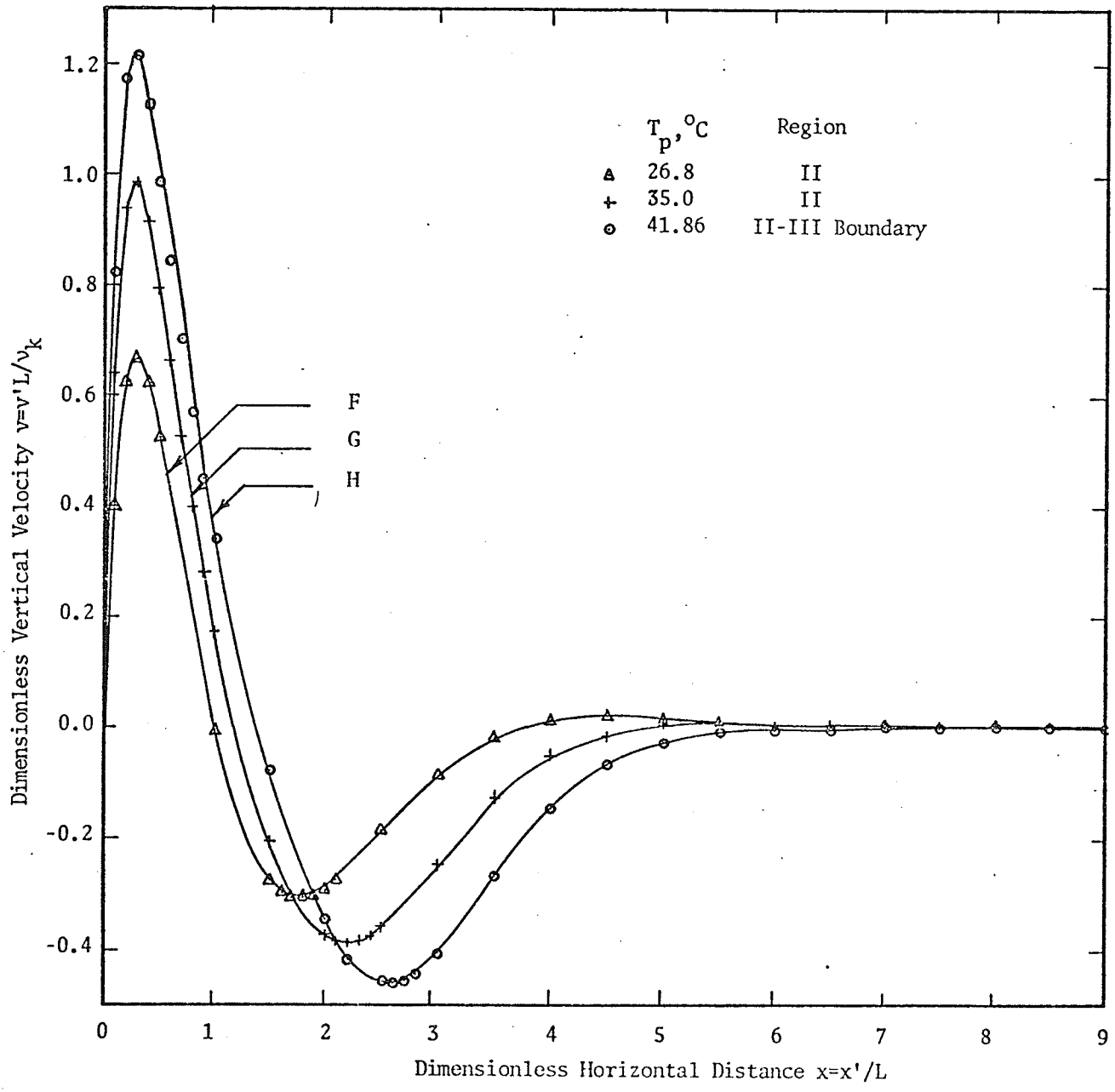

Fig. (7-2) : Vertical Velocity Profiles for Bi-Directional and Upward Uni-Directional flows for Bulk Temperature of 4°C .

maxima are shifted away from the plate as the dimensionless distance x increases. At the same time, the thickness of the buoyant layer increases. Near the right boundary, the velocity values were very low ($O(10^{-4} - 10^{-2})$) and they decreased as the plate temperature was increased.

The boundary between the bi-directional and the upward uni-directional regions, presented by curve H of Figure (7-2), was found to occur at a plate temperature of 41.86°C. Again, it has to be mentioned here that this boundary was predicted at a plate temperature of 26.8°C for the boundary-layer similarity solutions [Refs. 70,78]. It has to be emphasised, at this stage, that this boundary could not be determined precisely. This was due to the recirculating fluid near the right boundary, which existed for high values of the plate temperature. However, two techniques were used to predict this boundary; the first was by setting a minimum limit for the values of the velocities in the recirculating region in the vicinity of the right boundary. For velocity-values below this limit, the flow was assumed to be negligible. The second technique was by considering other plate and bulk temperatures to check the boundary. For the present work, a value of 0.5×10^{-4} was assigned as a sufficiently low value to determine the boundary between regions II and III. Also, some computer runs were performed to check the limits for the two regions by using several values of the plate and bulk temperatures (see Figure (7-3)) .

Above 41.86°C, the velocity profiles were similar to those for normal free convection described in Chapter 6, Section 6.1.2. Numerical values for the vertical non-dimensional velocities at a bulk temperature

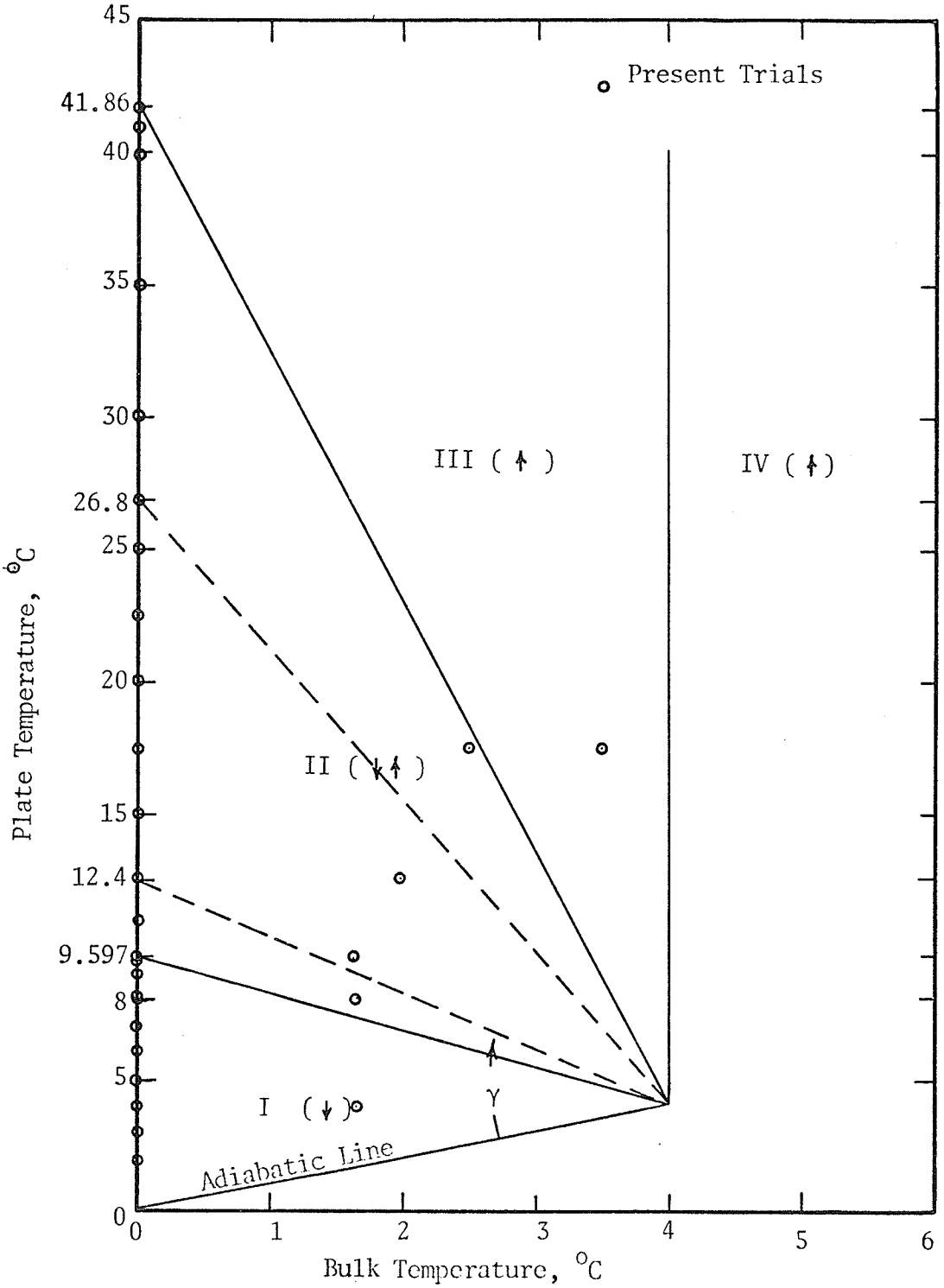

Fig. (7-3) : Map of Free Convection regions for water near 4°C .

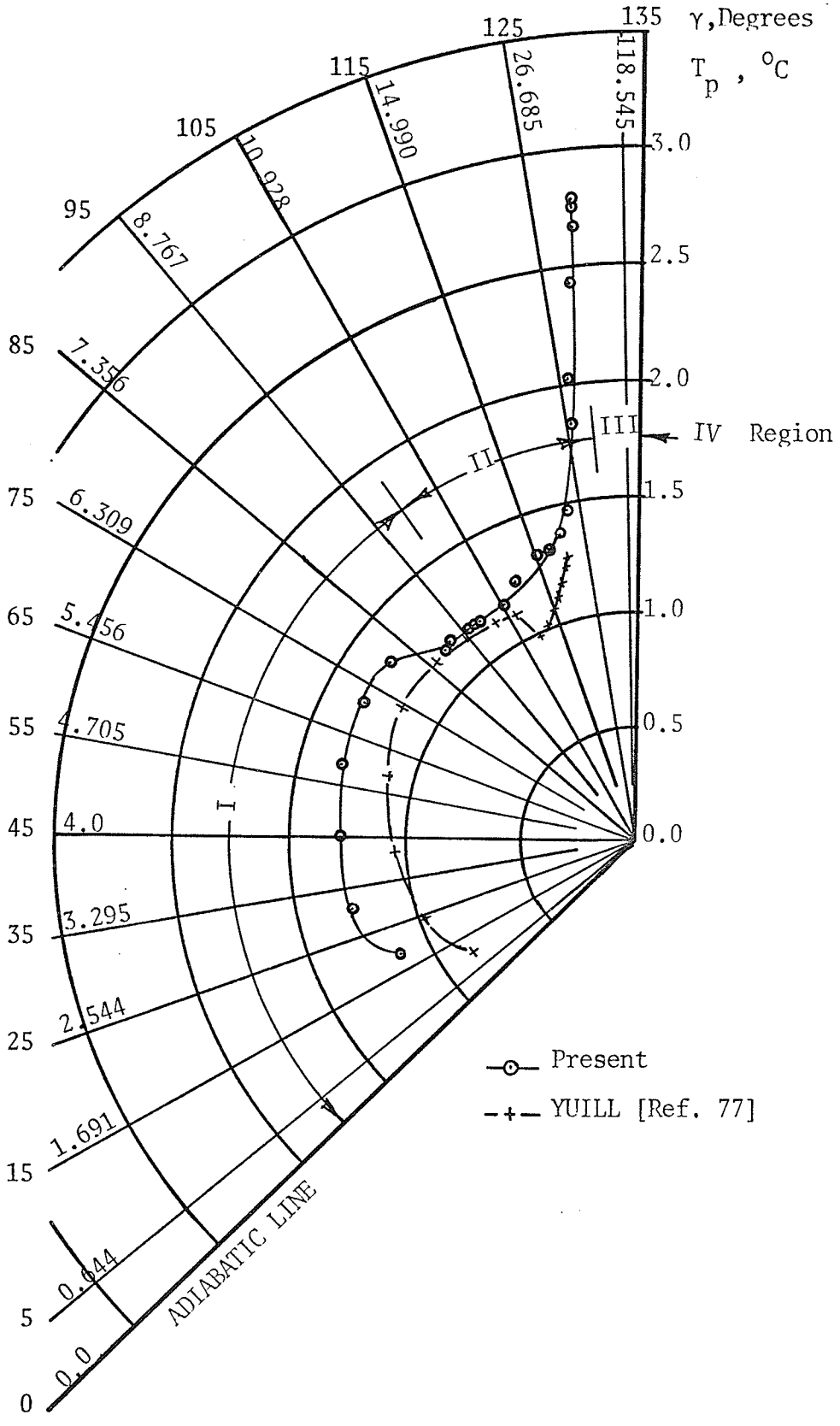

Fig. (7-4) : Average Nusselt Number, $\overline{Nu}$, vs the Angle γ and the Plate-Temperature, For Bulk-Temperature of 0°C .

of $0^{o}C$ and plate temperatures of 2.0, 8.0, 9.0, 9.597, 11.0, 26.8, 35.0 and $41.86^{o}C$ are presented in Tables (D-1) and (D-2) in Appendix D.

For all the aforementioned trials, the predicted free-convection flow regions are shown in Figure (7-3). The solid boundaries are for the present complete colution and the dashed ones are for the boundary-layer solution obtained by Yuill [Ref. 77]. Region I stands for the fully downward uni-directional flow. Region II presents the bi-directional flow and Regions III and IV are for fully upward un-directional flow.

For a bulk temperature of $0^{o}C$, the average Nusselt numbers were computed for different values of the plate temperature. In connection with Figure (7-3), an angle γ can be defined as the angle between the adiabatic line, and any line connecting the focus, at $T_p = 4^{o}C$ and $T_b = 4^{o}C$, and any plate temperature. If this angle is measured and plotted against the average Nusselt number for the corresponding plate temperature, Figure (7-4) can be obtained. From this Figure, it can be seen that as γ increased in Region I, the value of the average Nusselt number increased to reach a maximum value of 1.306 and then decreased to an approximately constant value of 1.172; when the plate temperature exceeded $9.597^{o}C$, the average Nusselt number started to increase with γ.

The behaviour of the variation of the Nusselt number with the plate temperature, shown in Figure (7-4), is close to the results obtained by Yuill [Ref. 77, Fig. 17] at high Grashof numbers. Yuill's results, which were obtained for a plate height of 15.0 cm., have been converted

to correspond to a plate-height of 0.1 cm., which was the value used in obtaining the present results.

Also, it can be seen that the behaviour of the variation of $\overline{Nu}$ with the plate temperature, depended on the convective flow regions for both solutions presented in Figure (7-4).

CHAPTER 8

CONCLUSIONS

The major objective of this work was the numerical solution of the Boussinesq-approximated Navier-Stokes and energy equations for free convection heat transfer from an isothermal vertical flat plate to fluids. Emphasis was placed on the case of free convection heat transfer to water near $4^{\circ}C$ from the plate.

The steady-state governing equations have been solved by using the Direct Substitution Simple Explicit (DSSE) method. With an ordinary grid system, solutions could be obtained for values of Grashof number up to 100. For values of Grashof number between 100 and 500, the DSSE method was found to be more successful if it was applied with a Temporary-nodes (TN) grid system. The relaxation method was used to solve the simultaneous algebric equations produced by the finite-difference expressions of the vorticity, stream-function and temperature . Under-relaxation was found to be most successful for the vorticity equation while over-relaxation was found to be the most suitable approach to the solution of the stream-function and temperature equations.

The solution of the time-dependent governing equations was also attempted. Simple Explicit (SE) and Alternating Direction Implicit (ADIP) techniques were tried. No final results were obtained because of the instability in the solution of the temperature equation. It was found that the finite-difference form of the stream-function equation should be modified to include the effect of the time-increment.

New set of boundary conditions were introduced to circumvent the instability problem of the numerical solution of the case studied in this work. They were called " the Open-Control-Volume" boundary conditions. This set of boundary conditions helped to eliminate the formation of eddies at the boundaries at infinity, and to forbid the generation of velocity " accumulation" in the vicinity of the plate.

For the case of free convection heat transfer to water near $4^{o}C$, several regions for the convective flow were observed. For a bulk temperature of $0^{o}C$, upward and downward uni-directional flow regions, and bi-directional region resulted for different values of the plate temperature. The average Nusselt number variation with both the γ-angle and the plate temperature showed a very good agreement with previous published results.

It should be mentioned that the free-surface boundary condition, imposed on the right boundary, was supposed to present a boundary at infinity where neither fluid-flow nor heat transfer occurred. However, for a value of the infinity-distance of 9.0 times the plate height, these circumstances were not satisfactorily satisfied, and it was found that the right-boundary was still influencing the solution and causing fluid recirculation.

REFERENCES

1. Aziz, K. and Hellums, J.D.: "Numerical Solution of the Three-Dimensional Equations of Motion for Laminar Natural Convection", Phys. of Fluids, 10, 314-324, 1966.

2. Barakat, H.Z. and Clark, J.A.: "On the Solution of the Diffusion Equations by Numerical Methods", Trans. ASME, J. Heat Transfer, 88, 421-427, 1966.

3. Batchelor, G.K.: "Heat Transfer by Free Convection across a Closed Cavity between Vertical Boundaries at Different Temperatures", Quart. of Appl. Math., 12(3), 209-233, 1954.

4. Bickley, W.G.: "Formulae for Numerical Differentiation", Math. Gazette, 25, 19-27, 1941.

5. Carré, B.A.: "The Determination of the Optimum Acceleration Factor for Successive Over-Relaxation", Computer J., 4, 73-78, 1961

6. Chiang,T., Ossin,A. and Tien,C.L.: "Laminar Free Convection from a Sphere", Trans. ASME, J. Heat Transfer, 86, 537-542, 1964.

7. Deardorff, J.W.: "A Numerical Study of Two-dimensional Parallel-Plate Convection", J. of Atmospheric Sciences, 21,419-438, 1964.

8. De Vahl Davis, G.: "Laminar Natural Convection in an Inclosed Rectangular Cavity", Int. J. Heat Mass Transfer, 11, 1675-1693, 1968.

9. ——— and Thomas, R.W.: "Natural Convection between Concentric Vertical Cylinders", Supl. II to Phys. of Fluids, 12, 198-207, 1969.

10. Dorsey, N.E.: "Properties of Ordinary Water Substance in all its Phases", Hafner, 1968.

11. Eckert, E.R.G. and Carlson, W.O.: "Natural Convection in an Air Layer Enclosed between two Vertical Plates with Different Temperatures", Int. J. Heat Mass Transfer, 2, 106-120, 1961.

12. ——— and Drake, R.M., Jr.: "Analysis of Heat and Mass Transfer", McGraw Hill, Inc., N.Y. 1972.

13. ——— and Jackson, T.W.: "Analysis of Turbulent Free-convection Boundary Layer on Flat Plate", NACA, Rept. 1015, 255-261, 1951.

14. Ede, A.J.: "Advances in Free Convection", Advances in Heat Transfer, Academic Press, vol. 4, 1967.

15. Elder, J.W.: "Numerical Experiments with Free Convection in a Vertical Slot", J. Fluid Mech., 24(4), 823-843, 1966.

16. Forsythe, G.E. and Wasow, W.R.: "Finite-Difference Methods for Partial Differential Equations", J. Wiley & Sons, Inc., 1960.

17. Fox, L.: "Numerical Solution of Ordinary and Partial Differential Equations", Pergamon Press, A. Wesley, Inc., 1962.

18. Frankel, S.P.: "Convergence Rates of Iterative Treatments of Partial Differential Equations", M.T.A.C., 4, 65-75, 1950.

19. Fromm, J.E.: "The Time Dependent Flow of an Incompressible Viscous Fluid", Methods in Computational Physics, Academic Press, vol. 3, 1964.

20. ——— : "Numerical Solutions of the Nonlinear Equations for a Heated Fluid Layer", Phys. of Fluids, 8(10), 1757-1769, 1965.

21. Gebhart, B.: "Heat Transfer", McGraw Hill, Inc., N.Y., 1971.

22. ——— : "Transient Natural Convection from Vertical Elements", Trans. ASME, J. Heat Transfer, 83, 61-70, 1961.

23. ——— : "Effect of Viscous Dissipation in Natural Convection", J. Fluid Mech., 14, 225-232, 1962.

24. ——— : and Mollendorf, J.: "Viscous Dissipation in External Natural Convection Flows", J. Fluid Mech., 38, 97-107, 1969.

25. Gosman,A.D., Pun,W.H., Runchall,A.K., Spalding,D.B. and Walfshtein, M. : "Heat and Mass Transfer in Recirculating Flows", Academic Press, 1969.

26. Hageman, L.A. and Kellogg, R.B.: "Estimating Optimum Over-Relaxation Parameters". Math. of Computation, 22, 60-68, 1968.

27. Hellums, J.D. and Churchill, S.W.: "Transient and Steady State, Free and Natural Convection, Numerical Solution; Part 1: The Isothermal Vertical Plate", A.I.Ch.E. Journal, 8, 690-692, 1962.

28. Illingworth, C.R.: "Unsteady Linear Flow of Gas near as Infinite Flat Plate",Proc. Cambridge Philosophical Society, 46, 603 613, 1950.

29. Jakob, M.: "Heat Transfer", J. Wiley & Sons, Inc. N.Y., vol. I, 1950.

30. Kettleborough, C.F.: "Transient Laminar Free Convection between Heated Vertical Plates Including Entrance Effect", Int. J. Heat Mass Transfer, 15, 883-896, 1972.

31. Kreyszig, E.: "Advanced Engineering Mathematics", J. Wiley & Sons, Inc., N.Y., 1972.

32. Kuo, H.L.: "Solution of the Non-Linear Equations of Cellular Convection and Heat Transfer", J. Fluid Mech., 10, 611-634, 1961.

33. Lester, W.G.S.: "Some Convergence Problems in the Numerical Solution of the Navier-Stokes Equations", A.R.C., R. & M. No.3239, 1960.

34. MacGregor, R.K. and Emery, A.F.: "Free Convection through Vertical Plane Layers - Moderate and High Prandtl Number Fluids", Trans. ASME, J. Heat Transfer, 91, 391-403, 1969.

35. Martini, W.R. and Churchill, S.W.: "Natural Convection inside a Horizontal Cylinder", A.I.Ch.E. Journal, 8(2), 251-257, 1960.

36. McAdams, W.H.: "Heat Transmission", McGraw Hill, Inc., N.Y., 1954.

37. Omar, A.M.E.: "Solution of Fields by Numerical Methods", Project Rep., Course No. 24.781, University of Manitoba, 1972.

38. Ostrach, S.: "An Analysis of Laminar Free-Convection Flow and Heat Transfer about a Flat Plate Parallel to the Direction of the Generating Body Force", NACA, Rept. 1111, 1953.

39. Ostrowski, A.: "On Over and Under Relaxation in the Theory of the Cyclic Step Iteration", M.T.A.C., 7, 152-159, 1953.

40. Parker,J.D., Boggs,J.H. and Blick,E.F.: "Introduction to Fluid Mechanics and Heat Transfer", A. Wesley Co., Inc., 1969.

41. Peaceman, D.W. and Rachford, H.H.,Jr.: "The Numerical Solution of Parabolic and Elliptic Differential Equations", J. Soc. Ind. Appl. Math., 3, 28-41, 1955.

42. Poots, G.: "Heat Transfer by Laminar Free Convection in Enclosed Plane Gas Layers", Quart. Journ. Mech. and Applied Math., 11(3), 257-273, 1958.

43. Randall, T.J.: "A Note on the Estimation of the Optimum Successive Overrelaxation Parameter for Laplace's Equation", Computer J., 10, 400-401, 1968.

44. Reid, J.K.: "A Method for Finding the Optimum Successive Over-relaxation Parameter", Computer J., 7, 200-204, 1966.

45. Roshsenow, W.M. and Choi, H.Y.: "Heat, Mass and Momentum Transfer", Prentice-Hall, Inc., Englewood Cliffs, N.J., 1961.

46. Rubel, A. and Landis, F.: "Numerical Study of Natural Convection in a Vertical Rectangular Enclosure", Supl. II to Phys. of Fluids, 208-213, 1969.

47. Rubel, A. and Landis, F.: "Laminar Natural Convection in a Rectangular Enclosure with Moderately Large Temperature Difference", Proc. of the Fourth Int. Conf. of Heat Transfer, Paris, 1970.

48. Runchal, A.K., Spalding, D.B. and Walfshtein, M.: "The Numerical Solution of the Elliptic Equations for Transport of Vorticity, Heat and Matter in Two-Dimensional Flows", Imperial Colledge, Rept. SF/TN/2, London, 1967.

49. Salvadori, M.G. and Baron, M.L.: "Numerical Methods in Engineering", Prentice-Hall, Inc., Englewood Cliffs, N.J., 1961.

50. Saunders, O.A.: "Natural Convection in Liquids", Proc. Roy. Soc., A172(948), 55-71. 1939.

51. Schechter, R.S.: "Natural-Convection Heat Transfer in Regions of Maximum Density", Ph.D. Thesis, University of Minnesotta, 1956.

52. ——— and Isbin, H.S.: "Natural-Convection Heat Transfer in Regions of Maximum Fluid Density", A.I.Ch.E. Journal, 4(1), 81-89, 1958.

53. Schenk, J. and Schenkels, F.A.M.: "Thermal Free Convection from an Ice Sphere in Water", Appl. Sci. Res., 19, 465-476, 1968.

54. Schlichting, H.: "Boundary Layer Theory", McGraw Hill Co., Inc., 1968.

55. Schmidt, E. and Beckmann, W.: "Das Temperature- und Geschwindigkeitsfeld vor einer Warme abgebenden senkrechten Platte bei naturlicher Konvektion", Tech. Mech und Thermodyn., 1(10), 342-349 and 391-406, 1930.

56. Shapiro, A.H.: "The Dynamics and Thermodynamics of Compressible Fluid Flow", Ronald Press Co., N.Y., vol. I, 1953.

57. Siegel, R.: "Transient Free Convection From a Vertical Falt Plate", Trans. ASME, 80, 347-359, 1958.

58. Smith, G.D.: "Numerical Solutions of Partial Differential Equations", Oxford University Press, 1965.

59. Southwell, R.V.: "Relaxation Methods in Engineering Science", Oxford University Press, 1951.

60. ——— : "Relaxation Methods in Theoretical Physics", Oxford University Press, 1956.

61. Sparrow, E.M. and Gregg, J.L.: "Laminar Free Convection from a Vertical Plate with Uniform Surface Heat Flux", Trans. ASME, 78, 435-440, 1956.

62. Sparrow, E.M. and Gregg, J.L.: "The Variable Fluid Property Problem in Free Cnvection", Trans. ASME, 80, 879-886, 1958.

63. ——— and ——— : "Similar Solutions for Free Convection from a Nonisothermal Vertical Plate", Trans. ASME, 80, 379-386, 1958.

64. Sugawara, S. and Michiyoshi, I.: "The Heat Transfer by Natural Convection in the Unsteady State on a Vertical Flat Wall", Proc. of the Japan National Congress for Appl. Mech., 1951.

65. Suriano, F.J. and Yang, K.T.: "Laminar Free Convection about Vertical and Horizontal Plates at Small and Moderate Grashof Numbers", Tech. Note 66-11, Dept. of Mech. Eng., Univ. of Notre-Dame, Indiana, 1966.

66. ——— , ——— and Donlon, J.A.: "Laminar Free Convection along a Vertical Plate at Extremely Small Grashof Numbers", Int. J. Heat Mass Transfer, 8, 815-831, 1965.

67. Thom, A. and Apelt, C.J.: "Note on the Convergence of Numerical Solutions of the Navier-Stokes Equations", A.R.C., R.&M. No.3061, 1956.

68. Thomas, R.W. and De Vahl Davis, G.: " Natural Convection in Annular and Rectangular Cavities. A Numerical Study", Proc. of the Fourth Int. Conf. of Heat Transfer, Paris, 1970.

69. Touloukian, Y.S., Hawkin, G.A. and Jakob, M.: "Heat Transfer by Free Convection from Heated Vertical Surfaces to Liquids", Trans. ASME, 70, 13-18, 1948.

70. Vanier, C.R. and Tien, C.: "Effect of Maximum Density and Melting on Natural Convection Heat Transfer from a Vertical Plate", Ch. E. Prog. Symp. Series, No. 82, 64, 240-254, 1968.

71. ——— and ——— : "Free Convection Melting of Ice Spheres", A.I.Ch.E. Journal, 16(1), 76-82, 1970.

72. Varga, R.S.: "Matrix Iterative Analysis", Prentice-Hall, Inc., Englewood Cliffs, 1962.

73. Wexler, A.: "Computation of Electomagnetic Fields", IEEE, MTT-17(8), 416-439, 1969.

74. Wilkes, J.O. and Churchill, S.W.: "The Finite-Difference Computation of Natural Convection in a Rectangular Enclosure", A.I. Ch. E. Journal, 12, 161-166, 1966.

75. Yang, K.T.: "Possible Similarity Solutions for Laminar Free Convection

on Vertical Plates and Cylenders", Trans. ASME, J. Appl. Mech., 82, 230-240, 1960.

76. Yang, K.T. and Jerger, E.W.: "First-Order Perturbations of Laminar Free Convection Boundary Layer on a Vertical Plate", Trans. ASME, J. Heat Transfer, 86, 107-115, 1964.

77. Yuill, G.K.: " Free Convection Heat Transfer From a Vertical Isothermal Plate to Water Near 4°C", Ph.D. Thesis, University of Minnesota, 1972.

78. ——— : "Free Convection Heat Transfer in Water Near 4°C", Dept. of Mech. Eng., Univ. of Manitoba, 1972.

APPENDIX A

Derivation of the Node-Coefficient of Volumetric Thermal Expansion, β_k

The density-temperature relationship is presented by Yuill [Ref. 78] as

$$\rho_o/\rho_k = 1 + D_1T_k + D_2T_k^2 + D_3T_k^3 \qquad (A.1)$$

where

ρ_k is the node-density of water at any node-temperature T_k,

ρ_o is the density of water at 0^oC
($\rho_o = 0.999551$ gm/cm^3),

D_1 is constant and equal to $-0.6669167 \times 10^{-4}$, $^oC^{-1}$,

D_2 is constant and equal to 0.871689×10^{-5}, $^oC^{-2}$,

D_3 is constant and equal to -0.647664×10^{-7}, $^oC^{-3}$,

and

k is subscript designating the node being considered for computation. It should be mentioned here that the density coefficients D_1, D_2 and D_3 have to be used in a temperature range of 0^oC to 20^oC.

The node-coefficient of volumetric thermal expansion β_k, on the other hand, can generally be defined as

$$\beta_k = -(d\rho_k/dT_k)/\rho_k \qquad (A.2)$$

Since neither $(d\rho_k/dT_k)$ nor ρ_k itself is constant, the value of β_k will change, therefore, from one node to another. The rate of change of the density with respect to temperature at any node k can

easily be derived from their relationship formula (A-1). The resulting form will be

$$\left(\frac{d\rho}{dT}\right)_k = -\rho_o\left(\frac{D_1 + 2D_2T + 3D_3T^2}{(1 + D_1T + D_2T^2 + D_3T^3)}\right) \qquad (A.3)$$

Equations (A.1) and (A.3) can now be substituted into equation (A.2). By carrying some algebraic rearrangements, the equation for the node-coefficient of volumetric expansion, β_k, can be obtained in the form

$$\beta_k = (D_1 + 2D_2T + 3D_3T^2)/(1 + D_1T + D_2T^2 + D_3T^3) \qquad (A.4)$$

at any node by substitutaing the values of the density-coeffucient constants D_1, D_2 and D_3, and the temperature at that node.

According to Vanier and Tien [Ref. 70], the standard deviatio of the computed D-values, from the data of Dorsey [Ref. 10], was found to be 0.54×10^{-6} for a temperature range of 0^oC to 20^oC. They also computed the density-coefficients for a temperature range of 0^oC to 35^oC. Their resulting values were: $D_1 = -.6226173 \times 10^{-4}\ {}^oC^{-1}$,

$D_2 = .807544 \times 10^{-5}\ {}^oC^{-2}$, and

$D_3 = -.439592 \times 10^{-7}\ {}^oC^{-3}$.

These values have a standard deviation of 0.57×10^{-5} from the same emperical data of Dorsey.

In the present work, it was found that the D-values computed by Vanier and Tien for the temperature range of 0^oC to 35^oC, can adequately be applied for a temperature range of 0^oC to 42^oC with a relative error of 0.00475% from the data of Dorsey.

APPENDIX B

Derivation of Some Finite-Difference Formulae

B.1 Forward 3-point one-sided derivative formula

In connection with the notations shown on Fig. (B-1), the value of any function f at point 1 can be expressed, by the use of the Taylor's expansion, in terms of the values of the function f and its derivatives at point 0 and the grid size h. The resulting equation will take the form

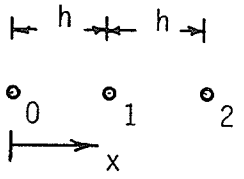

Fig. (B-1) : 3-points for forward formula.

$$f_1 = f_0 + hf_0' + \frac{h^2}{2!} f_0'' + \frac{h^3}{3!} f_0''' + O(h^4) \qquad (B.1)$$

with a truncation error of the order (h^4) .

Similarly, the value of the function f at point 2 can be expressed, in terms of the values of the function f and its derivatives at point 0, by applying the Taylor's expansion in the same manner, or by simply replacing h by 2h in equation (B.1). Either method will yield

$$f_2 = f_0 + 2hf_0' + \frac{4h^2}{2!} f_0'' + \frac{8h^3}{3!} f_0''' + O(h^4) \qquad (B.2)$$

with a truncation error of the order (h^4) .

The f_0''-term in equations (B.1) and (B.2) can be eliminated by multipling the former by 4 and then substituting from the latter. Also, if the f_0'''-terms are neglected, an expression for the first derivative of the function f at point 0 can be obtained in the form

$$f_0' = -\,(\,3f_0 - 4f_1 + f_2\,) \,/\, 2h + O(h^2) \qquad (B.3)$$

Equation (B.3) presents the forward 3-point one-sided derivative formula. The truncation error here is of the order (h^2) .

B.2 Backward 3-point one-sided derivative formula

Refering to Fig. (B.2), the Taylor's expansion for f_1 and f_2 can easily be written in terms of the function and its derivatives at point 0. By following the prescribed steps used to derive the forward formula, the backward 3-point one-sided derivative formula can be expressed as

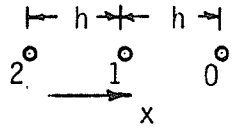

Fig (B.2) : 3-points for backward formula .

$$f_0' = (3f_0 - 4f_1 + f_2) / 2h + O(h^2) \qquad (B.4)$$

with a truncation error of the order (h^2) .

B.3 5-point second-derivative formula

Consider the five points -2, -1, 0, 1 and 2 shown on Fig. (B.3)

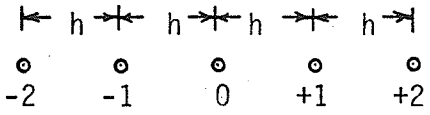

Fig. (B.3) : 5-points for second derivative formula.

By the use of the Taylor's expansion, the function f at the two points -1 and -2 can be expressed in terms of the values of the function and its derivatives at the point 0 as follows

$$f_1 = f_0 + hf_0' + \frac{h^2}{2!} f_0'' + \frac{h^3}{3!} f_0''' + \frac{h^4}{4!} f_0'''' + \frac{h^5}{5!} f_0''''' + \frac{h^6}{6!} f_0'''''' + O(h^7) \qquad (B.5)$$

and

$$f_{-1} = f_0 - hf_0' + \frac{h^2}{2!} f_0'' - \frac{h^3}{3!} f_0''' + \frac{h^4}{4!} f_0'''' - \frac{h^5}{5!} f_0''''' + \frac{h^6}{6!} f_0'''''' + O(h^7) \qquad (B.6)$$

Adding equations (B.5) and (b.6), the resulting equation will be

$$f_1 + f_{-1} = 2f_0 + h^2 f_0'' + \frac{h^4}{12} f_0'''' + O(h^6) \qquad (B.7)$$

By a similar manner, for points 2 and -2, the following expression can be obtained

$$f_2 + f_{-2} = 2f_0 + 4h^2 f_0'' + \frac{16}{12} h^4 f_0'''' + O(h^6) \qquad (B.8)$$

The f_0''''-term can be omitted from equations (B.7) and (B.8) by mutiplying the former by 16 and subtracting the result from the latter. Consequently, f_0'' can be expressed as

$$f_0'' = (-f_{-2} + 16f_{-1} - 30f_0 + 16f_1 - f_2) / 12h^2 + O(h^4) \qquad (B.9)$$

with a truncation error of the order of (h^4). Equation (B.9) presents the 5-point second-derivative formula .

B.4 Evaluation of the vorticity at a rigid-wall boundary-node

The 3-point one-sided derivative formula, equation (B.3), can be used to compute the vorticity ζ_0 at a pivotal boundary-point. If the notations of Fig. (B-1) are considerd, an expression for ζ_0 may be obtained in terms of ψ_0, ψ_1, ψ_2, ζ_1 and ζ_2 .

The procedure can be initiated by applying the Taylor's expansion to evaluate ψ_2 and ψ_1 in terms of the values of ψ and its derivatives at point 0. With some manipulations similar to that which are carried out in section B.1, and by applying the rigid-wall boundary condition $(\frac{\partial \psi}{\partial x})_0 = 0$, the equation

$$3\psi_0 - 4\psi_1 + \psi_2 = \frac{3h^3}{3} (\frac{\partial^3 \psi}{\partial x^3})_0 + O(h^2) \qquad (B.10)$$

can be obtained. On the other hand, the continuity equation (2.27) can be differentiated with respect to x to yield

$$\frac{\partial^3\psi}{\partial x^3} + \frac{\partial^2}{\partial y^2}\left(\frac{\partial\psi}{\partial x}\right) = -\frac{\partial\zeta}{\partial x} \qquad \text{(B.11)}$$

Since, at point 0, $\frac{\partial^2}{\partial y^2}\left(\frac{\partial\psi}{\partial x}\right) \to 0$, therefore, by making use of expression (B.3), equation (B.11) becomes

$$\left(\frac{\partial^3\psi}{\partial x^3}\right) = -\left(\frac{\partial\zeta}{\partial x}\right)_0 = \left(3\zeta_0 - 4\zeta_1 + \zeta_2\right) / 2h + O(h^2) \qquad \text{(B.12)}$$

Substituting (B.12) into (B.10) and solving for ζ_0, the result will be

$$\zeta_0 = \left(3\psi_0 - 4\psi_1 + \psi_2\right) / h^2 + \left(4\zeta_1 - \zeta_2\right) / 3 + O(h^2) \qquad \text{(B.13)}$$

Equation (B.13) presents the formula to be used to compute the vorticity ζ at the rigid-wall boundary-node 0 . The truncation error in this equation is of the order (h^2) .

The backward 3-point one-sided derivative formula can be used, on the other hand, for a similar derivation resulting in the same expression (B.13) for ζ_0 .

B.5 Evaluation of the temperature at a non-conducting boundary-node

The dimensionless steady-state temperature equation (2.26) can be written in the form

$$u\frac{\partial\theta}{\partial x} + v\frac{\partial\theta}{\partial y} = \frac{1}{Pr}\left\{\frac{\partial^2\theta}{\partial x^2} + \frac{\partial^2\theta}{\partial y^2}\right\} \qquad \text{(B.14)}$$

The stated boundary conditions at the boundary-node 0 of Fig. (B-4) are

$$u_0 = o \text{ and } \left(\frac{\partial^2\theta}{\partial y^2}\right)_0 = 0 \qquad \text{(B.15)}$$

Therefore, when equation (B.14) is applied at point 0 it becomes

$$v\frac{\partial\theta}{\partial y} = \frac{1}{Pr}\frac{\partial^2\theta}{\partial x^2} \qquad \text{(B.16)}$$

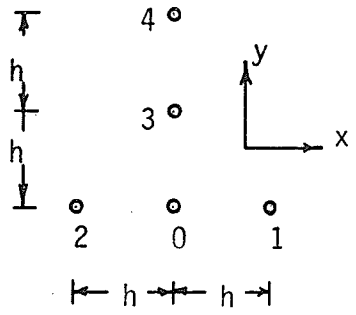

Fig. (B-4) : Five point to evaluate θ_0.

By the use of the 3-point one-sided derivative formula to substitute for $\partial\theta/\partial y$, and the finite-difference formula to substitute for $\partial^2\theta/\partial x^2$, equation (B.16) can be manipulated to yield an expression for θ_0 of the form

$$\theta_0 = \{(\theta_1+\theta_2)/Pr\, h+ \frac{v}{2} (4\theta_3-\theta_4)\}/\{ \frac{3}{2}v + \frac{2}{Pr\, h} \} \qquad (B.17)$$

with a truncation error of the order (h^2). Expression (B.17) presents the forward form. The backward form can similarly be derived and the resulting formula will be

$$\theta_0 = \{(\theta_1+\theta_2)/Pr\, h+ \frac{v}{2} (-4\theta_3+\theta_4)\}/\{-\frac{3}{2}v + \frac{2}{Pr\, h} \} \qquad (B.18)$$

with a truncation error of the order (h^2) .

B.6 Evaluation of the average Nusselt number $\overline{Nu}$

The heat transferred through the plate-water interface,at any of the plate-points, is governed by the equation

$$-k \left(\frac{\partial T_{y'}}{\partial x'}\right)_0 dy' = h_{y'} (T_p-T_b) dy' \qquad (B.19)$$

The dimensionless parameters defined by equations (2.16-a) and (2.16-c) can be introduced into equation (B.19). As a result, the

non-dimensional form of the above equation is

$$-k \left(\frac{\partial \theta}{\partial x}\right)_0 dy = h_y L \, dy \tag{B.20}$$

The total heat transfered from the plate into water can be obtained by integrating equation (B.20). Assuming k is constant, the resulting form will be

$$-k \int_{-.5}^{+.5} \left(\frac{\partial \theta}{\partial x}\right)_0 dy = L \int_{-.5}^{+.5} h_y \, dy \tag{B.21}$$

Now, if the convective heat transfer coefficient h_y is assumed to have its average value $\bar{h}$ along the plate, equation (B.21) becomes

$$-k \int_{-.5}^{+.5} \left(\frac{\partial \theta}{\partial x}\right)_0 dy = \bar{h} L \tag{B.22}$$

At this stage, the average Nusselt number $\overline{Nu}$ can be expressed as

$$\overline{Nu} = \frac{\bar{h}L}{k} = - \int_{-.5}^{+.5} \left(\frac{\partial \theta}{\partial x}\right)_0 dy \tag{B.23}$$

The temperature gradient at the plate $(\partial \theta / \partial x)_0$ can be computed numerically by using the 3-point one-sided derivative finite-difference formula. By carrying out that for all plate-pivotal points, the value of $\overline{Nu}$ can be computed by applying Simpson's rule for numerical integration [Ref. 31 p. 657] .

```
C
C
C
C
C                                   APPENDIX C
C                                   ----------
C
C
C     PROGRAM-LISTING (C-1) : UP-DOWN COMPUTATIONAL TECHNIQUE FOR
C                                   LAPLACIAN TEMPERATURE FIELDS .
C
C
C
C     <<<**MAIN**>>>
C
C     ************************************************************************
C     *                                                                      *
C     *          PROGRAMME TO COMPUTE LAPLACIAN TEMP. DIST.                  *
C     *                          USING                                       *
C     *                THE UP-DOWN COMPUTATIONAL TECHNIQUE                   *
C     *                                                                      *
C     ************************************************************************
C
      1       DIMENSION A(61,161)
      2       REWIND1
C
C$$$  FEED DATA THROUGH DATA CARDS
C
C$$$$ MESH DATA
      3       DATA IN,JN/61,161/,JL,JH,JL1,JH1/72,82,71,83/
C
C$$$$ ITERATION DATA
      4       DATA RSOU,RF/0.,1.6/
C
      5       INM=IN-1
      6       JNM=JN-1
C
C$$$$ INITIAL VALUES AND FIXED BOUNDARY CONDITIONS
C
      7       DO 2 I=1,IN
      8       DO 2 J=1,JN
      9     2 A(I,J)=0.
     10       DO 3 J=JL,JH
     11     3 A(1,J)=1.
     12       WRITE(6,769)
     13       NITER=0
C
C$$$  START OF THE ITERATIVE CYCLES
C
     14     1 CONTINUE
     15       NITER=NITER+1
     16       RSOU=0.
     17       SUM=0.
C
C$$$$ ITERATION AT THE INTERIOR NODES
C
C$$$  CHOICE OF UP OR DOWN WAY
     18       IF(NITER/2*2-NITER)50,51,50
C
C$$   UP WAY
C
     19    50 DO 8 J=2,JNM
     20       DO 8  I=2,INM
```

```
      OF=A(I,J)
      A(I,J)=.25*(A(I,J+1)+A(I,J-1)+A(I+1,J)+A(I-1,J))
      A(I,J)=(A(I,J)-OF)*RF+OF
      RSDU=RSDU+ABS(A(I,J)-OF)
      SUM=SUM+ABS(A(I,J))
    8 CONTINUE
      GO TO 53
C
C$$$  DOWN WAY
C
   51 DO 41 J=2,JNM
      M=JNM+2-J
      DO 41 I=2,INM
      OF=A(I,M)
      A(I,M)=.25*(A(I+1,M)+A(I-1,M)+A(I,M+1)+A(I,M-1))
      A(I,M)=OF+(A(I,M)-OF)*RF
      RSDU=RSDU+ABS(A(I,M)-OF)
      SUM=SUM+ABS(A(I,M))
   41 CONTINUE
C
C$$$  RESIDUAL OR DISPLACEMENT-NORM CACULATION
   53 RRSDU=RSDU/SUM
C
C$$$$ ITERATION AT THE BOUNDARY NODES
C
      DO 4 J=2,JL1
    4 A(1,J)=(4.*A(2,J)-A(3,J))/3.
      DO 5 J=JH1,JNM
    5 A(1,J)=(4.*A(2,J)-A(3,J))/3.
      DO 6 I=2,INM
      A(I,1)=(4.*A(I,2)-A(I,3))/3.
    6 A(I,JN)=(4.*A(I,JNM)-A(I,JN-2))/3.
      A(1,1)=.5*(A(1,2)+A(2,1))
      A(1,JN)=.5*(A(1,JNM)+A(2,JN))
C
C$$$  CHECK EXIT CRITERION
C
      IF(RRSDU.LT..005.OR.NITER.EQ.100) GO TO 20
      WRITE(6,772) NITER,RRSDU
      GO TO 1
   20 WRITE(6,772) NITER,RRSDU
C
C$$$  FINAL PRINT OUT
C
      DO 7 I=1,IN
    7 WRITE(6,771)(A(I,J),J=1,JN)
C
C$$$  FINAL WRITING ON TAPE
C
      WRITE(1)((A(I,J),J=1,JN),I=1,IN)
      ENDFILE1
      STOP
  769 FORMAT(1H1,50X,'RESULTS'//,4X,'NITER',3X,'REL. DISP. NORM'/)
  771 FORMAT(10E12.4)
  772 FORMAT(5X,I3,5X,E15.5)
      END
```

```
      C
      C
      C
      C     PROGRAM-LISTING (C-2) : SUBROUTINE AOCT TO CARRY ON THE ITERATIVE
      C                             CYCLE OVER THE INTERIOR NODES BY USING
      C                             THE DSSE METHOD WITH THE TEMPORARY-NODES
      C                             (TN) COMPUTATIONAL TECHNIQUE .
      C
      C
      C
      C     <<<** ACCT SUBPROGRAMME **>>>
      C
      1     SUBROUTINE ACCT(N1,N2,N3,N11,N21,AG,AR,IMIN,IMAX,JMIN,JMAX)
      C
      2     DIMENSION AR(N1,N2,N3),AG(N11,N21,N3)
      3     COMMON/CNUMBR/NT,NW,NF,NV,IE,IV
      4     COMMON/CGEO/IN,JN,INM,JNM,INMM,JNMM,JL,JH,JL1,JH1
      5     COMMON/CGEN/NMAX,NPRINT,IP,EPS,DISP(3),RF(3),SUM(3)
      6     COMMON/CPROP/PR,GR,H
      C
      C     ***************************************************************
      C     *                                                             *
      C     * SUBPROGRAMME TO MAKE USE AND CONTROL THE COMPUTATION PROCESS *
      C     * CARRIED OUT ACCORDING TO THE TN TECHNIQUE. THE DSSE ITERATIVE *
      C     * METHOD IS APPLIED FOR THE FINITE-DIFFERENCE CALCULATIONS .   *
      C     *                                                             *
      C     ***************************************************************
      C
      7     DO 5 J=JMIN,JMAX
      8     DO 5 I=IMIN,IMAX
      9     IF(J.EQ.1) GO TO 35
     10     IF(I.EQ.1) GO TO 33
      C
      C$$$  COMPUTATION AT THE TEMPORARY NODES C AND D
      C
     11     THC=0.25*(AR(I,J,NT)+AR(I-1,J,NT)+AG(I-1,J,NT)+AG(I-1,J-1,NT))
     $-PR*((AR(I,J,NT)-AR(I-1,J,NT))*(AG(I-1,J,NF)-AG(I-1,J-1,NF))
     $-(AG(I-1,J,NT)-AG(I-1,J-1,NT))*(AR(I,J,NF)-AR(I-1,J,NF)))/16.
     12     ZEC=0.25*(AR(I,J,NW)+AR(I-1,J,NW)+AG(I-1,J,NW)+AG(I-1,J-1,NW))
     $    -((AR(I,J,NW)-AR(I-1,J,NW))*(AG(I-1,J,NF)-AG(I-1,J-1,NF))
     $-(AG(I-1,J,NW)-AG(I-1,J-1,NW))*(AR(I,J,NF)-AR(I-1,J,NF)))/16.
     $+GR*H*(AR(I,J,NT)-AR(I-1,J,NT))/8.
     13     FYC=.25*(AR(I,J,NF)+AR(I-1,J,NF)+AG(I-1,J,NF)+AG(I-1,J-1,NF)+ZEC*(
     $H**2))
     14     THD=0.25*(AG(I,J-1,NT)+AG(I-1,J-1,NT)+AR(I,J,NT)+AR(I,J-1,NT))
     $-PR*((AG(I,J-1,NT)-AG(I-1,J-1,NT))*(AR(I,J,NF)-AR(I,J-1,NF))
     $-(AR(I,J,NT)-AR(I,J-1,NT))*(AG(I,J-1,NF)-AG(I-1,J-1,NF)))/16.
     15     ZED=0.25*(AG(I,J-1,NW)+AG(I-1,J-1,NW)+AR(I,J,NW)+AR(I,J-1,NW))
     $    -((AG(I,J-1,NW)-AG(I-1,J-1,NW))*(AR(I,J,NF)-AR(I,J-1,NF))
     $-(AR(I,J,NW)-AR(I,J-1,NW))*(AG(I,J-1,NF)-AG(I-1,J-1,NF)))/16.
     $+GR*H*(AG(I,J-1,NT)-AG(I-1,J-1,NT))/8.
     16     FYD=.25*(AG(I,J-1,NF)+AG(I-1,J-1,NF)+AR(I,J,NF)+AR(I,J-1,NF)+ZED*(
     $H**2))
     17     GO TO 33
      C
      C$$$  CONDITIONS IN THE VICINITY OF THE LOWER BOUNDARY
      C
     18  35 THA=0.
     19     FYA=0.
     20     ZEA=0.
      C
      C$$$  CONDITIONS IN THE VICINITY OF THE L.H.S.-BOUNDARY
      C
```

```
      IF(I.EQ.1) GO TO 44
      GO TO 36
C
C$$$  COMPUTATION AT THE TEMPORARY NODE A
   33 THA=0.25*(AR(I+1,J,NT)+AR(I,J,NT)+AG(I,J,NT)+AG(I,J-1,NT))
     $-PR*((AR(I+1,J,NT)-AR(I,J,NT))*(AG(I,J,NF)-AG(I,J-1,NF))
     $-(AG(I,J,NT)-AG(I,J-1,NT))*(AR(I+1,J,NF)-AR(I,J,NF)))/16.
      ZEA=0.25*(AR(I+1,J,NW)+AR(I,J,NW)+AG(I,J,NW)+AG(I,J-1,NW))
     $    -((AR(I+1,J,NW)-AR(I,J,NW))*(AG(I,J,NF)-AG(I,J-1,NF))
     $-(AG(I,J,NW)-AG(I,J-1,NW))*(AR(I+1,J,NF)-AR(I,J,NF)))/16.
     $+GR*H*(AR(I+1,J,NT)-AR(I,J,NT))/8.
      FYA=0.25*(AR(I+1,J,NF)+AR(I,J,NF)+AG(I,J,NF)+AG(I,J-1,NF)+ZEA*(H**
     $2))
      IF(I.EQ.1) GO TO 44
      GO TO 36
C
C$$$  COMPUTATION AT THE TEMPORARY NODE B
C
   44 THB=0.25*(AR(I,J+1,NT)+AR(I,J,NT)+2.*AG(I,J,NT))
      ZEB=0.25*(AR(I,J+1,NW)+AR(I,J,NW)+2.*AG(I,J,NW))
      FYB=0.25*(AR(I,J+1,NF)+AR(I,J,NF)+2.*AG(I,J,NF))
      GO TO 34
   36 THB=0.25*(AG(I,J,NT)+AG(I-1,J,NT)+AR(I,J+1,NT)+AR(I,J,NT))
     $-PR*((AG(I,J,NT)-AG(I-1,J,NT))*(AR(I,J+1,NF)-AR(I,J,NF))
     $-(AR(I,J+1,NT)-AR(I,J,NT))*(AG(I,J,NF)-AG(I-1,J,NF)))/16.
      ZEB=0.25*(AG(I,J,NW)+AG(I-1,J,NW)+AR(I,J+1,NW)+AR(I,J,NW))
     $    -((AG(I,J,NW)-AG(I-1,J,NW))*(AR(I,J+1,NF)-AR(I,J,NF))
     $-(AR(I,J+1,NW)-AR(I,J,NW))*(AG(I,J,NF)-AG(I-1,J,NF)))/16.
     $+GR*H*(AG(I,J,NT)-AG(I-1,J,NT))/8.
      FYB=.25*(AG(I,J,NF)+AG(I-1,J,NF)+AR(I,J+1,NF)+AR(I,J,NF)+ZEB*(H**2
     $))
C
C$$$  CONDITIONS IN THE VICINITY OF THE R.H.S. AND THE UPPER BOUNDARIES
C
      IF(J.EQ.JNM.AND.I.EQ.INM) GO TO 40
      IF(I.EQ.INM) GO TO 41
      GO TO 34
   40 THE=0.
      ZEE=0.
      FYE=0.
      GO TO 30
   41 THE=0.
      ZEE=0.
      FYE=0.
      IF(J.EQ.JNM) GO TO 43
      GO TO 32
C
C$$$  COMPUTATION AT THE TEMPORARY NODE E
C
   34 THE=0.25*(AG(I+1,J,NT)+AG(I,J,NT)+AR(I+1,J+1,NT)+AR(I+1,J,NT))
     $-PR*((AG(I+1,J,NT)-AG(I,J,NT))*(AR(I+1,J+1,NF)-AR(I+1,J,NF))
     $-(AR(I+1,J+1,NT)-AR(I+1,J,NT))*(AG(I+1,J,NF)-AG(I,J,NF)))/16.
      ZEE=0.25*(AG(I+1,J,NW)+AG(I,J,NW)+AR(I+1,J+1,NW)+AR(I+1,J,NW))
     $    -((AG(I+1,J,NW)-AG(I,J,NW))*(AR(I+1,J+1,NF)-AR(I+1,J,NF))
     $-(AR(I+1,J+1,NW)-AR(I+1,J,NW))*(AG(I+1,J,NF)-AG(I,J,NF)))/16.
     $+GR*H*(AG(I+1,J,NT)-AG(I,J,NT))/8.
      FYE=.25*(AG(I+1,J,NF)+AG(I,J,NF)+AR(I+1,J+1,NF)+AR(I+1,J,NF)+ZEE*(
     $H**2))
   30 IF(J.EQ.JNM)GO TO 43
      GO TO 32
   43 THF=0.25*(AR(I+1,J+1,NT)+AR(I,J+1,NT)+2.*AG(I,J,NT))
      ZEF=0.
      FYF=0.
      GO TO 31
C
C$$$  COMPUTATION AT THE TEMPORARY NODE F
```

```
      C
   56    32   THE=0.25*(AR(I+1,J+1,NT)+AR(I,J+1,NT)+AG(I,J+1,NT)+AG(I,J,NT))
     $-PP*((AR(I+1,J+1,NT)-AR(I,J+1,NT))*(AG(I,J+1,NF)-AG(I,J,NF))
     $-(AG(I,J+1,NT)-AG(I,J,NT))*(AR(I+1,J+1,NF)-AR(I,J+1,NF)))/16.
   57         ZEF=0.25*(AR(I+1,J+1,NW)+AR(I,J+1,NW)+AG(I,J+1,NW)+AG(I,J,NW))
     $    -((AR(I+1,J+1,NW)-AR(I,J+1,NW))*(AG(I,J+1,NF)-AG(I,J,NF))
     $-(AG(I,J+1,NW)-AG(I,J,NW))*(AR(I+1,J+1,NF)-AR(I,J+1,NF)))/16.
     $+GP*H*(AR(I+1,J+1,NT)-AR(I,J+1,NT))/8.
   58         FYE=.25*(AR(I+1,J+1,NF)+AR(I,J+1,NF)+AG(I,J+1,NF)+AG(I,J,NF)+ZEF*(
     $H**2))
   59    31   CONTINUE
   60         IF(J.EQ.JNM.AND.I.EQ.INM) GO TO 42
   61         IF(I.EQ.1.OR.J.EQ.1) GO TO 46
      C
      C$$$  EVALUATION OF VARIABLES AT RCUNC NODES
      C
   62    42   ORT=AR(I,J,NT)
   63         ORW=AR(I,J,NW)
   64         ORF=AR(I,J,NF)
   65         AR(I,J,NF)=0.25*(FYA+FYB+FYC+FYD+AR(I,J,NW)*(H**2))
   66         AR(I,J,NT)=0.25*(THA+THB+THC+THD)
     $-PP*((THA-THC)*(FYB-FYD)-(THB-THD)*(FYA-FYC))/16.
   67         AR(I,J,NW)=0.25*(ZEA+ZEB+ZEC+ZED)
     $-((ZEA-ZEC)*(FYB-FYD)-(ZEB-ZED)*(FYA-FYC))/16.
     $+GP*H*(THA-THC)/8.
   68         DRT=(AR(I,J,NT)-ORT)*RF(NT)
   69         DRW=(AR(I,J,NW)-ORW)*RF(NW)
   70         DRF=(AR(I,J,NF)-ORF)*RF(NF)
   71         AR(I,J,NT)=ORT+DRT
   72         AR(I,J,NW)=ORW+DRW
   73         AR(I,J,NF)=ORF+DRF
   74         DISP(NT)=DISP(NT)+ABS(DRT)
   75         DISP(NW)=DISP(NW)+ABS(DRW)
   76         DISP(NF)=DISP(NF)+ABS(DRF)
   77         SUM(NT)=SUM(NT)+ABS(AR(I,J,NT))
   78         SUM(NW)=SUM(NW)+ABS(AR(I,J,NW))
   79         SUM(NF)=SUM(NF)+ABS(AR(I,J,NF))
      C
      C$$$  EVALUATION OF VARIABLES AT CROSS NODES
      C
   80    46   CGT=AG(I,J,NT)
   81         CGW=AG(I,J,NW)
   82         CGF=AG(I,J,NF)
   83         AG(I,J,NF)=0.25*(FYE+FYF+FYB+FYA+AG(I,J,NW)*(H**2))
   84         AG(I,J,NT)=0.25*(THE+THF+THB+THA)
     $-PP*((THE-THB)*(FYF-FYA)-(THF-THA)*(FYE-FYB))/16.
   85         AG(I,J,NW)=0.25*(ZEE+ZEF+ZEB+ZEA)
     $-((ZEE-ZEB)*(FYF-FYA)-(ZEF-ZEA)*(FYE-FYB))/16.
     $+GP*H*(THE-THB)/8.
   86         DGT=(AG(I,J,NT)-OGT)*RF(NT)
   87         DGW=(AG(I,J,NW)-OGW)*RF(NW)
   88         DGF=(AG(I,J,NF)-OGF)*RF(NF)
   89         AG(I,J,NT)=OGT+DGT
   90         AG(I,J,NW)=OGW+DGW
   91         AG(I,J,NF)=OGF+DGF
   92         DISP(NT)=DISP(NT)+ABS(DGT)
   93         DISP(NW)=DISP(NW)+ABS(DGW)
   94         DISP(NF)=DISP(NF)+ABS(DGF)
   95         SUM(NT)=SUM(NT)+ABS(AG(I,J,NT))
   96         SUM(NW)=SUM(NW)+ABS(AG(I,J,NW))
   97         SUM(NF)=SUM(NF)+ABS(AG(I,J,NF))
   98    5    CONTINUE
   99         RETURN
  100         END
```

```
      C
      C
      C
      C     PROGRAM-LISTING (C-3) : MAIN SUBROUTINE FOR THE MODIFIED ADIP
      C                             METHOD .
      C
      C
      C
      C     <<<*** MAIN ***>>>
      C
      C
      C
      1     DIMENSION A(91,101,6),GR(91,101),SL(31)
      C
      2     COMMON/CNAMES/ATITLE(27),ANAME(9,7),ASYMBL(6)
      3     COMMON/CNUMB/NT,NW,NF,NU,NV,NC,NG,IE,IV
      4     COMMON/CGEC/IN,JN,INM,JNM,JL,JH,JL1,JH1
      5     COMMON/CPRINT/NMAX,NPRINT,IP,EPS1,EPS2
      6     COMMON/CPRCP/RCREF,ZMUREF,PR
      7     COMMON/CSCR/RF(3),DC1(3),DC2(3),DT(3),SUM,SUMF
      8     COMMON/CSCL/H,DELT
      9     COMMON/CBETA/TPLATE,TBULK,D1,D2,D3,CL,G
      C
      C
      C     ***************************************************************
      C     *                                                             *
      C     *          IMPROVED ALTERNATIVE DIRECTION IMPLICIT METHOD     *
      C     *                          A.D.I.P.                           *
      C     *                                                             *
      C     ***************************************************************
      C
      C
     10     REWIND3
      C
     11     FT=1.+DELT/H/H/PR
     12     FZ=1.+DELT/H/H
      C
      C$$$$ READ ALPHAMERIC INFORMATION FOR HEADING,NAMES AND  SYMBLES
      C
     13     READ(5,201) ATITLE,ANAME
     14     READ(5,202) ASYMBL
      C
      C$$$$ WRITE PROBLEM SPESIFICATIONS
      C
     15     WRITE(6,203) ATITLE
     16     WRITE(6,204)(K,(ANAME(L,K),L=1,9),K=1,IE)
     17     WRITE(6,205) RCREF,ZMUREF,PR,(RF(K),K=1,3),EPS1,EPS2
      C
      C$$$$ FEED THE INITIAL VALUES
      C
     18     CALL INIT(IN,JN,IV,A)
      C
     19     NCOUNT=0
     20   1 CONTINUE
     21     TT=DC1(NT)+DC2(NT)
     22     WW=DC1(NW)+DC2(NW)
     23     FF=DC1(NF)+DC2(NF)
     24     NCOUNT=NCOUNT+1
     25     WRITE(6,206) NCOUNT
     26     WRITE(6,217) DELT
      C
      C$$$$ TEMPERATURE SUBCYCLE FOR THE FIRST HALF TIME FROM N TO N+1/2
      C
     27     DO 102 I=1,IN
```

```
      28            DO 102 J=1,JN
      29      102   A(I,J,NC)=A(I,J,NT)
      30            NITER=0
      31            WRITE(6,207) ASYMPL (NT)
      32      2     CONTINUE
      33            DC1(NT)=0.
      34            SUM=0.
      35            NITER=NITER+1
      36            DO 103 J=2,JNM
      37            DO 103 I=2,INM
      38            OF=A(I,J,NC)
      39            A(I,J,NC)=A(I,J,NT)/FT
      40            A(I,J,NC)=A(I,J,NC)-.25*(DELT/H/FT)*(A(I,J,NU)*(A(I+1,J,NC)-A(I-1,
     $J,NC))+A(I,J,NV)*(A(I,J+1,NT)-A(I,J-1,NT)))
      41            A(I,J,NC)=A(I,J,NC)+.5*(DELT/H/H/PR/FT)*((A(I-1,J,NO)+A(I+1,J,NO)
     $)+(A(I,J-1,NT)+A(I,J+1,NT)-2.*A(I,J,NT)))
      42            D=(A(I,J,NC)-OF)*RF(NT)
      43            A(I,J,NC)=OF+D
      44            IF(A(I,J,NC).LT.0.) GO TO 333
      45            SUM=SUM+ABS(A(I,J,NO))
      46            DC1(NT)=DC1(NT)+ABS(D)
      47      103   CONTINUE
      48            CALL BOUND(A,IN,JN,IV,NT,NC)
      49            DC1(NT)=DC1(NT)/SUM
      50            WRITE(6,208) NITER,DC1(NT)
      51            IF(DC1(NT).GT.EPS1) GO TO 2
            C
            C$$$  EVALUATION OF GRASHOF NUMBERS
            C
      52            DO 112 J=2,JNM
      53            DO 112 I=2,INM
      54            T=TBULK+A(I,J,NC)*(TPLATE-TBULK)
      55            TDNM=1.+D1*T+D2*T*T+D3*T*T*T
      56            TNM=D1+2.*D2*T+3.*D3*T*T
      57            ROP=ROREF/TDNM
      58            BETAP=TNM/TDNM
      59            ZNUP=ZNUREF/ROP
      60            GR(I,J)=G*(BETAP/ZNUP**2)*(CL**3*(TPLATE-TBULK))
      61      112   CONTINUE
      62            WRITE(6,214)(GR(2,J),J=JL,JH)
            C
            C*$$$ VORTICITY AND STREAM-FUNCTION SUB-CYCLES FOR THE FIRST HALF
            C     CYCLE FROM N TO N+1/2
            C
      63            DO 105 I=1,IN
      64            DO 105 J=1,JN
      65      105   A(I,J,NC)=A(I,J,NW)
      66            NITER=0
      67            WRITE(6,210)(ASYMBL(K),K=2,3)
      68      4     CONTINUE
      69            DC1(NW)=0.
      70            DC1(NF)=0.
      71            SUM=0.
      72            SUMF=0.
      73            NITER=NITER+1
      74            DO 106 J=2,JNM
      75            DO 106 I=2,INM
      76            OF=A(I,J,NC)
      77            A(I,J,NC)=.25*GR(I,J)*(DELT/H/FZ)*(A(I+1,J,NT)-A(I-1,J,NT))
      78            A(I,J,NC)=A(I,J,NC)+A(I,J,NW)/FZ
      79            A(I,J,NC)=A(I,J,NC)-.25*(DELT/H/FZ)*(A(I,J,NU)*(A(I+1,J,NO)-A(I-1,
     *J,NO))+A(I,J,NV)*(A(I,J+1,NW)-A(I,J-1,NW)))
      80            A(I,J,NC)=A(I,J,NC)+.5*(DELT/H**2/FZ)*((A(I-1,J,NO)+A(I+1,J,NO))
     $+(A(I,J+1,NW)+A(I,J-1,NW)-2.*A(I,J,NW)))
      81            D=(A(I,J,NC)-OF)*RF(NW)
      82            A(I,J,NC)=OF+D
```

```
      SUM=SUM+ABS(A(I,J,NO))
      DC1(NW)=DC1(NW)+ABS(D)
C
C$$$$ STREAM-FUNCTION COMPLEMENTARY CYCLE
C
      CF=A(I,J,NF)
      A(I,J,NF)=.25*(A(I,J,NO)*H*H+A(I+1,J,NF)+A(I-1,J,NF)+A(I,J+1,NF)+
     $A(I,J-1,NF))
      D=(A(I,J,NF)-CF)*RF(NF)
      A(I,J,NF)=CF+D
      SUMF=SUMF+ABS(A(I,J,NF))
      DC1(NF)=DC1(NF)+ABS(D)
  106 CONTINUE
      DC1(NF)=DC1(NF)/SUMF
      DC1(NW)=DC1(NW)/SUM
      WRITE(6,211) NITER,DC1(NW),DC1(NF)
      CALL BOUND(A,IN,JN,IV,NW,NC)
      CALL VELOST(A,IN,JN,IV)
      IF(DC1(NW).GT.EPS1.OR.DC1(NF).GT.EPS1) GO TO 4
C
C$$$  TEMPERATURE SUBCYCLE FOR THE SECOND HALF TIME FROM N+1/2 TO N+1
C
      NITER=0
      WRITE(6,209) ASYMBL(NT)
    3 CONTINUE
      DC2(NT)=0.
      SUM=0.
      NITER=NITER+1
      DO 104 J=2,JNM
      DO 104 I=2,INM
      CF=A(I,J,NT)
      A(I,J,NT)=A(I,J,NC)/FT
      A(I,J,NT)=A(I,J,NT)-.25*(DELT/H/FT)*(A(I,J,NU)*(A(I+1,J,NO)-A(I-1,
     $J,NO))+A(I,J,NV)*(A(I,J+1,NT)-A(I,J-1,NT)))
      A(I,J,NT)=A(I,J,NT)+.5*(DELT/H**2/FT/PR)*(A(I-1,J,NO)+A(I+1,J,NO)-
     $2.*A(I,J,NC)+A(I,J+1,NT)+A(I,J-1,NT))
      D=(A(I,J,NT)-CF)*RF(NT)
      A(I,J,NT)=CF+D
      IF(A(I,J,NT).LT.0.) GO TO 333
      DC2(NT)=DC2(NT)+ABS(D)
      SUM=SUM+ABS(A(I,J,NT))
  104 CONTINUE
      CALL BOUND(A,IN,JN,IV,NT,NT)
      DC2(NT)=DC2(NT)/SUM
      WRITE(6,208) NITER,DC2(NT)
      IF(DC2(NT).GT.EPS1) GO TO 3
C
C$$$  EVALUATION OF GRASHOF NUMBERS
C
      DO 113 J=2,JNM
      DO 113 I=2,INM
      T=TBULK+A(I,J,NT)*(TPLATE-TBULK)
      TDNM=1.+D1*T+D2*T*T+D3*T*T*T
      TNM=D1+2.*D2*T+3.*D3*T*T
      ROP=RGREF/TDNM
      BETAP=TNM/TDNM
      ZNUP=ZNUREF/ROP
      GR(I,J)=G*(BETAP/ZNUP**2)*(CL**3*(TPLATE-TBULK))
  113 CONTINUE
      WRITE(6,214)(GR(2,J),J=JL,JF)
C
C$$$  VORTICITY AND STREAM FUNCTION SUBCYCLES FOR THE SECOND HALF TIME
C     FROM N+1/2 TO N+1
C
      NITER=0
      WRITE(6,212) (ASYMBL(K),K=2,3)
```

```
133     5     CONTINUE
134           DC2(NW)=0.
135           DC2(NF)=0.
136           SUM=0.
137           SUMF=0.
138           NITER=NITER+1
139           DO 107 J=2,JM
140           DO 107 I=2,IM
141           CF=A(I,J,NW)
142           A(I,J,NW)=A(I,J,NC)/FZ
143           A(I,J,NW)=A(I,J,NW)-.25*(DELT/H/FZ)*(A(I,J,NU)*(A(I+1,J,NC)-A(I-1,
             $J,NC))+A(I,J,NV)*(A(I,J+1,NW)-A(I,J-1,NW)))
144           A(I,J,NW)=A(I,J,NW)+.25*GP(I,J)*(DELT/H/FZ)*(A(I+1,J,NT)-A(I-1,J,N
             $T))
145           A(I,J,NW)=A(I,J,NW)+.5*(DELT/H**2/FZ)*((A(I+1,J,NC)+A(I-1,J,NC)-2.
             $*A(I,J,NC))+(A(I,J+1,NW)+A(I,J-1,NW)))
146           D=(A(I,J,NW)-CF)*RF(NW)
147           A(I,J,NW)=CF+D
148           SUM=SUM+ABS(A(I,J,NW))
149           DC2(NW)=DC2(NW)+ABS(D)
      C
      C$$$  STREAM FUNCTION COMPLEMENTARY CYCLE
      C
150           CF=A(I,J,NF)
151           A(I,J,NF)=.25*(A(I,J,NW)*H*H+A(I+1,J,NF)+A(I-1,J,NF)+A(I,J+1,NF)+
             $A(I,J-1,NF))
152           D=(A(I,J,NF)-CF)*RF(NF)
153           A(I,J,NF)=CF+D
154           DC2(NF)=DC2(NF)+ABS(D)
155           SUMF=SUMF+ABS(A(I,J,NF))
156    107    CONTINUE
157           DC2(NW)=DC2(NW)/SUM
158           DC2(NF)=DC2(NF)/SUMF
159           WRITE(6,211) NITER,DC2(NW),DC2(NF)
160           CALL BOUND(A,IN,JN,IV,NW,NW)
161           CALL VELDST(A,IN,JN,IV)
162           IF(DC2(NW).GT.EPS1.OR.DC2(NF).GT.EPS1) GO TO 5
      C
      C$$$  CALCULATION OF THE RELATIVE DISPLACEMENT NORM BETWEEN TWO
      C     SUCCESSIVE TIME-STEPS
      C
163           DT(NT)=ABS(DC1(NT)+DC2(NT)-TT)
164           DT(NW)=ABS(DC1(NW)+DC2(NW)-WW)
165           DT(NF)=ABS(DC1(NF)+DC2(NF)-FF)
166           WRITE(6,213)(ASYMPL(K),K=1,IE),(DT(K),K=1,IE)
      C
      C$$$  CHECK MAXIMUM NUMBER OF COMPUTATIONAL STEPS
      C
167           IF(NCOUNT.EQ.NMAX) GO TO 900
      C
      C$$$  CHECK PRINT-OUT STEP
      C
168           IF((NCOUNT+NPRINT-IP)/NPRINT.NE.NCOUNT/NPRINT) GO TO 899
169           CALL PRINT(A,IN,JN,IV,ANAME,1,5)
170           CALL NLSLT(IN,JN,IV,A,SL)
      C
      C$$$  CHECK EXIT CRITERION
      C
171    899    DDT=0.
172           DO 313 K=1,3
173           IF(DDT.LT.DT(K)) DDT=DT(K)
174    313    CONTINUE
      C
      C$$$  EVALUATION OF THE TIME-INCREMENT AS A FUNCTION OF GR
      C
175           FACTOR=.48*GP(2,JH)**.5/H+4.*PR/H**2
```

```
      DELT=1./FACTOR
      IF(DDT.GT.EPS2) GO TO 1
C
C$$$  FINAL PRINT OUT
C
  900 CALL PRINT(A,IN,JN,IV,ANAME,1,5)
C
C$$$  EVALUATION OF THE AVERAGE NUSSELT NUMBER
C
      CALL NUSLT(IN,JN,IV,A,SL)
C
C$$$  WRITE ON TAPE
C
      WRITE(3)(((A(I,J,K),J=1,JN),I=1,IN),K=1,5)
      ENDFILE3
C
C$$$  PUCH OUT FOR PLOTS
C
      GO TO 444
  333 WRITE(6,216)
  444 STOP
C
  201 FORMAT(9A4)
  202 FORMAT(6A6)
  203 FORMAT(1H1,24X,'IMPROVED ALTERNATIVE DIRECTION IMPLICIT METHOD IS
     $UNDER CONSIDERATION'/25X'----------------------------------
     $----------'//1X,27A4/1H-'THE DEPENDENT VARIABLES
     $ BEING CONSIDERED ARE,'//)
  204 FORMAT(1HO,9X,I1,'.  ',9A4/)
  205 FORMAT(1H ,'THE PARAMETERS USED IN THE SOLUTION ARE,'//,1X,
     $'THE REFERENCE DENSITY ..........ROREF=',E12.4/,1X,
     $'THE REFERENCE VISCOSITY ..... ZMUREF=',E12.4/,1X,
     $'THE PRANDTL NUMBER ..............  PR=',E12.4/,1X,
     $'THE SPATIAL RELAXATION FACTORS .. RFS=',E12.4/38X,'=',E12.4/,38X,
     $'=',E12.4,',AND'/1X,
     $'THE EXIT CRITERION ..........SPATIAL=',E12.4/,33X,'TIME =',E12.4
     $//)
  206 FORMAT(1H1//,1X,'*****************************************'/,1X,
     $'* NUMBER OF  THE TIME STEP BEING DONE =',I3,'*'/,1X,'*********
     $*****************************')
  207 FORMAT(1HO,'NITER',8X,A6,05X,'(AT FIRST HALF TIME)')
  208 FORMAT(1H ,I4,5X,E12.4)
  209 FORMAT(1HO,'NITER',8X,A6,5X,'(AT SECOND HALF TIME)')
  210 FORMAT(1HO,'NITER',8X,A6,15X,A6,05X,'(AT FIRST HALF TIME)')
  211 FORMAT(1H ,I4,5X,E12.4,10X,E12.4)
  212 FORMAT(1HO'NITER',8X,A6,15X,A6,05X,'(AT SECOND HALF TIME)')
  213 FORMAT(1HO,'*****************************************************
     $******'/1X,'* THE DIFFERENCE BETWEEN TWO SUCCESSIVE TIME STEP AVER
     $AGES *'/'*****************************************************
     $****'//12X,A6,2(15X,A6)/9X,E12.4,2(09X,E12.4)///)
  214 FORMAT(1HO,'GRASHOF NUMBERS FOR THE NODES RIGHT IN FRONT OF THE PL
     $ATE,'/,1X,'(BASED ON PLATE HEIGHT L BUT FOR DIFFERENT BETAS),ARE,'
     $//,6(5X,E15.6))
  216 FORMAT(1HO,1X,'NEGATIVE VALUES OF TEMPERATURE')
  217 FORMAT(1HO,'TIME-INTERVAL VALUE DELT =',E12.4)
      END
```

APPENDIX D

Tables for Some Resulting Numerical Values

TABLE (D-1) : Vertical-Velocity Values at y=0 and T_b=0

	T_p , °C				
x	2	8	9	9.597	11
0.1	$-.2022^{-1}$*	$-.1423^{-1}$	$-.5976^{-2}$	$-.5699^{-4}$	$.1674^{-1}$
0.2	$-.3957^{-1}$	$-.3908^{-1}$	$-.2689^{-1}$	$-.1790^{-1}$	$.8205^{-2}$
0.3	$-.5223^{-1}$	$-.6148^{-1}$	$-.4903^{-1}$	$-.3957^{-1}$	$-.1138^{-1}$
0.4	$-.5927^{-1}$	$-.7922^{-1}$	$-.6872^{-1}$	$-.6039^{-1}$	$-.3470^{-1}$
0.5	$-.6190^{-1}$	$-.9157^{-1}$	$-.8416^{-1}$	$-.7781^{-1}$	$-.5721^{-1}$
0.6	$-.6122^{-1}$	$-.9866^{-1}$	$-.9472^{-1}$	$-.9071^{-1}$	$-.7634^{-1}$
0.7	$-.5817^{-1}$	$-.1010$	$-.1005$	$-.9864^{-1}$	$-.9089^{-1}$
0.8	$-.5349^{-1}$	$-.9942^{-1}$	$-.1019$	$-.1024$	$-.1005$
0.9	$-.4776^{-1}$	$-.9460^{-1}$	$-.9964^{-1}$	$-.1015$	$-.1053$
1.0	$-.4142^{-1}$	$-.8733^{-1}$	$-.9433^{-1}$	$-.9810^{-1}$	$-.1058$
1.5	$-.9915^{-2}$	$-.3515^{-1}$	$-.4460^{-1}$	$-.5075^{-1}$	$-.6677^{-1}$
2.0	$.1111^{-1}$	$.1027^{-1}$	$.4734^{-2}$	$.7427^{-3}$	$-.1069^{-1}$
2.5	$.2034^{-1}$	$.3412^{-1}$	$.3278^{-1}$	$.3141^{-1}$	$.2655^{-1}$
3.0	$.2171^{-1}$	$.4041^{-1}$	$.4156^{-1}$	$.4185^{-1}$	$.4138^{-1}$
3.5	$.1917^{-1}$	$.3698^{-1}$	$.3906^{-1}$	$.4005^{-1}$	$.4162^{-1}$
4.0	$.1531^{-1}$	$.2982^{-1}$	$.3193^{-1}$	$.3303^{-1}$	$.3514^{-1}$
4.5	$.1146^{-1}$	$.2228^{-1}$	$.2404^{-1}$	$.2499^{-1}$	$.2692^{-1}$
5.0	$.8209^{-2}$	$.1580^{-1}$	$.1713^{-1}$	$.1786^{-1}$	$.1938^{-1}$
5.5	$.5685^{-2}$	$.1080^{-1}$	$.1174^{-1}$	$.1226^{-1}$	$.1336^{-1}$
6.0	$.3835^{-2}$	$.7185^{-2}$	$.7820^{-2}$	$.8172^{-2}$	$.8924^{-2}$
6.5	$.2533^{-2}$	$.4680^{-2}$	$.5095^{-2}$	$.5328^{-2}$	$.5824^{-2}$
7.0	$.1646^{-2}$	$.3006^{-2}$	$.3274^{-2}$	$.3423^{-2}$	$.3742^{-2}$
7.5	$.1052^{-2}$	$.1919^{-2}$	$.2090^{-2}$	$.2184^{-2}$	$.2387^{-2}$
8.0	$.6556^{-3}$	$.1227^{-2}$	$.1336^{-2}$	$.1396^{-2}$	$.1526^{-2}$
8.5	$.3826^{-3}$	$.7664^{-3}$	$.8530^{-3}$	$.8731^{-3}$	$.9550^{-3}$
9.0	$.1994^{-3}$	$.4401^{-3}$	$.4811^{-3}$	$.5043^{-3}$	$.5549^{-3}$

* This means the number printed times 10 to the power shown as superscript .

TABLE (D-2) : Vertical-Velocity Values at $y=0$ and $T_b=0$

x	T_p , °C 26.8	35	41.86
0.1	.4095	.6407	$.8266_{+1}$
0.2	.6226	.9362	$.1172_{+1}$
0.3	.6686	.9854	$.1212_{+1}$
0.4	.6250	.9158	$.1123_{+1}$
0.5	.5259	.7968	.9880
0.6	.4127	.6622	.8429
0.7	.2965	.5277	.7018
0.8	.1854	.4003	.5704
0.9	$.8373^{-1}$*	.2831	.4503
1.0	$-.6418^{-2}$	.1769	.3415
1.5	-.2741	-.2028	$-.7530^{-1}$
1.7	-.3046	-.2943	-.2005
1.9	-.3020	-.3537	-.3045
2.1	-.2757	-.3821	-.3842
2.3	-.2352	-.3819	-.4362
2.5	-.1887	-.3583	-.4589
2.7	-.1425	-.3183	-.4536
2.9	-.1008	-.2692	-.4349
3.0	$-.8226^{-1}$	-.2434	-.4038
3.5	$-.1618^{-1}$	-.1258	-.2678
4.0	$.1326^{-1}$	$-.4935^{-1}$	-.1433
4.5	$.2132^{-1}$	$-.1161^{-1}$	$-.6465^{-1}$
5.0	$.1986^{-1}$	$.2884^{-2}$	$-.2492^{-1}$
5.5	$.1542^{-1}$	$.6443^{-2}$	$-.7936^{-2}$
6.0	$.1090^{-1}$	$.5885^{-2}$	$-.1772^{-2}$
6.5	$.7270^{-2}$	$.4294^{-2}$	$-.1290^{-4}$
7.0	$.4679^{-2}$	$.2815^{-2}$	$.2413^{-3}$
7.5	$.2956^{-2}$	$.1744^{-2}$	$.1244^{-3}$
8.0	$.1871^{-2}$	$.1072^{-2}$	$.1517^{-4}$
8.5	$.1201^{-2}$	$.7099^{-3}$	$.3523^{-4}$
9.0	$.7932^{-3}$	$.5673^{-3}$	$.1906^{-4}$

* This means the number printed times 10 to the power shown as superscript .

APPENDIX E

Convergence, Accuracy and Reliability of the Results

The stability and convergence of the iterative procedure, used to obtain the final results, was controlled by three sets of values of the relaxation factors for three ranges of the number of the iterative steps. Figure (E-1) shows these ranges and the ω-values associated with each one for the three dependent variables. This approach of using ranges was found to eliminate the numerical instability which was always occurring after 80 iterative steps, and causing the appearance of negative values in the temperature field. This is obvious in Figure (E-1) where, it can be seen that the use of ranges improved the rate of convergence.

The accuracy of the results can be presented, on the other hand, by the following analysis:

The results were obtained using relative displacement norms, defined by equation (5.6), of less than 1%. For the temperature equation, this exit criterion was reached after 50 iterations and then it decreased smoothly until it reached a value of 0.209×10^{-2} at the $130^{\underline{th}}$ iterative step. The vorticity equation also converged smoothly. The relative displacement norm for this case reached a value less than 1% after 105 iterations and continued decreasing to reach a value of 0.821×10^{-2} at the $130^{\underline{th}}$ terminating iterative-step. On the other hand, the convergence of the stream-function equation was comparatively slower than that of the temperature and vorticity equations. Here, at the last 30 iterative steps

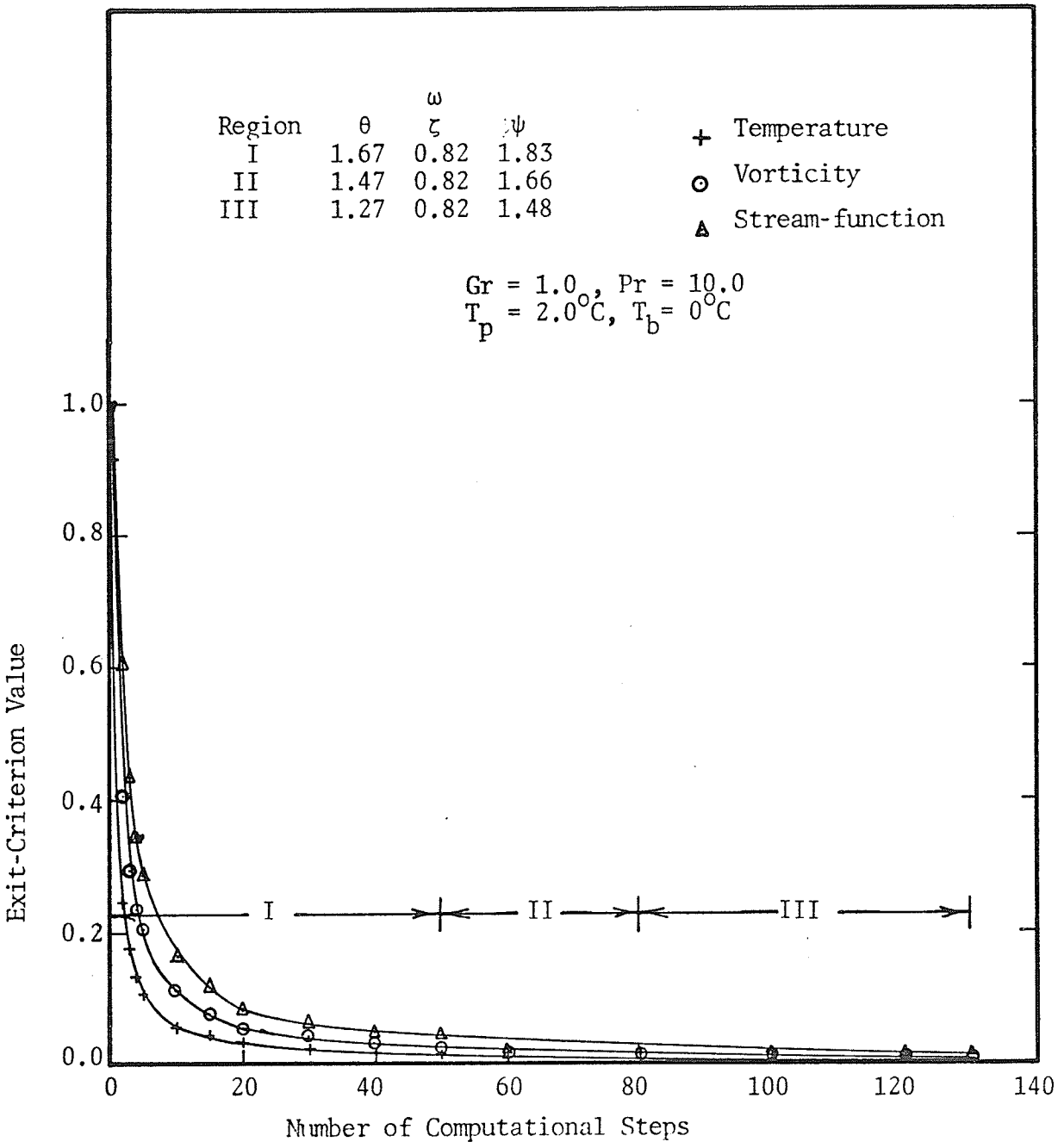

Fig. (E-1) : Convergence Rate of the Three Dependent Variables under Consideration.

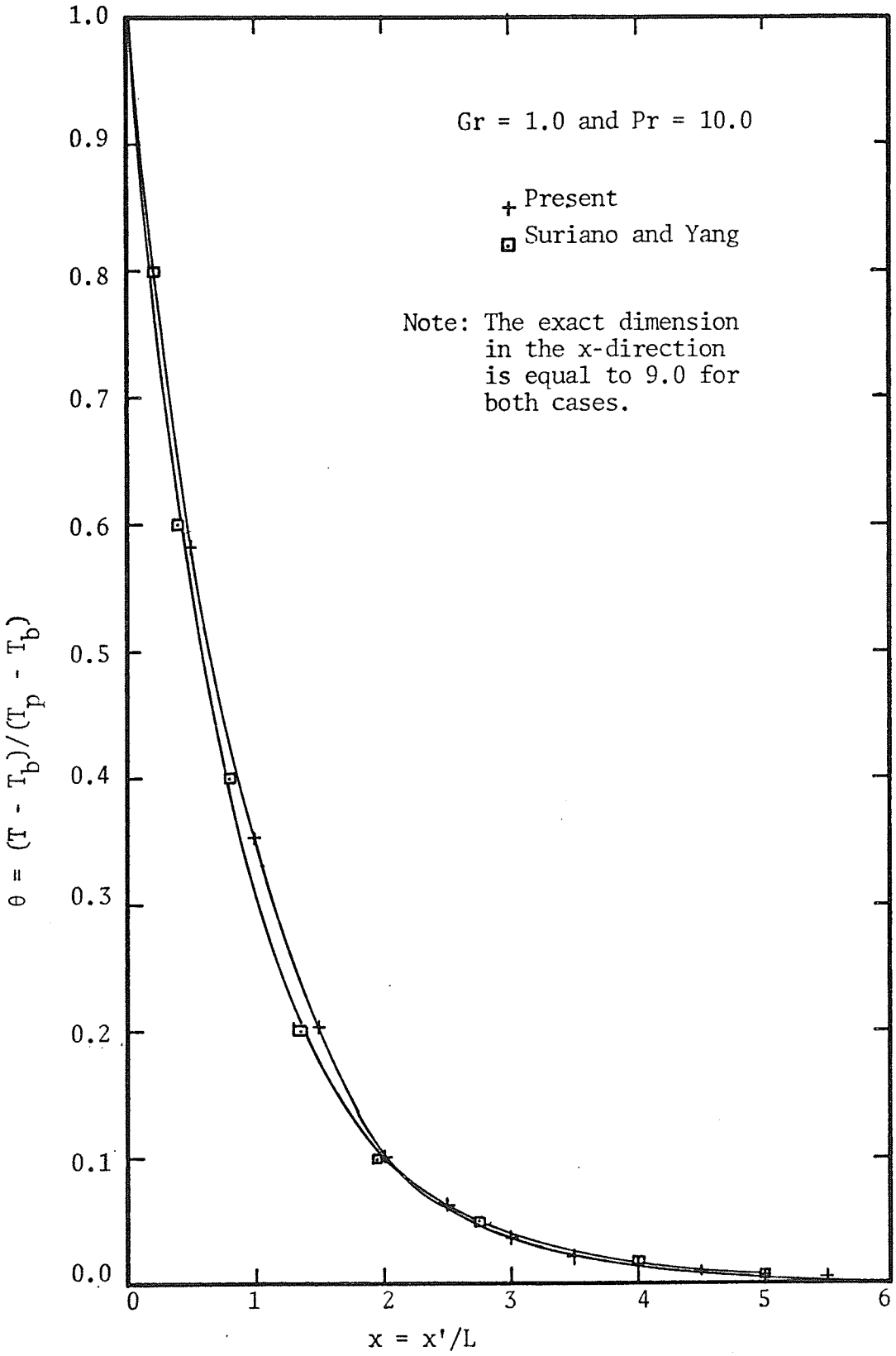

Fig. (E-2): Dimensionless temperature profiles for the present and Suriano and Yang results for the same boundary conditions and numerical parameters.

the value of the relative displacement norm decreased only from 0.0112 to 0.0107. Subsequently, it was felt that more iterative steps would be a waste of computer time.

From the above analysis of accuracy, it can be seen that the results were obtained after a certain stage at which the computed values had reached almost constant figures. Also, it can be seen that the convergence was smooth without any unstable oscillations.

At this stage, the reliability of the results might be questined. For this reason, the present DSSE approach was tested by using the same boundary conditions and all other parameters of the solution obtained by Suriano and Yang [Ref. 65], and comparing the results obtained. The two temperature profiles, shown in Figure (E-2), illustrate the agreement which was found. The average Nusselt number obtained from the present program was 1.24, and that obtained by Suriano and Yang was 1.279, less than 2.5% higher. The agreement between the results obtained by these two independent programs indicates the reliability of both.